Universidade Vigo

# Smart nanohydrogels for controlled release of food preservatives

por Clara Fuciños González

Memoria para optar al título de Doctora por la Universidad de Vigo con Mención de Doctora Internacional

Ourense 2012

Los doctores María Luisa Rúa Rodríguez, Profesora Titular, y Lorenzo Miguel Pastrana Castro, Catedrático, del Departamento de Química Analítica y Alimentaria de la Universidad de Vigo,

CERTIFICAN:

que la memoria titulada: “Smart nanohydrogels for controlled release of food preservatives”,

presentada por Doña Clara Fuciños González para optar al Grado de Doctor Internacional en Ciencia y Tecnología de Alimentos, fue realizada en el Departamento de Química Analítica y Alimentaria de la Facultad de Ciencias de Ourense (Universidad de Vigo) bajo nuetra dirección, y considerando que constituye trabajo de Tesis Doctoral, autorizamos su presentación en la Universidad de Vigo.

Para que así conste, expedimos y firmamos el siguiente certificado en Ourense, a 3 de Septiembre de 2012.

Fdo. María Luisa Rúa Rodríguez

Fdo. Lorenzo Miguel Pastrana Castro

# Contents

# Enfoque, justificación y objetivos

En la actualidad la gran mayoría de los alimentos se comercializan envasados con la finalidad principal de protegerlos y aislarlos del entorno para que conserven sus características físicas, químicas y microbiológicas ya que se trata de productos que sufren un rápido deterioro durante el almacenamiento por causa de la acción de organismos vivos (principalmente microorganismos) o de condiciones ambientales como la temperatura y la humedad. Sin embargo, los cambios en las formas de vida de las sociedades industriales han propiciado que el envase satisfaga también otras necesidades adicionales relacionadas con la comunicación, el marketing y la conveniencia para el consumidor, de modo que, hoy en día, los envases son uno de los factores determinantes de la elección de compra por parte de los consumidores. Estas nuevas necesidades han propiciado un gran desarrollo tecnológico del envasado de alimentos que ha supuesto cambios profundos en el diseño, los materiales y los procesos de envasado. Estos avances permiten que ahora, por ejemplo, el consumidor disponga de productos más naturales, menos procesados o que puedan ser cocinados o consumidos en el propio envase y en porciones adaptadas a sus necesidades de consumo.

Este es el contexto en el que en los últimos años el concepto de envasado activo de alimentos se ha desarrollado e implementado en la práctica. Así, hoy se dispone de materiales de envasado y dispositivos que interaccionan con el alimento o con la atmósfera que le rodea induciendo cambios positivos en ellos.

Uno de los aspectos del envasado activo de alimentos en los que con mayor intensidad se ha trabajado es el de los envases antimicrobianos, de los que ya existen incluso

aplicaciones comerciales. Se trata de materiales que, al incorporar sustancias antimicrobianas de naturaleza muy diversa (plata, etanol, antibióticos) y en algunos casos liberarlas, son capaces de inhibir el crecimiento microbiano en los alimentos en contacto con ellos.

A pesar de ello, hasta la fecha, cuando existe liberación de las sustancias antimicrobianas al alimento ésta se hace generalmente mediante mecanismos de difusión pasiva, de modo que no existe un control efectivo real del proceso más que aquel que determine las constantes de difusión durante las síntesis de los materiales y el gradiente de concentración del antimicrobiano entre el material y el alimento. Así, en estos sistemas se da la paradoja de que en el momento en el que el alimento es más seguro desde el punto de vista microbiológico que es cuando se envasa recién procesado, es cuando el flujo de antimicrobiano desde el envase al alimento es mayor. Esta poco satisfactoria circunstancia es particularmente relevante cuando se trata de alimentos refrigerados o incluso congelados ya que en estos casos el mantenimiento de la cadena de frío suele ser suficiente para asegurar que el alimento llega al consumidor en condiciones adecuadas y sólo si se rompe esta cadena y la temperatura del producto alcanza valores adecuados para el crecimiento microbiano existe un riesgo real. Como no siempre se puede garantizar la integridad de la cadena del frío los productores de alimentos optan por la garantía adicional que le ofrece el envasado activo aún siendo conscientes que estará en muchos casos liberando innecesariamente el conservante hacia el alimento.

Por todo ello se hace necesario diseñar sistemas de aplicación en el envasado activo de alimentos que permitan liberar los antimicrobianos bajo demanda sólo cuando sea necesario y como respuesta a cambios ambientales que puedan suponer un riesgo para la seguridad y estabilidad del alimento.

Precisamente y con este enfoque esta memoria explora la posibilidad del uso de nanohidrogeles "inteligentes" para la liberación controlada de conservantes alimentarios. Así, el principal objetivo de esta tesis es el estudio de la capacidad los nanohidrogeles de poli (N-isopropilacrilamida) (PNIPA) para trasportar y liberar de pimaricina como respuesta

a estímulos externos de temperatura así como el estudio de la efectividad antimicrobiana del sistema propuesto con el fin de evaluar su potencial en el envasado activo de alimentos.

En el **Capitulo 1** el principal objetivo es proporcionar una visión general del estado actual del envasado activo de alimentos y las aportaciones que la nanotecnología puede hacer dentro de este campo. o de este campo. Asimismo se pretende describir las principales ventajas e inconvenientes del uso de la pimaricina como substituto de conservantes químicos usados en el tratamiento de alimentos, así como las principales características de los nanohidrogeles de poli (N-isopropilacrilamida) que los hacen adecuados para el transporte y liberación de pimaricina y para su posterior aplicación en el envasado activo de alimentos.

En el **Capítulo 2** el principal objetivo es la caracterización de los nanohidrogeles de PNIPA sintetizados con diferente grado de hidrofilia mediante la adición de ácido acrílico (AA) como comonómero con el fin de entender mejor los factores que afectan a la liberación de pimaricina desde estos nanohidrogeles. El primer subobjetivo es el estudio del tamaño de partícula y carga superficial de los nanohidrogeles sintetizados. El segundo subobjetivo es el estudio de las propiedades termodinámicas de los nanohidrogeles de PNIPA/AA en función de su composición y bajo diferentes condiciones ambientales.

En el **Capítulo 3** el principal objetivo es la evaluación de la capacidad de los nanohidrogeles de PNIPA/AA para transportar y liberar pimaricina en función de su composición y de las condiciones ambientales con el fin de evaluar su posible aplicación en el envasado activo de alimentos. El primer subobjetivo es evaluar la capacidad de los nanohidrogeles de PNIPA/AA para encapsular pimaricina en función de la composición del nanohidrogel. El segundo subobjetivo es evaluar la capacidad de los nanohidrogeles de PNIPA/AA para liberar pimaricina como respuesta a estímulos externos (temperatura y pH) en función de su composición.

En el **Capítulo 4** el principal objetivo es evaluar la efectividad del nanohidrogel cargado con pimaricina para controlar la contaminación por hongos en queso. Para ello

el primer subobjetivo es la evaluación de la efectividad antimicrobiana en sistemas modelo basados en placas de agar contaminadas con un microorganismo indicador y almacenadas en condiciones favorables y desfavorables para la estabilidad química de la pimaricina con el fin de evaluar el efecto protector del nanohidrogel. El segundo subobjetivo es la evaluación de la efectividad antimicrobiana en un alimento real con el fin de controlar la contaminación de quesos de la DOP Arzúa-Ulloa almacenados bajo diferentes condiciones de térmicas simulando una rotura en la cadena de frío. El tercer subobjetivo es la puesta a punto de un método de cuantificación de los hongos totales en muestras de queso empleando PCR cuantitativa.

En el **Capítulo 5** el principal objetivo es evaluar la efectividad del nanohidrogel cargado con pimaricina para controlar la contaminación por hongos en zumo de uva. Para ello el primer subobjetivo es la puesta a punto de un método para cuantificar pimaricina mediante cromatografía líquida en medio de cultivo y en zumo de uva. El segundo subobjetivo es la construcción de curvas dosis-respuesta para el cálculo de la dosis inhibitoria 50 ($IC_{50}$) de la pimaricina en medio de cultivo y en zumo de uva. El tercer subobjetivo es la evaluación de la actividad antimicrobiana en sistemas modelo basados en un medio de cultivo contaminado con un microorganismo indicador. El cuarto subobjetivo es la evaluación de la actividad antimicrobiana antimicrobiana en una bebida real con el fin de controlar la contaminación de zumo de uva almacenados bajo condiciones de abuso térmico.

CHAPTER 1

# Introduction

The global food packaging industry has a lot to contribute not only in addressing food losses but also in ensuring food safety as well as enhancing global food trade, which is a key to economic development of varying economies. If there is an industry sector that is equally, if not more dynamic than the food sector, it is none other than the packaging industry. Food accounts for 50% of the global consumer packaging industry valued at US$ 380 billion as of 2009. If the beverage sector is to be added, that will even increase to 69% [115].

The continued quest for innovation in food and beverage packaging is mostly driven by consumer needs and demands influenced by changing global trends, such as increased life expectancy, fewer organizations investing in food production and distribution, and regionally abundant and diverse food supply [22]. All this combined with the interest of consumers for healthy eating combined with its active lifestyles is the key to the success of the ready-to-eat food products. However the stability of these products is compromised due to contamination by moulds and yeasts generating a serious problem of preservation. Standard thermal treatments do not allow maintaining the organoleptic characteristics of the product and chemical preservatives like sulphites may cause allergy problems. Therefore, in recent years, the interest in antimicrobials for extending the shelf life of food products has focused on using natural substances such as essential oils (allyl isotiocyanate), bacteriocins (nisin) and pimaricin.

## 1.1. Pimaricin

Pimaricin (natamycin) is a polyene macrolide fungicide produced by submerged aerobic fermentation of *Streptomyces natalensis* and related species. It is widely used in the food industry as a preservative on the surface of cheese, fruits and other non-sterile products, such as meat and sausages [61, 17]. Pimaricin presents a broad spectrum of activity and any development of resistance has not been reported.

Pimaricin (MW = 665.75 g $mol^{-1}$) forms a cylindrical structure due to the alignment of the hydroxyl groups of its amphipathic chain towards each other (Figure 1). The exterior of the cylinder is completely non-polar.

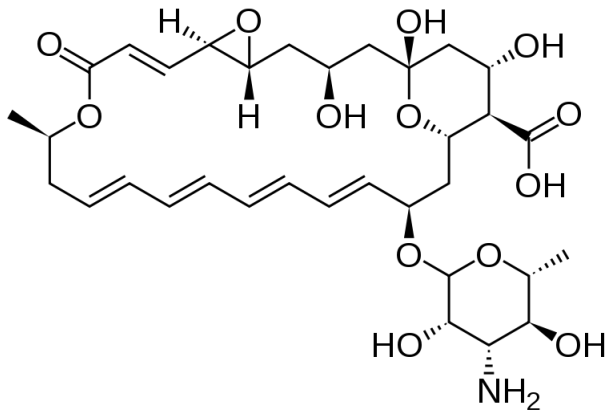


FIGURE 1. Pimaricin molecule

Pimaricin has several advantages to use as food preservative: it is not toxic; it has no influence on the taste and appearance; it has a favourable consumer perception because it is a natural ingredient; it is active a low concentrations; and it has no antibacterial activity so the natural ripening process in fermented products is not influenced in a negative way for its action [183].

Nevertheless some important technological disadvantages limit its food applications: pimaricin low solubility reduces its use to surface treatments applications; and the

chemical stability in acidic conditions and under light radiation is low. This last disadvantage is important in food products that are normally exposed to high-intensity fluorescent lighting in the retail dairy case, until consumer purchase and storage [99, 183].

The mode of action of pimaricin is directly related to the presence of sterols in the cell membrane of organisms. Polyene antibiotics binds irreversibly to sterol in the cell membranes, forming a polar pore through which small ions such as $K^+$, $H^+$, amino acids and other metabolites can pass freely, disrupting the cell's ionic control and killing the cell [183]. However, Welscher et al. [204, 205] appointed that pimaricin did not change the permeability in ergosterol containing membranes as its mode of action are related to the interference in the process of vacuole fusion in a sterol dependent manner and the inhibition of the function of the transport proteins preventing the uptake of different important substrates.

Pimaricin has minimum inhibitory concentration (MIC) value less than 10 ppm and, in general, yeasts are more sensitive than moulds with MIC values for most yeast even lower than 3 ppm. Under normal hygienic and processing conditions 30 ppm of dissolved pimaricin is enough to prevent fungal growth, because the solubility is much higher than the MIC value [183]. Türe et al. [190] reported a MIC value for pimaricin included into methyl cellulose and wheat gluten films for *A. niger* and *P. roquefortii* of 0.2 mg and 0.1 mg per g of solution, respectively. Fajardo et al. [59] obtained a minimum inhibitory concentration of pimaricin included into chitosan films applied in cheeses of 0.50, 0.50, 0.25 and 0.06 mg $mL^{-1}$ for *A. niger*, *P. crustosum*, *P. roquefortii* and *P. commune*, respectively.

Pimaricin was approved as a GRAS (Generally Recognized As Safe) agent by Food and Drug Administration (FDA) in the United States [183] and also designated as a natural preservative by the European Union (E-235). The "Codex General Standard for Food Additives" (GSFA, Codex STAN 192-1995) sets forth the conditions under which permitted food additives may be used in all foods. GSFA provisions for Pimaricin are listed in Table 1 on the next page.

TABLE 1. «Codex General Standard for Food Additives» (GSFA) provisions for pimaricin

| Food category | Maximum Level | Notes |
|---|---|---|
| Cheese analogues | 40 mg $kg^{-1}$ | 1,2 |
| Cured (including salted) and dried non-heat treated processed comminuted meat, poultry, and game products | 20 mg $kg^{-1}$ | 1,3 |
| Cured (including salted) and dried non-heat treated processed meat, poultry, and game products in whole pieces or cuts | 6 mg $kg^{-1}$ | |
| Processed cheese | 40 mg $kg^{-1}$ | 1,2 |
| Ripened cheese | 40 mg $kg^{-1}$ | 1,2 |
| Unripened cheese | 40 mg $kg^{-1}$ | 1,2 |
| Whey protein cheese | 40 mg $kg^{-1}$ | 1,2 |

[1]Surface treatment.

[2]Equivalent to 2 mg dm-2 surface application to a maximum depth of 5 mm.

[3]Equivalent to 1 mg dm-2 surface application to a maximum depth of 5 mm.

Pimaricin is mainly used in cheese, so one of the most important problems for the quality and shelf life of cheese is mould development on the surface because of the post-process contamination during handling and packaging of the product [136] leading to

economical losses and health problems owing to mycotoxins [219]. Pimaricin is normally applied in these products as an aqueous suspension by spraying the surface or soaking the cheese in a solution of pimaricin [192].

At present the sulfur dioxide ($SO_2$) is one of the most widely used substances in the preservation of beverages such as wine, to prevent rancidity and oxidative deterioration by spoilage microorganism. However, allergies caused by $SO_2$-derived compounds, namely the sulfites, are becoming more frequent. Although in the literature are still few studies about these of pimaricin for preventing contamination of beverages as pimaricin is not yet approved for use in drinks in beverages in Spain and the European Union, its use might be an alternative to prolong the shelf life and improve the quality of these products. Shirk and Clark [173] use pimaricin in fresh orange juice preventing its spoilage during 8 weeks. Bärwald [9] use pimaricin in apple juice obtaining the fully inhibition of inoculated yeast during 25 days. Medina et al. [122] found that the presence of pimaricin in grape juice prevented *A. carbonarius* growth, main fungus responsible for contaminating wine, grapes, grape juice and vine fruits, when applied to the medium at a concentration of 20 ng $ml^{-1}$ and it has also been shown that natamycin is able to control OTA production as well.

However, pimaricin, like other food preservatives, is usually added at high concentrations to food bulk during manufacturing in order to extend the shelf life, keeping an effective concentration during all the storage, although initial microbial load in a processed food is usually low. Nevertheless it is possible to reduce preservative concentration (and consequently consumers intake) maintaining suitable levels of food safety by using a delivery system as proposed in active packaging technologies. In addition, when there is continuous contact between preservatives and microorganisms, microbial resistance can develop and so the preservative becomes ineffective. This occurs frequently when antimicrobials are added directly to the food product. Smart active packaging can reduce this effect.

## 1.2. Active and smart packaging

Traditional food packaging are passive and inert barriers designed to protect food against adverse effects of the environment that acts protecting food from external influences, like microorganisms, oxygen, off-odours, light etc. and, by doing so, guaranteeing convenience in food handling and preserving the food quality for an extended time period. The key safety objective for these traditional materials in contact with foods is to be as inert as possible, i.e., there should be a minimum of interaction between food and packaging [50].

In the last decades, however, one of the most innovative developments in the area of food packaging is the active and smart packaging based on the interaction of packages with food and environment playing a dynamic role in food preservation [22, 50].

The purpose of active packaging is the extension of the shelf life of the food and the maintenance and even the improvement of its quality [197]. On the other hand, smart packaging responds to environmental conditions or repairs them or alerts the consumers to contamination and/or the presence of pathogens [165]. However, there is an important distinction between package functions that are smart, and those that become active in response to a triggering event, for example, filling, exposure to ultraviolet radiation, release of pressure etc., and then continue until the process is exhausted [102].

Good examples of smart packaging are the so-called time–temperature indicators (TTIs) that show an irreversible change in a physical characteristic, usually colour or shape, in response to temperature changes. These observable changes are expected to mimic and correlate with the change of a quality parameter of the food that experiences the same temperature history [102]. Colorimetric indicators can be incorporated into a food packaging materials or attached to the inside or outside of a package to detect and monitor changes in the conditions of packed products by visual colour variations [22].

TABLE 2. Overview of studies on smart packaging technologies for food applications (based on Kuswandi et al. [102])

| Smart packaging system | Technology | Working principle | Application | References |
|---|---|---|---|---|
| Time-temperature indicators | thermochromic dye | colour changes of a heat-sensitive dye or pigment like anthocyanin | Plastic containers of pouring syrup and orange juice pack labels | 214, 113, 166 |
| | | melting and diffusion of a safe dye (MonitorMark™, Timestrips®) | frozen or refrigerated foods: fresh seafood, fresh produce, airline catering, school meals, home delivery diets, food retailing, restaurants —fridge and freezer checking against power outages—, pizza dough delivery | 180, 215 |
| | thermochromic polymers | colour changes of a polymer diacetylene based (Fresh-Check®) | pre-packed perishable foods | 210 |
| | enzymatic reactions | colour change due to the reaction of a lipase plus a pH indicating dye and the substrate, consisting primarily of triglycerides (CheckPoint®) | beef, poultry, pork, seafood, high value packaged fruits, salad mixes, airline catering, prepared foods | 216 |

| Smart packaging system | Technology | Working principle | Application | References |
|---|---|---|---|---|
| | | starch-iodine clathrate compound whose color was according to the degree of polymerization in presence of amylase | different foodstuffs | 218 |
| | lactic acid diffusion | color changes associated with the pH variation | fruits and vegetables | 202 |
| Microbial growth indicators | $CO_2$ sensors | colour change of a pH-dye | intermediate-moisture desserts, packed fermented vegetable product, sausage gravy or tomato soup | 135, 119, 151, 84 |
| | | fluorescent change of a luminiscent-dye | | 128 |
| | $H_2S$ sensors | colour change of agarose immobilised myoglobin | packed poultry | 178, 179 |
| | Total Volatile Basic Nitrogen compounds sensors | colour change of a pH sensitive dye (bromocresol green) in presence of basic volatile spoilage compounds (FreshTag®) | fish and seafood spoilage | 142, 141, 211 |

| Smart packaging system | Technology | Working principle | Application | References |
|---|---|---|---|---|
| | foodborne pathogens sensors | conducting polymers where the change in resistance correlates to the amount of gas released during microbe metabolism | chicken meat spoilage | 7, 67 |
| | | silica nanospheres filled with a fluorescent dye that light up after antibody-antigen contact | *E. coli* 0157 detection in meat | 143 |
| | | colour changes due to the microbial protein binding with a dye linked with a silk fibrils | food packaging | 103 |
| | | specific pathogen detection based on immunochemical reaction in a bar code | raw meat products, juices and beverages spoilage | 71 |
| Ripeness indicator | aroma sensors | color change due to the presence of aromas released during fruit ripening (ripeSense®) | fruit pears, kiwifruit, melon, mango, avocado, and other stone fruit | 200, 213 |
| | ethylene sensors | radio frequency identification tags for ethylene sensing | perishable goods and foodstuffs | 92 |

| Smart packaging system | Technology | Working principle | Application | References |
|---|---|---|---|---|
| Leak indicators | $O_2$ sensors | colour changes due to the oxidation of a redox dye in presence of $O_2$ (Ageless Eye) | chill-stored food, such as fish products, moist cakes and biscuits, sausage gravy or tomato soup | 119, 177, 212 |

Smart packaging systems may also include biosensors, which incorporate integrated optics, immunoassay or surface chemistry, to detect chemicals, pathogens and toxins in food [11, 159] , sensors to indicate fruit ripeness, or radio frequency identification [201]. Table 2 on page 19 list some smart packaging that already exist in the market and concepts that are under development.

Active packages (AP) are designed to prevent sensorial or toxicological problems and improve product quality and acceptability, using the possible interactions between food and package. Based on the nature of the expected spoilage, two categories of active substances have been used in active packaging systems: scavengers and releasing .

Scavengers systems included those active on $O_2$, ethylene, and moisture, of which some are currently commercially available.

Within the second category release of active substances such as antimicrobials or antioxidants are among the most referenced. A number of antimicrobial substances have been including like organic acids (benzoic acid, sorbates), enzymes (lysozyme, glucose oxidase), bacteriocins (nisin, pediocin), fungicides (benomyl, imazalil), polymers (predominantly chitosan), natural extracts, antibiotics, triclosan, and silver compounds [10]. There are commercially available active food packaging systems such as those containing silver and triclosan as antimicrobial substances but their use in the food packaging industry is limited, mainly due to concerns about their applicability and safety [52, 198 from 10].

Examples of scientific studies on active agent delivery devices for food packaging applications are listed in Table 3 on the next page.

In most of the cited examples active compounds are incorporated into polymeric films that allow the active principle either to migrate into the food either to act on the food surface. Synthetic polymers derived from petroleum have thus far dominated the applications in antimicrobial food-packaging films (Polyethylene (PE), Polypropylene (PP), Polyethylene terephthalate (PET), Polystyrene (PS), Ethylene-vinyl acetate (EVA), among others) [10, 93].

TABLE 3. Overview of studies on active packaging systems for food applications

| Matrix | Bioactive compound | Application | References |
|---|---|---|---|
| Polyethylene | lactocin 705/lactocin AL705/nisin | inhibition of *Listeria* growth in ready-to-eat products | 118 |
| | synthetic peptide E14LKK | *E. coli* inhibition | 184 |
| | bacteriocin 32Y by *Lact. curvatus* | inhibition of *L. monocytogenes* growth during the storage of meat products | 120 |
| Polyethylene coated with hydroxypropyl methyl cellulose | nisin | *K. rhizophila* inhibition | 43 |
| Low-density polyethylene | benzoic anhydride | control of surface mould growth in foods such as cheese | 207 |
| | sodium benzoate | *B. subtilis* inhibition in foodstuffs (cheese, sausage, etc.) | 194 |
| | potassium sorbate | *B. subtilis* inhibition in foodstuffs (cheese, sausage, etc.) | 194, 80 |
| | sodium nitrite | *A. niger* and *B. subtilis* inhibition in foodstuffs (cheese, sausage, etc.) | 194 |
| | hexamethylenetetramine | improvement of orange juice and cooked ham shelf life | 53 |

| Matrix | Bioactive compound | Application | References |
|---|---|---|---|
| | nisin | inhibit microbial population during the storage of milk | 121 |
| Polyamide-coated low-density polyethylene | *trans*-cinnamaldehyde | antimicrobial activity in food products | 79 |
| Polyamide | allyl isothiocyanate | antimicrobial activity in food products | 108 |
| High density polyethylene | potassium sorbate | antimicrobial activity in food products | 80 |
| Polypropylene | potassium sorbate | antimicrobial activity in food products | 80 |
| Polyethylene terephthalate | sodium benzoate | *B. subtilis* inhibition in foodstuffs (cheese, sausage, etc.) | 194 |
| | sodium nitrite | *A. niger* and *B. subtilis* inhibition in foodstuffs (cheese, sausage, etc.) | 194 |
| | potassium sorbate | *B. subtilis* inhibition in foodstuffs (cheese, sausage, etc.) | 194, 80 |
| Polystyrene | sodium benzoate | *B. subtilis* inhibition in foodstuffs (cheese, sausage, etc.) | 194 |
| | sodium nitrite | *A. niger* and *B. subtilis* inhibition in foodstuffs (cheese, sausage, etc.) | 194 |

| Matrix | Bioactive compound | Application | References |
|---|---|---|---|
| | potassium sorbate | *B. subtilis* inhibition in foodstuffs (cheese, sausage, etc.) | 194 |
| Surface-modified polystyrene resin | synthetic peptide 6K8L | *E. coli* O157: H7, *L. monocytogenes*, *S. aureus*, *P. fluorescens*, and *K. marxianus* inhibition | 5 |
| Vinyl acetate-ethylene | nisin/α-tocopherol | inhibition of *M. flavus* growth and retardation lipid oxidation in the in milk cream | 104 |
| Polylactic acid | silver-based antimicrobial | inhibition of Gram-negative *Salmonella* spp. | 26 |
| Poly (maleic acid-co-olefine) | sodium benzoate | *B. subtilis* inhibition in foodstuffs (cheese, sausage, etc.) | 194 |
| | sodium nitrite | *A. niger* and *B. subtilis* inhibition in foodstuffs (cheese, sausage, etc.) | 194 |
| | potassium sorbate | *B. subtilis* inhibition in foodstuffs (cheese, sausage, etc.) | 194 |
| Poly(ethylene-co-methacrylate acid) | benzoic acid and sorbic acid | fungal growth inhibition (*A. niger* and *Penicillium* sp.) | 206 |
| Poly (vinyl alcohol) | lemongrass essential oils | *E. coli* and *S. aureus* inhibition | 105 |
| | lysozyme | *M. lysodeikticus* inhibition | 25 |

| Matrix | Bioactive compound | Application | References |
|---|---|---|---|
| Ethylene-vinyl alcohol | silver nitrate | inhibition of *L. monocytogenes* and *Salmonella spp.* in different food products | 132 |
| Cellulose | nisin | inhibition of pathogens (*Staphylococcus* sp. and psychrotrophic bacteria) growth in cheese (sliced mozzarella) and ham sliced | 149, 163 |
| | pimaricin | inhibition of moulds and yeasts in sliced mozzarella cheese | 149 |
| | lacticin 3147 | inhibition of pathogens growth in cheese and ham sliced | 163 |
| | pediocin | inhibition of *L. innocua* and *Salmonella* sp. growth in sliced ham | 160 |
| Cellophane | nisin | inhibition of the total aerobic bacteria growth in fresh veal meat | 74 |
| Cellulose acetate | lysozyme | *E. coli* inhibition | 70 |
| Solid wax paraffin | cinnamon oil | improve the bakery products shelf life | 154 |
| Chitosan | propionic acid | increase the processed meats shelf life | 139 |
| | acetic acid | increase the processed meats shelf life | 139 |

| Matrix | Bioactive compound | Application | References |
|---|---|---|---|
| | nisin | inhibiting growth of *S. aureus*, *L. monocytogenes* and *B. cereus* | 150 |
| | potassium sorbate | inhibiting growth of *S. aureus*, *L. monocytogenes* and *B. cereus* | 150 |
| | garlic oil | inhibiting growth of *S. aureus*, *L. monocytogenes* and *B. cereus* | 150 |
| Alginate | enterocins | inhibition of *L. monocytogenes* growth in cooked ham | 116 |
| Galactomannan | extracts from *G. triacanthos* | antioxidant activity in food products | 33 |
| | nisin | inhibition of *L. monocytogenes* growth on Ricotta cheese | 117, 34 |
| Zein | thymol | inhibition of cells and spores of *B. cereus*, *C. lusitaniae* and *Pseudomonas* spp. | 133 |
| | lysozyme/chickpea albumin extract/BSA/disodium EDTA | inhibition of *E. coli* and *B. subtilis* growth and antioxidant activity | 69 |
| Soy protein | grape seed extract/nisin/EDTA | inhibition of *L. monocytogenes* growth in ready-to-eat food products | 176 |

| Matrix | Bioactive compound | Application | References |
|---|---|---|---|
| | grape seed extract/green tea extract/nisin | inhibition of *L. monocytogenes* growth in ready-to-eat meat pproducts (full fat turkey frankfurters) | 188 |
| *k*-Carrageenan | ovotransferrin/ EDTA | inhibition of total microbes and *E. coli* growth in fresh chicken breast | 168 |
| | potassium sorbate | yeast, mold and selective bacteria inhibition | 42 |
| Whey protein | oregano and garlic essential oils | inhibition of *S. aureus*, *S. enteritidis*, *L. monocytogenes*, *E. coli* and *L. plantarum* growth | 170 |
| | lysozyme | increase the smoked salmon shelf life | 131, 125 |
| | grape seed extract/nisin/malic acid/EDTA | inhibition of *L. monocytogenes*, *S. typhimurium* and *E. coli* O157:H7 in ready-to-eat poultry products (turkey frankfurter system) | 66 |
| | *p*-aminobenzoic acid/sorbic acid | inhibition of *L. monocytogenes*, *E. coli* O157:H7 and *Salmonella enterica* subsp. enterica serovar *Typhimurium* DT104 in sliced bologna and summer sausage | 28, 29 |
| Milk protein | oregano/pimento essential oils | increase the beef muscle slice shelf life | 140 |

| Matrix | Bioactive compound | Application | References |
|---|---|---|---|
| Apple puree | oregano, cinnamon, and lemongrass oils | inhibition of *E. coli* O157:H7 in fresh-cut fruit surfaces | 156 |

A number of coatings and edible films derived from biopolymers or chemically synthesized from bioderived polymers have also been studied for antimicrobial applications. Among the most used stand cellulose derivatives, alginate, wheat gluten, zein, beeswax, whey protein, chitosan, soy protein, etc [10]. Table 3 on page 24 also includes a number of polymers used in active devices for food packaging applications.

In the case of the pimaricin, antimicrobial studied in this work, several approaches to include it in packaging films to avoid mould spoilage have been reported. For example, chitosan-based edible films [59], wheat gluten and methyl cellulose biopolymers [192, 191] and polyethylene films coated with commercially available polyvinylchloride (PVC) lacquer coatings [81], whey protein films [148], alginate-based coatings [134], cellulose-based films [136].

However, thermosensitive nanohydrogels have never been assayed for this purpose.

## 1.3. Food nanotechnology

The National Nanotechnology Initiative (Arlington, VA, USA) defines nanotechnology as "the understanding and control of matter at dimensions of roughly 1-100 nm, where unique phenomena enable novel applications. Encompassing nanoscale science, engineering and technology, nanotechnology involves imaging, measuring, modelling, and manipulating matter at this length scale".

Nanotechnology has potential applications in all aspects of food chain including storage, quality monitoring, food processing, and food packaging. Nanotechnology applications in the food industry range from smart packaging to creation of on-demand interactive food that allows consumers to modify food, depending on the nutritional needs and tastes [131].

Nonetheless, many of the nanotechnological developments might be currently either too expensive or too impractical to implement on a commercial scale. For this reason, it is said that nanoscale techniques are most cost-effective in different sectors of the food

industry, such us development of new functional materials, food formulations, and food processing at microscale and nanoscale levels, product development, and storage.

Among the emerging applications of nanotechnology in the food industry are the following [15]:

- Bacteria identification and food-quality monitoring.
- Active and smart food packaging systems.
- Nanoencapsulation of bioactive food compounds (e.g. micelles, liposomes, nanoemulsions, biopolymeric nanoparticles).

Below are described some relevant general aspects of these three areas and Table 4 on the next page summarizes some particular promising nanotechnology applications for food and bioprocessing industries.

Quality assurance and safety of food and bioprocess industry is of utmost importance because consumers demand safe and wholesome food as well as governments impose stringent regulations to ensure food safety and feed hygiene. Sensors or systems for rapid detection of microbial contamination or spoilage of food components, for food quality control, and for abuse detection at source and during production chain is possible through nanotechnology [131].

The main purpose of food packaging is to increase food shelf life by avoiding spoilage, microbial contamination, or the loss of food nutrient. Nanotechnology offers higher hopes in food packaging by promising longer shelf life, safer packaging, better traceability of food products, and healthier food. Polymer nanocomposite technology holds the key to future advances in flexible, intelligent, and active packaging [131]. If so, nanotechnology can provide solutions for food packaging by modifying the permeation behaviour of foils, increasing barrier properties (mechanical, chemical, and microbial), providing antimicrobial properties, and by improving heat-resistance properties [21, 35].

TABLE 4. Promising nanotechnology applications for food and bioprocessing industries (based on Neethirajan and Jayas [131])

| Area | Technology | Description | Benefits | References |
|---|---|---|---|---|
| Food quality monitoring | nanosensors | electronic tongue sensitive to gases release during food processing | antimicrobial; health benefits; degradation detection during processing and storage | 158 |
| Bacteria identification | reflectve interferometry using nanotechnology | optical detection of biomolecules in complex mixtures | food quality assurance; detection of *E. coli* in foods | 85 |
| | silicon/gold nanorod array | fluorescent dyes are attached to antibodies that become visible under microbial contamination | food quality assurance; detection of *Salmonella* in foods | 64 |
| | nanoparticles that bind to cell surfaces | antibiotic-functioning nanocarbohydrate particles | detection and elimination of *C. jejuni* through the animal's feces | 186 |
| | nano bioluminescent spray | reacts with the pathogens on food producing a visual glow | detection of food-related pathogens (*Salmonella* and *E. coli*) | 91 |
| | biofunctional magnetic nanoparticle | bioluminescence detection of immobilized bacteria | detection of *E. coli* in pasteurized milk | 41 |
| | antibody-conjugated silica fluorescent nanoparticles | immunoassay for in situ pathogen quantification | pathogenic bacteria detection such as *E. coli* O157:H7 | 224 |

| Area | Technology | Description | Benefits | References |
|---|---|---|---|---|
| Antimicrobial packaging | nanoscale dirt repelent coating | | self- cleaning surfaces; barrier properties | 130 |
| | antimicrobial nanoparticles | silver oxide and zinc oxide nanoparticles | antimicrobial (*S. aureus* and *E. coli* inhibition); health benefits | 181, 94 |
| | electrospun blend nanofibers from chitosan | the addition of poly(ethylene oxide) allows to obtain fibers from chitosan to use as food packaging | provides naturly antimicrobial properties | 100 |
| Improved food storage | polymers bonded with nanocrystals | the material works by introducing nanocrystals into the plastic that essentially create a maze from which oxygen molecules find it difficult to escape | increase the shelf life in packaged beverages (beer, fruit juice and soft drinks) | 209 |

| Area | Technology | Description | Benefits | References |
|---|---|---|---|---|
| | biodegradable bio-nanocomposites made from natural biopolymers | bio-nanocomposites prepared with starch and protein using a melt intercalation or a solvent intercalation method | enhanced organoleptic characteristics of food, such as appearance, odor, and flavor; extended shelf life and improved quality of usually non-packaged items | 223 |
| | | bio-nanocomposites prepared with biodegradable polyesters (polyhydroxyalkanoates, poly(lactic acid), etc.) | improve stiffness, permeability, crystallinity and thermal stability of food packaging | 16 |
| | encapsulation of a phase changing material in a biopolymeric matrix using the electrospinning technique | dodecane nanoencapsulation into a zein matrix | development of new smart packaging materials with the ability to maintain temperature control in the cold chain | 147 |

| Area | Technology | Description | Benefits | References |
|---|---|---|---|---|
| Tracking, tracing, and brand protection | invisible nanobarcodes with batch information which can be encrypted directly onto the food products and packaging | use a scanning probe molecule-coated tip to deposit a chemically engineered ink material to create nanolithographic pattern onto the food surface (Dip Pen Nanolithography) | offers food safety by allowing the brand owners to monitor their supply chains without having to share company information to distributors and wholesalers | 221 |
| | | nanodisks of gold functionalized with dye molecules that emit a unique light spectrum when illuminated with a laser beam | DNA detection and as tags for tracking food products. | 129 |
| | | nanobarcode detection system that fluoresces under ultraviolet light in a combination of color that can be read by a computer scanner | pathogen detection in food and biological samples | 107 |
| Encapsulation and delivery | nanoencapsulation of bioactive substances | encapsulation of tuna fish oil (source of omega-3 fatty acids) | taste masking; targeted delivery of nutrients; protection from degradation of bread | 131 |

| Area | Technology | Description | Benefits | References |
|---|---|---|---|---|
| | nanoncapsulation with calcium alginate | encapsulation of live probiotic species | improve the yogurt as a therapeutic functional food. | 95 |
| | nanoncapsulation with starch by spray coating | encapsulation of bifidobacteria | protection and controlled release | 137 |
| | nanoencapsulaton of supplements | encapsulation of lycopene (antioxidant from tomato) | protection from degradation during processing | 8 |
| | nanoencapsulation and stabilization of hydrophobic nutraceutical substances on casein micelles | encapsulation of vitamin $D_2$ utilizing the natural self-assembly tendency of bovine caseins | enrichment of non-fat or low-fat food products | 167 |
| | active nanofibers prepared by electrospinning technique | encapsulation of β-carotene | stabilization of light sensitive added-value food components | 62 |
| | self-assembled nanotubes from α-lactalbumin | encapsulation of bioactive substances | protection of sensitive health-promoting ingredients | 72 |

Nanotechnology has also shown greater potential in improving the efficiency of delivery of nutraceuticals and bioactive compounds in functional foods to improve human health. Nanotechnology can enhance solubility, improve bioavailability, and protect the stability of micronutrients and bioactive compounds during processing, storage and distribution [38]. In addition, moisture-triggered controlled release, pH-triggered controlled release or consecutive delivery of multiple active ingredients might be implemented [171].

The size and the structure of food influence the functionality by providing the taste, texture, and stability properties. Nanotechnology can help in controlling the size and structure of food in order to adapt to that consumers want. Scaling down the size of food molecules to nanosized crystals creates more particles for an overall greater surface area. Smaller particles improve food's spreadability and stability, and permits to reduce extra stabilizers and thickeners to achieve a desirable food texture of emulsion based foods [68]. In this way, it is possible to develop healthier low-fat food products with desirable sensory properties; ingredients with improved properties or the removal of certain additives without loss of stability. The later includes, for example, removal of allergens such as peanut protein in emulsions, and in smart-aids for processing foods [131].

Nanotechnology can help food industries in providing authentication, and track and trace features of a food product for avoiding counterfeiting; preventing adulteration and diversion of products destined for a specific market.

**1.3.1. Nanomaterial's legal regulations.** Different countries are trying to include nanomaterials in their current regulations. Blasco and Picó [15] have listed The European Union legislation applicable to nanomaterials in food as follows:

- General for chemical compounds (REACH). European Community legislation concerned with chemicals and their safe use and dealing with the Registration, Evaluation, Authorisation and restriction of Chemical Substances.

- Novel foods regulation (Regulation (EC) No 258/97). Novel foods are foods and food ingredients that have not been used for human consumption to a significant degree in the EC before 15 May 1997, and the Regulation subjects all novel foods and foods manufactured using novel processes to a mandatory pre-market approval system. In January 2008, the European Commission published a proposal to revise and update the Novel Foods Regulation. Various proposals have been discussed by the Commission, Parliament and Council (The draft Regulation is currently going through the co-decision procedure). A definition of nanomaterials has been introduced at the request of the European Parliament, and supported by the Council. Discussions are continuing on how to bring nanotechnologies specifically into the revised Regulation.
- Food additives (Directive 89/107/EC and associated legislation). Only additives explicitly authorized may be used in food. In December 2008, a new Regulation was passed (Regulation EC/1333/2008), which set out a common authorization procedure for additives, enzymes and flavourings. From early 2010, a list of approved additives, including vitamins and minerals, came into force. The Commission on the basis of an Opinion from the EFSA decided inclusion of additives on the list. Those included often had limits set on their use, for example, restrictions on the quantities permitted for use. The new regulations also specify that, where the starting material used, or the process by which an additive is produced, is significantly different (for example, through a change in particle size), it must go through a fresh authorization process, including a new safety evaluation.
- Food supplements (Directive 2002/46/EC). States that only vitamins and minerals on an approved list may be used as food supplements. New substances may be considered for inclusion on the list, but only after a safety assessment by EFSA.

- Food-contact materials (Regulation EC/1935/2004). All materials those are intended to come into contact with foodstuffs, either directly or indirectly. The Commission or Member States may request the EFSA to conduct a safety evaluation of any substance or compound used in the manufacture of a food contact material. Certain materials, including plastics, are subject to additional measures. The Commission has proposed updating the Regulation governing food-contact plastics to specify that a deliberately-altered particle size should not be used, even behind a migration barrier, without specific authorization.

## 1.4. Smart nanohydrogels as active packaging

Hydrogels have been widely studied as drug delivery systems [19, 31, 96, 187] and they are defined as a three-dimensional network with flexible chains capable of imbibing high amounts of water (more than 90% wt.) [146]. Its hydrophilicity is due to the presence in its molecular structure of hydrophilic functional groups such as: OH, COOH, $CONH_2$, CONH, $SO_3H$, etc. Despite their high water absorbing affinity, hydrogels show a swelling behaviour instead of being dissolved in the aqueous surrounding environment due to existence of weak cohesive forces (such van der Waals forces and hydrogen bonds) and covalent or ionic bonds. The equilibrium state of the swollen hydrogel is the result of the balance between osmotic forces caused by water entering into the macromolecular network and cohesive forces exerted by macromolecular chains that make opposition to this expansion [97, 78].

In the presence of proper functional groups, hydrogels have the property of undergoing reversible volume phase transitions in response to environmental factors, such as temperature, ionic strength, and pH [6]. Temperature-sensitive (thermoresponsive) and pH-responsive have gained considerable attention due to their ability for repeated swelling–deswelling conversion in response to the environmental temperature [23, 55 from 78] or pH changes [145, 193, 169, 83, 20, 2, 63, 174, 175, 12 from 78], respectively.

**1.4.1. Volume phase transitions of hydrogels.** Many polymer systems in which the biomolecule release responds to different external stimuli have been developed, such polymers are known as "smart polymers". Most research works have been focused on the effect of pH and temperature, due to the importance of these variables on physiological, biological and chemical systems.

The transitions occurred in polymers owed to external stimulus, result from the competition between repulsive intermolecular forces, that act to expand the polymer network, and an attractive force that acts to shrink it. Ilmain et al. [89] described, as described below, the different types of interactions that take place in these volume phase transitions:

- *Van der Waals interaction*: Van der Waals interaction causes a phase transition in hydrophilic gels in mixed solvents, such as an acrylamide gel in an acetone–water mixture. Van der Waals forces are responsible for polymer-polymer affinity. Acetone, in this case is a bad non-polar solvent, which added to water increases the attractive interactions between molecules and causes the collapse of the gel. This transition is also observed near the threshold concentration by changing the temperature. At higher temperatures the gel swells and with a decrease the gel collapses.
- *Hydrophobic interaction*: because of its low solubility, the hydrophobic groups dissolution in water is generally associated with an increase in the free energy of the system ($\Delta G > 0$). This dissolution is slightly exothermic ($\Delta H < 0$) and hence the entropy of the system must decrease ($\Delta G = AH - T \cdot \Delta S$). This can be interpreted as a consequence of the greater degree of packing and order adopted by water molecules (hydration cell) around the dissolved hydrophobic molecules compared with the structure of pure water. This behaviour is called hydrophobic effect. When two hydrophobic groups interact to form an aggregate, the release from the hydration cell of some water molecules to free water was produced, causing an increase in system entropy ($\Delta S > 0$). Although heat is needed to

break the cell hydration ($\Delta H > 0$), the decrease in free energy of the system ($\Delta G < 0$) promotes the aggregation of hydrophobic molecules. This type of interaction is responsible of the phase transition of poly (*N*-isopropylacrylamide) gels, which swell at low temperature and collapse with increasing temperature. This type of temperature dependence is contrary to the Van der Waals interactions.

- *Hydrogen bonding*: A hydrogen bond is the attractive force between the hydrogen attached to an electronegative atom of one molecule and an electronegative atom of a different molecule. Usually the electronegative atom is O and N. Moreover, the hydrogen bond has a directional preference, i.e., requires a particular configuration of either a sequence located in the polymer (intrachain hydrogen bonding) or sequences of the polymer (interchain links).
- *Electrostatic interaction*: The electrostatic interaction is inversely proportional to the dielectric constant of the medium. In synthetic polymers can be introduced charges in the chain by copolymerization processes or partial ionization, resulting in a strong electrostatic repulsion in the system. As the charges cannot be displaced because they are attached to the chain, the counterions tend to be located near them to maintain the electroneutrality of the system. As a result, a Donnan potential is created inside and outside the hydrogel, overriding the internal osmotic pressure, so that the hydrogel swells.

In any case, we must to take into account that often will be more than one type of interaction responsible for the behaviour of the gel, although some predominate over the others [54].

**1.4.2. *N*-isopropylacrylamide based hydrogels.** *N*-isopropylacrylamide (NIPA) is a neutral monomer derived from acrylic acid resulting thermosensitive hydrogels. The fact of presenting hydrophilic amide groups and hydrophobic isopropyl side chain in makes poly (*N*-isopropylacrylamide) (PNIPA) (Figure 2 on the facing page) a polymer soluble in both, water at room temperature and in organic solvents of low polarity.

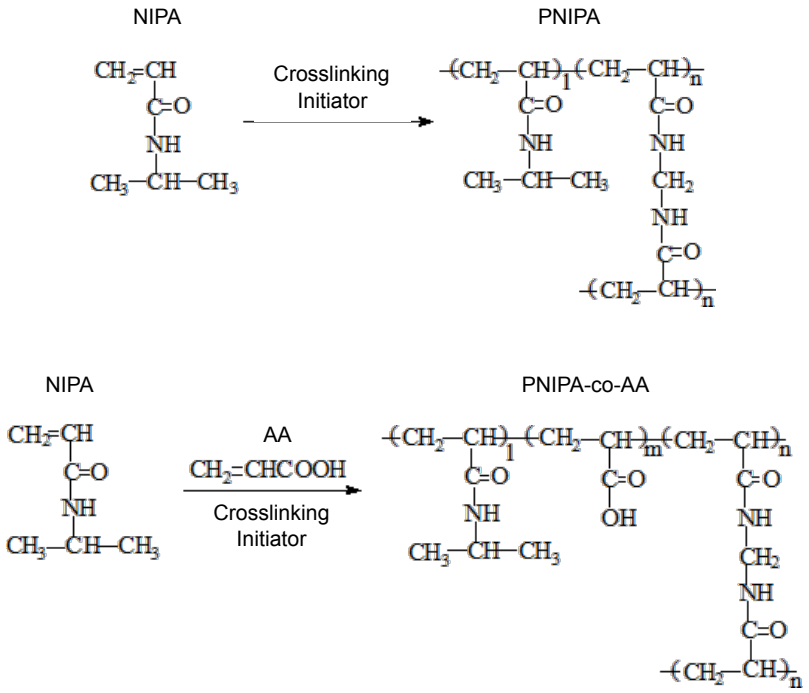


FIGURE 2. Poly (*N*-isopropylacrylamide) (PNIPA) and *N*-isopropylacrylamide copolymerized with acrylic acid (PNIPA-co-AA).

PNIPA hydrogels have a hydrophilic/hydrophobic balance in the side chains that will allow the formation of hydrogen bonds between water molecules and hydrophilic groups of the hydrogel. Below its lower critical solution temperature (LCST), the strong hydrogen bond between the hydrophilic groups and water exceeds the unfavourable free energy associated with exposure of hydrophobic groups to water, leading to good polymer solubility. As the temperature increases above the LCST, these interactions are destroyed and the hydrophobic interactions among the hydrophobic groups are strengthened dramatically and abruptly, which leads to the collapse of the polymer chains and thus the phase transition of the hydrogel network [164, 222, 45].

Since the collapse pattern can be easily modulated varying the polymer composition, the release behaviour can varies allowing a precise deliver control of the previously

loaded active principle. Thus, the addition of hydrophilic ionic comonomers, such as acrylic, methacrylic or itaconic acid to the PNIPA polymer led to an increase of the overall polymer hydrophilicity, strengthening polymer–water interactions and leading to an increase of the LCST [164, 45, 57, 124, 110]. Stile et al. [185] explained as hydrophilic AA tends to increase the LCST of PNIPA-co-AA polymers because the ionized -COO- groups are sufficiently soluble to counteract the aggregation of the hydrophobic temperature-sensitive elements. Also, the repulsion of the -COO- groups or the formation of hydrogen bonds between the amide groups in NIPAAm and the -COO- groups in AA may impede the collapse induced by the NIPAAm components, increasing the LCST. In addition appointed that the PNIPA-co-AA hydrogel exhibited a broader transition than the PNIPA hydrogel, indicating decreased swelling thermosensitivity, so copolymer hydrogels composed of NIPA and a more hydrophilic monomer have demonstrated decreased swelling thermosensitivity because the monomer prevents the formation of a compact shrunken structure.

PNIPA hydrogels have been widely investigated, in relation to its on/off behaviour, in biomedical applications and many other fields, such as in drug delivery systems [77, 13, 208, 189], immobilization of enzymes [40, 123] and gene carriers [86, 101]. However this type of hydrogels have not been studied for its application as active packaging of foods.

1.4.2.1. *N-isopropylacrylamide based nanohydrogels.* PNIPA nanohydrogel is a cross-linked polymeric network that swell to a particle size ranging from 10 to 1000 nm.

The techniques to synthesize nanoparticle can be divided into physical techniques, where the nanoparticles are obtained by mechanical division of the material; and chemical techniques, where the nanoparticles are obtained by nucleation and growth of precursor species [88]. Chemical techniques can be divided into:

- chemical co-precipitation
- electrochemical
- sonochemical
- sol-gel processing

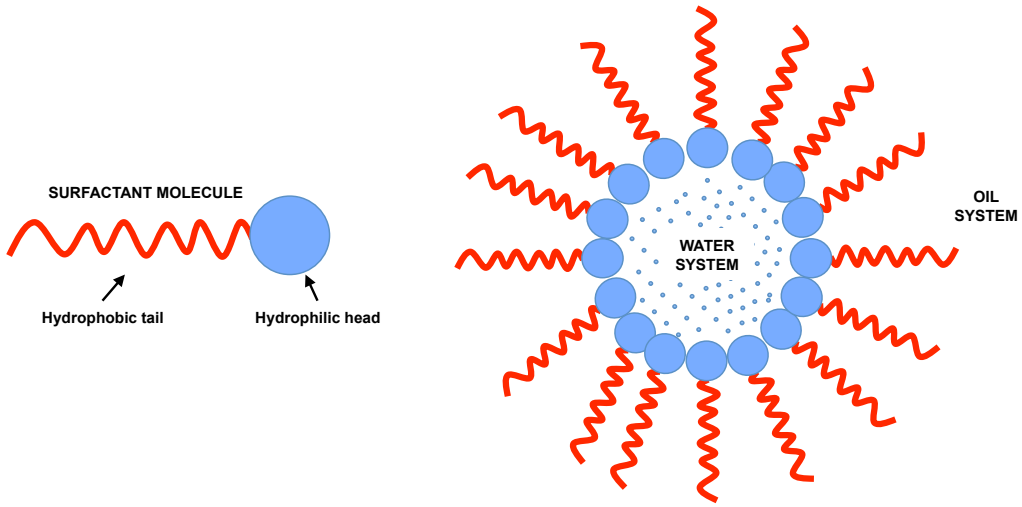


FIGURE 3. Diagram of micelles in inverse water-in-oil (W/O) microemulsions [58].

- microemulsions

All these techniques require the presence of a stabilizing agent in order to prevent aggregation of the resultant nanoparticles.

Microemulsions are isotropic, optically transparent, and thermodynamically stable dispersion systems consisting of water, oil, and suitable surfactants. Microemulsion polymerization can be divided into oil-in-water (direct), water-in-oil (reverse), and water-in-oil-in-water (double) according to the precursor microemulsions [58]. Water-in-oil (W/O) microemulsion polymerization (Figure 3) has been widely used to synthesize hydrogel nanoparticles of controlled size and shape [58, 76, 13, 14], due to their ability to mix reactants efficiently at the molecular level and enable the formation of shell and core structured nanocatalysts through sequential synthesis [88].

Since PNIPA nanohydrogels are biocompatible and non-toxic , is commonly used as carrier or deliver device in anticancer applications and therefore suitable for use in food. Furthermore nanohydrogels have the advantage of having the characteristics of hydrogels (flexibility, hydrophilicity, great capacity to absorb water) linked to the advantages of nanoparticles. Additionally the nanoscale and low hydrophobicity of PNIPA particles

is compatible with their oral ingestion because they have a low immune response and are able to glomerular filtration in kidney [203].

PNIPA nanohydrogels can be used to encapsulate functional ingredients with one or more targets functions such us protect them against degradation during food processing, storage and usage, carrying it to the site of action, and controlling its release as in active packaging. In this last application, nanoscale has several advantages which are, better dispersion of nanoparticles in the food packaging material and the possibility of controlling the release rate as a response to specific environmental conditions (for example, pH, ionic strength, or temperature).

Thermally sensitive and nontoxic poly(N-isopropylacrylamide) (PNIPA) hydrogels are widely used. Some applications include the controlled release of glucose and insulin [3] and 5-fluorouracil [13] in pharmaceutical applications as well as antifungals and macromolecules such as benzoic acid and its sodium salt [47], and bovine serum albumin [127, 226].

However applications within the food area are very scarce and practically limited to the encapsulation and controlled release of pimaricin [65], whose results are included in this thesis.

CHAPTER 2

# Physico-chemical characterization of poly (*N*-isopropylacrylamide) nanohydrogels for the pimaricin controlled release

In this chapter we study the physico-chemical characterization of poly (*N*-isopropylacrylamide) (PNIPA) nanohydrogels synthesized with different grades of hydrophilicity by adding acrylic acid (AA) as comonomer in order to gain a better understanding of the factors that influence the pimaricin release from PNIPA/AA nanohydrogels for further application in active food packaging.

## 2.1. Materials and Methods

**2.1.1. Materials.** *N*-isopropylacrylamide (NIPA) (99%, stabilized) was from Acros Organics (Geel, Belgium) and was used as received. Acrylic acid (stabilized with hydroquinone monomethyl ether) for synthesis, N,N´-methylenebisacrylamide (NMBA) for synthesis and sodium bisulfite ($NaHSO_3$) for analysis were from Merck (Darmstadt, Germany). Isoparaffinic synthetic hydrocarbon (98%, Isopar$^{TM}$ M) was from Esso Chemie (Cologne, Germany). Sorbitan sesquiolate (98%, Span$^{TM}$ 83) and PEG-40 sorbitol hexaoleate (98%, Atlas$^{TM}$ G-1086) were from Uniquema (Wilmington, DE, USA). Clorophorm stabilized with ethanol and diethyl ether (stabilized with ~6 ppm of BHT) were from Panreac (Barcelona, Spain).

**2.1.2. Synthesis of PNIPA/AA nanohydrogels.** The microemulsion polymerization experiments were conducted in water-in-oil (W/O) systems. The W/O microemulsion composition was 58% aqueous phase (AP), 17% oil phase (OP) and 25% surfactant (ST).

TABLE 5. Composition of the PNIPA/AA nanohydrogels

| Nomenclature | $m_{PNIPA}/m_{monomer}$ | $m_{AA}/m_{monomer}$ | $m_{CL}/m_{monomer}$ |
|---|---|---|---|
| PNIPA(3) | 1.00 | 0.00 | 0.03 |
| PNIPA(5) | 1.00 | 0.00 | 0.05 |
| PNIPA-5AA(3) | 0.95 | 0.05 | 0.03 |
| PNIPA-5AA(5) | 0.95 | 0.05 | 0.05 |
| PNIPA-10AA(3) | 0.90 | 0.10 | 0.03 |
| PNIPA-10AA(5) | 0.90 | 0.10 | 0.05 |
| PNIPA-20AA(3) | 0.80 | 0.20 | 0.03 |
| PNIPA-20AA(5) | 0.80 | 0.20 | 0.05 |

NIPA: N-isopropilacrylamide
AA: acrylic acid
CL: cross-linking (N,N'-methylenebisacrylamide)

The AP consisted of 80% water and 20% monomers. Mass ratios of NIPA to AA based on the monomers are showed in the Table 5. To preserve the shape and size of the particles during handling we used NMBA as cross-linking agent (CL) in the proportions indicated in Table 5. The OP consisted entirely of Isopar™ M, which was mixed directly with surfactants (ST) Atlas™ G-1086 ($m_{Atlas\ G\text{-}1086}/m_{ST}$ = 0.97) and Span™ 83 ($m_{Span\ 83}/m_{ST}$ = 0.03).

Both phases were solubilized then mixed in a 100 mL reactor thermostatized at 25 °C, equipped with mechanical stirring and a thermal sensor. To eliminate oxygen, 10 min before the polymerization began (by adding the initiator at a ratio $m_{NaHSO_3}/m_{monomer}$ = 0.01) and during the entire reaction, the reaction medium was purged by bubbling nitrogen through it. The polymerization conversion was monitored via the temperature increase inside the glass reactor. The polymer was purified using selective precipitation

with chloroform and diethyl ether. The pure polymer was dried overnight in an oven (50 °C) and then ground in a colloid mill (IKA®-Werke GmbH & Co. KG, Staufen, Germany).

**2.1.3. Measurement of mean particle size and zeta potential.** Zeta potential (Zp) and mean particle size (Z-average) was analysed by a dynamic light scattering (DLS) measurement technique using Zetasizer Nano ZS (Malvern Instruments, Worcestershire, UK) at 25 °C. Nanohydrogel samples were prepared dispersing PNIPA powder in distilled water (0.5 mg $mL^{-1}$) by agitation during 3 hours at ambient temperature to allow a proper swelling of the nanoparticles. Each analysis was performed in triplicate.

**2.1.4. Measurement of gel phase transition temperature.** The phase transition phenomenon of the polymer suspensions (12.5 mg $mL^{-1}$) was examined by two methods:

- *Optical density (OD).* The phase transition was examined by measuring the OD of polymer suspensions at 500 nm using a spectrophotometer with a Peltier temperature control module (Beckman Coulter Inc., Brea, CA, USA) at temperature intervals from 15 to 50 °C with increments of 2 °C between each measurement.
- *Differential scanning calorimetry (DSC).* DSC scans (Micro DCS III, Seratam) of nanohydrogel suspensions were performed from 10 to 50 °C with the reference ampule containing distilled water. Scans were run at 0.25 °C $min^{-1}$.

**2.1.5. Statistical analysis.** The differences between the results were evaluated by analysis of variance (ANOVA) followed by Bonferroni post-tests for multiple comparisons using with GraphPad Prism™ 5 (GraphPad Software Inc., San Diego, CA, USA).

## 2.2. Results and Discussion

**2.2.1. Mean particle size and zeta potential.** Since the nanoparticles were allowed to swell for 3 h in the solvent, the Z-average values could be used as an indicator of their swelling properties; the swelling degree being a result of the balance between two opposite forces, the osmotic pressure, which tends to expand the gel, and the elasticity of the polymer, which acts to shrink the gel network. Elasticity is, in turn, strongly influenced

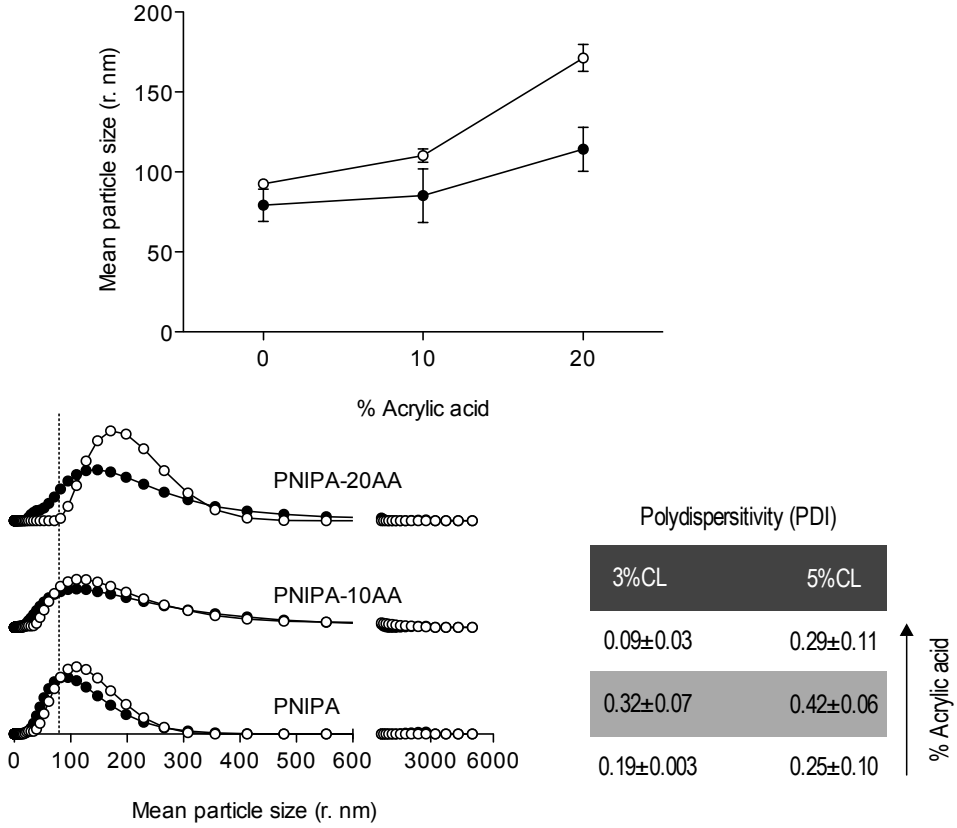


FIGURE 4. Mean particle size (Z-average) of PNIPA/AA nanohydrogels with 3% (○) and 5% (●) of cross-linking agent (CL), in distilled water at 25 °C.

by the cross-linking degree of the gel matrix. According to Otake et al. [138], Inomata et al. [90], Çaykara et al. [30], the increasing of cross-linking points in the gel matrix will arrest the formation of any hydration structure near the cosslinking points, which drecreases the volume changes assotiated with thermal transitions in PNIPA gels. Therefore, nanoparticles' rigidity is expected to increase as the CL-percentage is increased.

Figure 4 shows the Z-average values for nanohydrogel particles synthetized with different percentages of AA and CL. A polydispersity index (PDI) of 1 indicates large variations in particle size; a reported value of 0 means that size variation is absent. Z-average of PNIPA/AA nanohydrogels synthesized ranged from 79 to 171 nm with a PDI

below 0.5. Thus, the PDI values indicate limited variation in particle size, especially for the less cross-linked nanohydrogel without acrylic acid (PNIPA(3)).

In accordance with the theory [138, 90, 30] and previous reports [217, 114, 109], 3% CL gels resulted more elastic than 5% CL gels for all the conditions studied. In addition, both for 3% and 5% CL nanoparticles, the higher the AA content, the higher the Z-average (i.e., higher elasticity), which could be due to the increase in repulsive interactions between moieties with charges of the same sign. In addition, the osmotic pressure by counter ions would also contribute to the expanding force giving a more swelled nanoparticle [106]. On the other hand, this behaviour is more intense in 3% CL gels, which at 20% AA shows a size increment relative to the gel size at 0% AA equal to 1.3-fold the increment for 5% CL gels. In this case, a simultaneous increase in the AA-content and the CL-degree might have produced a higher attractive interaction between AA and NIPA chains, yielding a more rigid structure .

A two-way ANOVA analysis ($\alpha = 0.05$ for a 95% confidence) of the Z-average variation shows that both CL-percentage and AA-content effects were statistically significant ($p < 0.0001$). More over, the interaction of these two factors was also significant ($p = 0.0093$), i.e., the CL effect on Z-average changed as a function of the AA-content. So, swelling degree differences between 3% and 5% CL nanoparticles become higher as the AA-content increases.

With regard to the Zp results, the effect of the CL-degree is significant only ($p < 0.01$) for the PNIPA homopolymers (Figure 5 on the next page). PNIPA(5) is more negatively charged than PNIPA(3) gels, despite neither of them having ionized groups. The bottom of the Figure 5 shows that the PNIPA(5) nanohydrogel showed two Zp peaks, the first one close to neutrality, as expected for PNIPA, and the second one negatively charged. Since the cross-linker (NMBA) presents two carbonyl groups, the lower Zp value might be related to the number of exposed carbonyl oxygen atoms, which possess a partial negative charge due to the polarity of the carbon-oxygen bond.

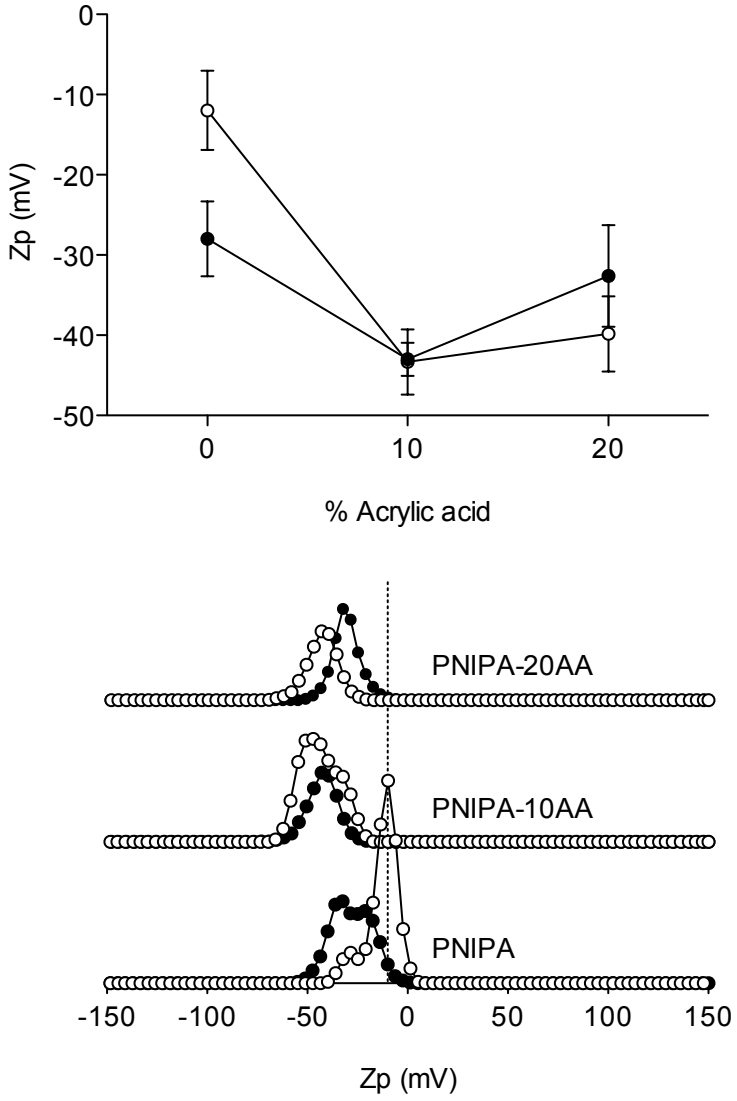


FIGURE 5. Zeta potential (Zp) of PNIPA/AA nanohydrogels with 3% (○) and 5% (●) of cross-linking agent (CL), in distilled water at 25 °C.

PNIPA copolimerized with AA (PNIPA-co-AA) nanohydrogels have always a lower Zp value than PNIPA nanohydrogels without AA. AA incorporation promoted a great increase in the surface charge of the nanohydrogels. In these cases, the contribution of the CL to

the surface charge is comparatively low and hence can be neglected. As a result, PNIPA-co-AA nanohydrogels showed a single Zp peak (botton of the Figure 5 on the facing page). On the other hand, there was a tendency to reduce the Zp value when the AA-content increased from 10 to 20 (top of the Figure 5 on the preceding page). Although, the Zp decrease was not significant ($p > 0.05$) in 3% CL nanohydrogel, the Zp change resulted significant for 5% CL nanohydrogels. This effect might be a consequence of two factors:

- Ionized carboxyl groups (-$COO^-$) of AA that provide negative charge to the polymer can interact among themselves trough hydrogen bonds or with the amide groups of NIPA. These interactions are benefited by increasing the CL-percentage since the polymeric matrix will be tighter and the reactants will be closer.

- According to the Hendersson-Hasselbach equation the pH of the PNIPA-co-AA suspensions will decrease when we increase the proportion of -$COO^-$ from the AA as in this case the suspension was not buffered. This diminution in pH causes the protonation of -$COO^-$ decreasing the surface charge (Zp) of the polymer.

### 2.2.2. Thermodynamic properties associated with the nanohydrogel collapse.

2.2.2.1. *Temperature-induced collapse.* The swelling/collapse behaviour is one of the most intensely studied aspects of hydrogels as these properties determine their efficiency as carriers in smart delivery systems. The thermally-induced collapse transitions are measured either spectroscopically or calorimetrically. However, from thermal transition curves, critical parameters such as the $T_m$ are often estimated using graphical methods, which do not provide confidence intervals and give little information on the physical changes accompanying the collapse.

Nonetheless, the simplicity of the collapse transition and its reversibility allow a detailed thermodynamical description of the collapse process by analogy to the Van't Hoff analysis of the unfolding of globular proteins .

A typical collapse curve is shown in Figure 6 on the following page. In this case the hydrogel collapse was monitored by measuring the molar absortivity, but any spectroscopic parameter can be used . To allow an easy comparison of nanohydrogels with

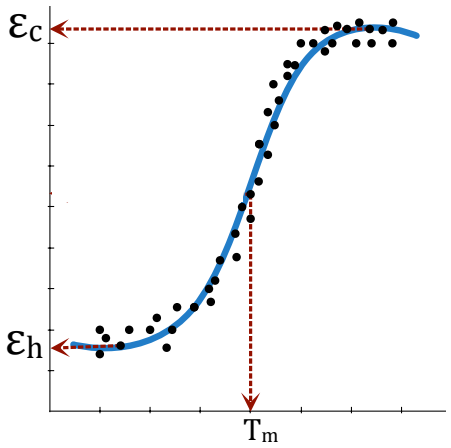


FIGURE 6. Typical collapse curve of a PNIPA nanohydrogel exposed to increasing temperatures. ε is the mean molar absortivity of the structural unit ($M^{-1}$ $cm^{-1}$) at collapsed state ($\varepsilon_c$) and swelled state ($\varepsilon_s$).

different molecular weights, we considered the mean molar absortivity of the repeating structural unit, which reports the molar absortivity for individual structural units instead of whole nanohydrogel molecules:

$$\varepsilon = \frac{A \cdot MMSU}{C \cdot l} \tag{1}$$

where ε is the mean molar absortivity of the structural unit ($M^{-1}$ $cm^{-1}$), $A$ is the absorbance at 500 nm, *MMSU* is the molecular mass of the structural unit (g $mol^{-1}$), $C$ is the nanohydrogel concentration (g $L^{-1}$) and $l$ is the optical path length (cm).

Values of ε characteristic of the swelled state ($\varepsilon_s$) and of the collapsed state ($\varepsilon_c$) can be obtained from the bottom and top plateaus of the curve. At any temperature ($T$) in the transition the hydrogel would be collapsed at a certain level. Assuming a simple two-state equilibrium , without stable collapsed intermediates ($Swelled \rightleftharpoons Collapsed$), a partially collapsed hydrogel is mathematically equivalent to considering the coexistence of a fraction of swelled hydrogels ($f_s$) in equilibrium with a fraction of collapsed hydrogels ($f_c$). Therefore, at any point in the collapse curve:

(2) $$\varepsilon = f_h \cdot \varepsilon_h + f_c \cdot \varepsilon_c$$

since, $f_h + f_c = 1$,

(3) $$\varepsilon = \varepsilon_h + f_c \left(\varepsilon_c - \varepsilon_h\right)$$

and the fraction of nanohydrogel collapsed at any point:

(4) $$f_c = \frac{\varepsilon - \varepsilon_h}{\varepsilon_c - \varepsilon_h}$$

Thus, the apparent equilibrium constant of collapse ($K_c$) is:

(5) $$K_c = \frac{[C]}{[H]} = \frac{f_c}{1 - f_c}$$

and from this equation,

(6) $$f_c = \frac{K_c}{1 + K_c}$$

On the other hand, at equilibrium (when $\triangle G = 0$), the standard free energy change ($\triangle G^o$) accompanying the collapse at a temperature $T$ is related to the equilibrium constant ($K_c$) between the swelled and the collapsed states by:

(7) $$\triangle G_T^o = -R \cdot T \cdot \ln K_c \Longrightarrow K_c = e^{-\frac{\triangle G_T^o}{RT}}$$

where $R$ is the gas constant (8.314 J $mol^{-1}$ $K^{-1}$) and $T$ is the absolute temperature (K). In addition, from the Gibbs free energy definition:

$$\triangle G_T^o = \triangle H_T^o - T \cdot \triangle S_T^o \tag{8}$$

where $\triangle H_T^o$ and $\triangle S_T^o$ are the enthalpy and entropy changes accompanying the collapse at temperature *T*.

When the hydrogel collapses (i.e., changes its thermodynamic state), a molar heat capacity change ($\triangle C_p$) is observed due to restructuring of the solvent molecules around exposed moieties of the hydrogel . Assuming that $\triangle C_p$ between the swelled and collapsed states of the gel is independent of the temperature in the experimental domain , the temperature dependences of $\triangle H_T^o$ and $\triangle S_T^o$ can be calculated according to the Kirchhoff's law:

$$\triangle H_T^o = \triangle H_m^o + \triangle C_p \left(T - T_m\right) \tag{9}$$

$$\triangle S_T^o = \triangle S_m^o + \triangle C_p \cdot \ln\left(\frac{T}{T_m}\right) \tag{10}$$

where $\triangle H_m^o$ and $\triangle S_m^o$ and are the enthalpy and entropy changes at the midpoint of the collapse transition (i.e., when $T = T_m$).

Substituting values of Equations 9 and 10 into Equation 8 we get:

$$\triangle G_T^o = \triangle H_m^o + \triangle C_p \left(T - T_m\right) - T \cdot \triangle S_m^o - T \cdot \triangle C_p \cdot \ln\left(\frac{T}{T_m}\right) \tag{11}$$

At $T = T_m$ we have the same concentration of swelled and collapsed gel, so $K_c = \frac{[C]}{[S]} = 1$ (from Equation 5 on the previous page), $\triangle G_{T=T_m}^o = -R \cdot T \cdot \ln K_c = -R \cdot T \cdot \ln 1 = 0$ (from Equation 7 on the preceding page), and $\triangle G_{T=T_m}^o = 0 = \triangle H_m^o - T_m \cdot \triangle S_m^o$ (from Equation 8).

Therefore $\triangle S_m^o = \frac{\triangle H_m^o}{T_m}$. Substituting $\triangle S_m^o$ into Equation 11 we get:

$$\triangle G_T^o = \triangle H_m^o \left(1 - \frac{T}{T_m}\right) + \triangle C_p \left[(T - T_m) - T \cdot \ln\left(\frac{T}{T_m}\right)\right] \tag{12}$$

Finally, rearranging Equations 3, 6, 7 and 12 one obtains:

$$\varepsilon = \varepsilon_c - \frac{\varepsilon_c - \varepsilon_s}{1 + e^{-\left(\frac{(T-T_m)(T_m \cdot \triangle C_p - \triangle H_m^o)}{R \cdot T \cdot T_m}\right)} \left(\frac{T}{T_m}\right)^{\frac{\triangle C_p}{R}}} \tag{13}$$

The results of fitting the experimental data of ε variation with temperature, depicted graphically in Figure 7 on the next page, show that homopolymer PNIPA nanohydrogels present a sharp volume phase transition while there is not well defined lower critical solution temperature (LCST) transition for the PNIPA-co-AA nanohydrogels. It has been demonstrated that physical properties such as LCST of PNIPA nanohydrogels can be modulated by copolymerization with hydrophilic monomers [57, 36]. Thus, hydrogen bonds between water and acrylic acid, in addition to those established with the PNIPA structure, will be form in PNIPA-co-AA nanohydrogels. As hydrophobic interactions are greatly responsible for the collapse of the nanohydrogel above the LCST, presence of acrylic acid might also affect the deswelling rate giving rise to a more hydrated collapse state. This stronger hydrogen bond interaction also have be suggested for Chen et al. [39] to explain this change in LCST behaviour with PNIPA-co-AA nanohydrogels. So the collapsing of polymer nanoparticles happens in higher temperature due to more energy is required to destroy the hydrogen bonds. This behaviour was also observed with other hydrophilic copolymers, so Milašinović et al. [124] observed a similar behaviour when increasing the hydrophilicity degree by increasing the percentage of itaconic acid. Thus, the LCST was situated on 34.2 °C for the PNIPA homopolymer with a sharp phase transition that became less pronounced for hydrogels with 5 and 10% of itaconic acid, and practically did not exist with 15% of itaconic acid.

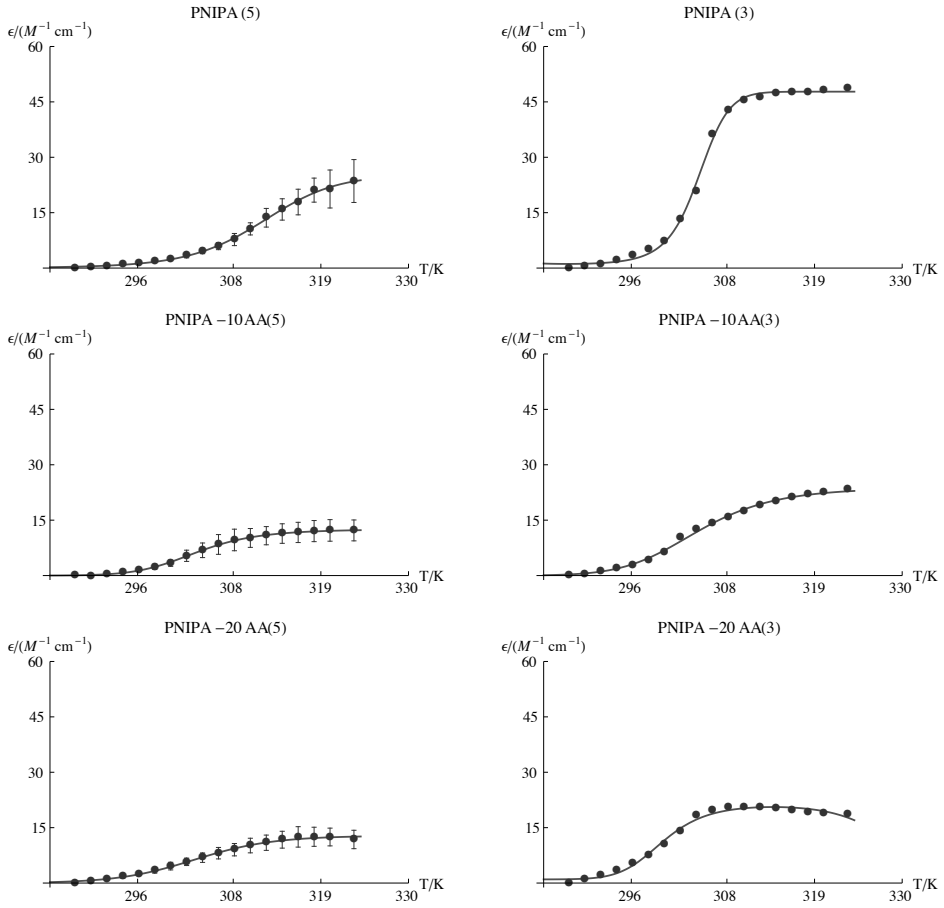


FIGURE 7. Variation of the mean molar absortivity (ε, $M^{-1}$ $cm^{-1}$) of the structural unit of PNIPA/AA nanohydrogel aqueous solutions (12.5 mg $mL^{-1}$), synthesized with 3% and 5% of cross-linking agent (CL), as function of temperature (T, K). The lines are the fitting curves generated from Equation 13 on the preceding page.

Respect to the CL effect, as we explained in Section 2.2.1, the nanohydrogels with low CL-percentages show higher variations between swelled and collapsed state due to its higher elasticity (Figure 7).

In addition, volume phase transition from swell to collapse state should be an endothermic process involving a greater transition heat due to the formation of hydrophobic interactions [138] and the disappearance of the polymer–water interactions [138, 46]. So

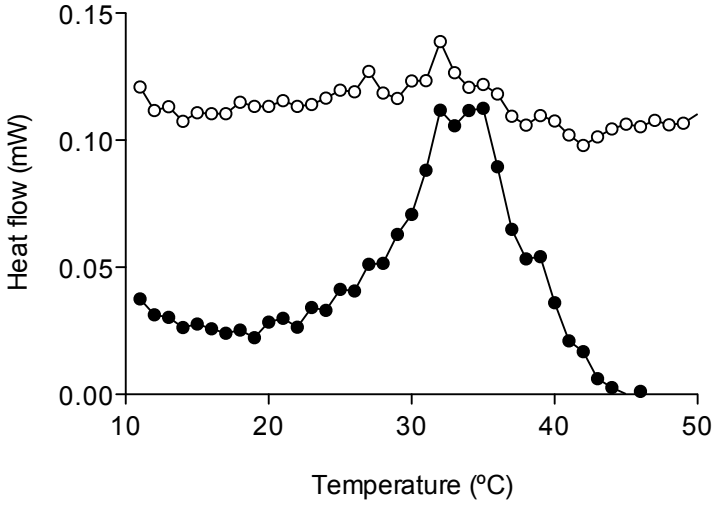


FIGURE 8. Differential scanning calorimetry (DSC) analysis of the nanohydrogel aqueous solutions (12.5 mg $mL^{-1}$) of PNIPA(5) (●) and PNIPA-20AA(5) (○) nanohydrogels.

the effect of the AA incorporation as comonomer in the NIPA polymer could be studied by DSC measurements. In the heat flow curve (Figure 8) of PNIPA homopolymer appears an endothermic peak, which could be attributed to its LCST (around 33 °C). However, DSC profile of PNIPA-20AA(5) polymer virtually no peak appears or is less intense, consistent with the results obtained with optical density measurements (Figure 7 on the facing page).

2.2.2.2. *Simultaneous temperature and pH-induced collapse.* In this case, the observed accompanying the collapse transition mediated by temperature and pH change would be the sum of two contributions, a free energy change due to a gel state change mediated by temperature (Equation 12 on page 57, and a free energy change due to a gel state change mediated by pH. Assuming that follows a profile similar to that associated with the temperature change:

$$\triangle G^o_{pH} = \triangle H^o_{pH_m}\left(1 - \frac{pH}{pH_m}\right) + \triangle C_p\left[(pH - pH_m) - pH \cdot \ln\left(\frac{pH}{pH_m}\right)\right] \tag{14}$$

where $\triangle H^o_{pH_m}$ and $\triangle S^o_{pH_m}$ are the enthalpy and entropy changes at the midpoint of the collapse transition (i.e., when $pH = pH_m$).

Thus, the overall $\triangle G^o$ would be:

$$\triangle GT^o_{T,pH} = \triangle G^o_T + \triangle G^o_{pH} \tag{15}$$

and Equation 7 on page 55 would become:

$$K_c = e^{-\frac{\triangle G^o_{T,pH}}{R \cdot T}} \tag{16}$$

Finally, rearranging Equations 3, 6, 12, 14, 15 and 16 one obtains:

$$\varepsilon = \varepsilon_h + \frac{\varepsilon_c - \varepsilon_h}{1+e^{\left(\frac{\triangle H^o_{T_m} + \triangle H^o_{pH_m} - \triangle H^o_{T_m}\left(\frac{T}{T_m}\right) - \triangle H^o_{pH_m}\left(\frac{pH}{pH_m}\right) + \triangle C_p((T-T_m)+(pH-pH_m))}{R \cdot T}\right)}} \cdot \frac{1}{\left(\frac{T}{T_m}\right)^{-\frac{\triangle C_p}{R}}\left(\frac{pH}{pH_m}\right)^{-\frac{\triangle C_p \cdot pH}{R \cdot T}}} \tag{17}$$

In Figure 9 on the next page the results of fitting the experimental data of ε variation with temperature and pH, after their fitting with Equation 17, showed how the response of the gels with or without acrylic to the temperature as a function of pH is very different. PNIPA-20AA(5) nanohydrogel is more swollen at high pHs where the temperature does practically not affect. As the pH lower the nanohydrogel collapses, i.e. OD increases, and also increases the influence of temperature. This occured until the nanohydrogel is sufficiently collapsed due to the effect of pH decreasing the effect of temperature again.

When the value of pH is increased above the $pK_a$ of AA (4.35), the ionization of its carboxylic group is occurred. This fact will affect the LCST since the ionized -$COO^-$ groups are even more hydrophilic, dissapearing the swelling transition phenomena of the hydrogel. However, in acidic media the carboxylic groups are not ionized, and can

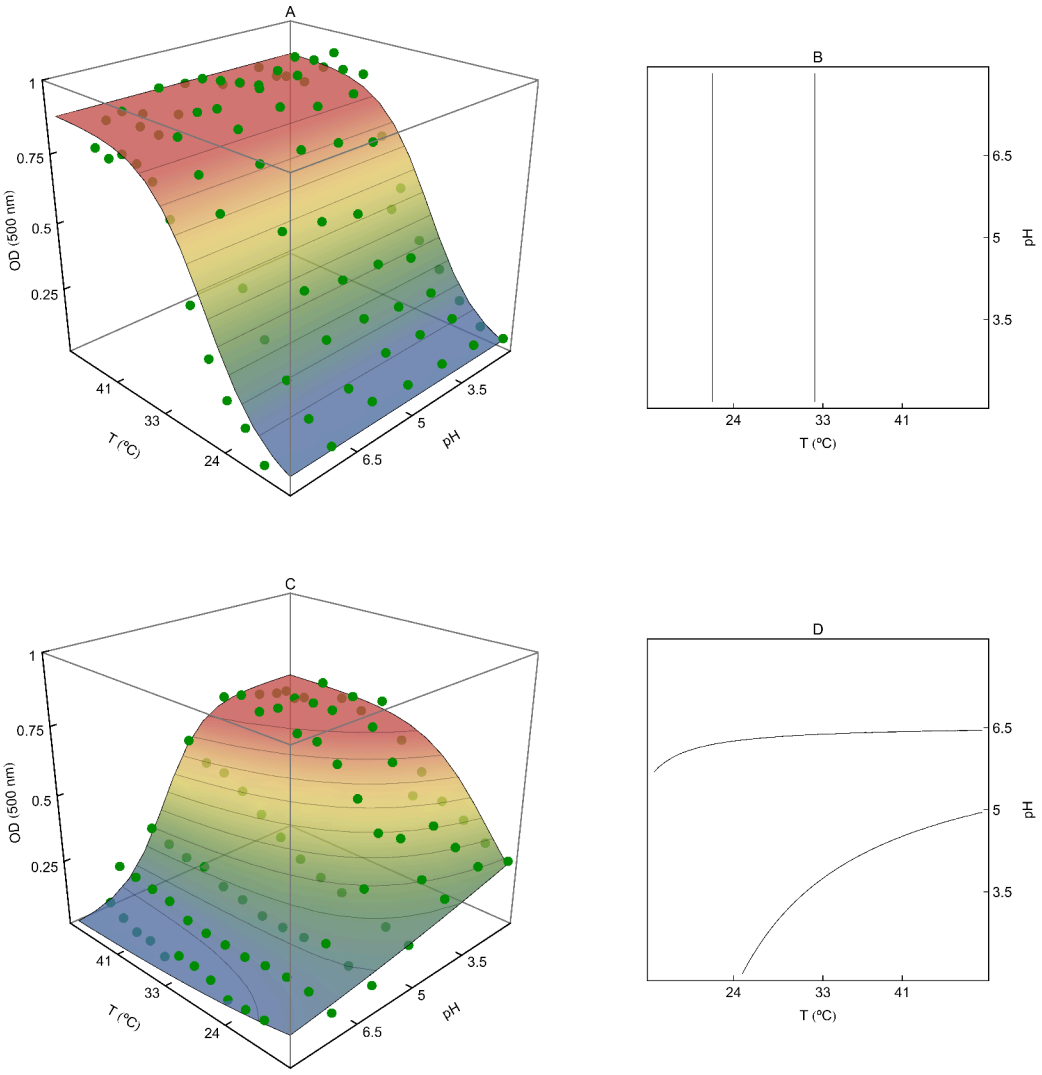


FIGURE 9. Variation of the mean molar absortivity (ε, $M^{-1}$ $cm^{-1}$) of the structural unit of PNIPA/AA nanohydrogel aqueous solutions (12.5 mg $mL^{-1}$), synthesized with 5% of cross-linking agent (CL), as function of temperatures (T, K) and pH. The surface represents the fitting of the experimental data with the Equation 17 on the facing page.

also take place an additional physical cross-linking resulting from the dimerization of the carboxylic groups by hydrogen bonds resulting in the collapse of the gel [37].

However the pH has no influence in PNIPA(5) nanohydrogel (Figure 9 on the previous page) because of the absence of ionizable groups in the homopolymer. Díez-Peña [54] refleted this bahaviour with PNIPA nanohydrogels copolymerized with methacrylic acid and Yoo et al. [220] in hydrogels of PNIPA copolymerized with AA.

2.2.2.3. *Simultaneous temperature and methanol-induced collapse.* Using the same assumptions as for the temperature and pH-induced collapse, the mean molar absortivity profile associated to a hydrogel collapse mediated by a change on temperature and methanol concentration would be:

$$\varepsilon = \varepsilon_h + \frac{\varepsilon_c - \varepsilon_h}{1+e^{\left(\frac{\triangle H^o_{T_m} + \triangle H^o_{MeOH_m} - \triangle H^o_{T_m}\left(\frac{T}{T_m}\right) - \triangle H^o_{MeOH_m}\left(\frac{MeOH}{MeOH_m}\right) + \triangle C_p((T-T_m)+(MeOH-MeOH_m))}{R\cdot T}\right)}} \cdot \frac{1}{\left(\frac{T}{T_m}\right)^{-\frac{\triangle C_p}{R}}\left(\frac{MeOH}{MeOH_m}\right)^{-\frac{\triangle C_p \cdot MeOH}{R\cdot T}}} \tag{18}$$

where *MeOH* is the methanol concentration and $MeOH_m$ is the methanol concentration at the midpoint of the collapse transition.

The variation of the ε as function of the volume fraction of methanol (v/v) and temperature after their fitting with Equation 18, is shown in Figure 10 on the next page. For both, pure PNIPA and PNIPA-co-AA, the nanohydrogel is more collapsed when the volume fraction of methanol (v/v) is around 0.4 and then reswelled on increasing the alcohol concentration further. In the same way that in the previous experiments, PNIPA-20AA(5) nanohydrogel shows similar behaviour to PNIPA(5) but the collapse is less intense.

This observed behaviour has been referenced in previous studies with PNIPA hydrogels where it was related with a phenomenon known as cononsolvency, i.e., pure water and pure alcohol are both good solvents for PNIPA but are not apparently for mixtures of the two over a certain concentration range [48]. This phenomenon of cononsolvency is produced by the formation of clathrate structures, consisting of water molecules which

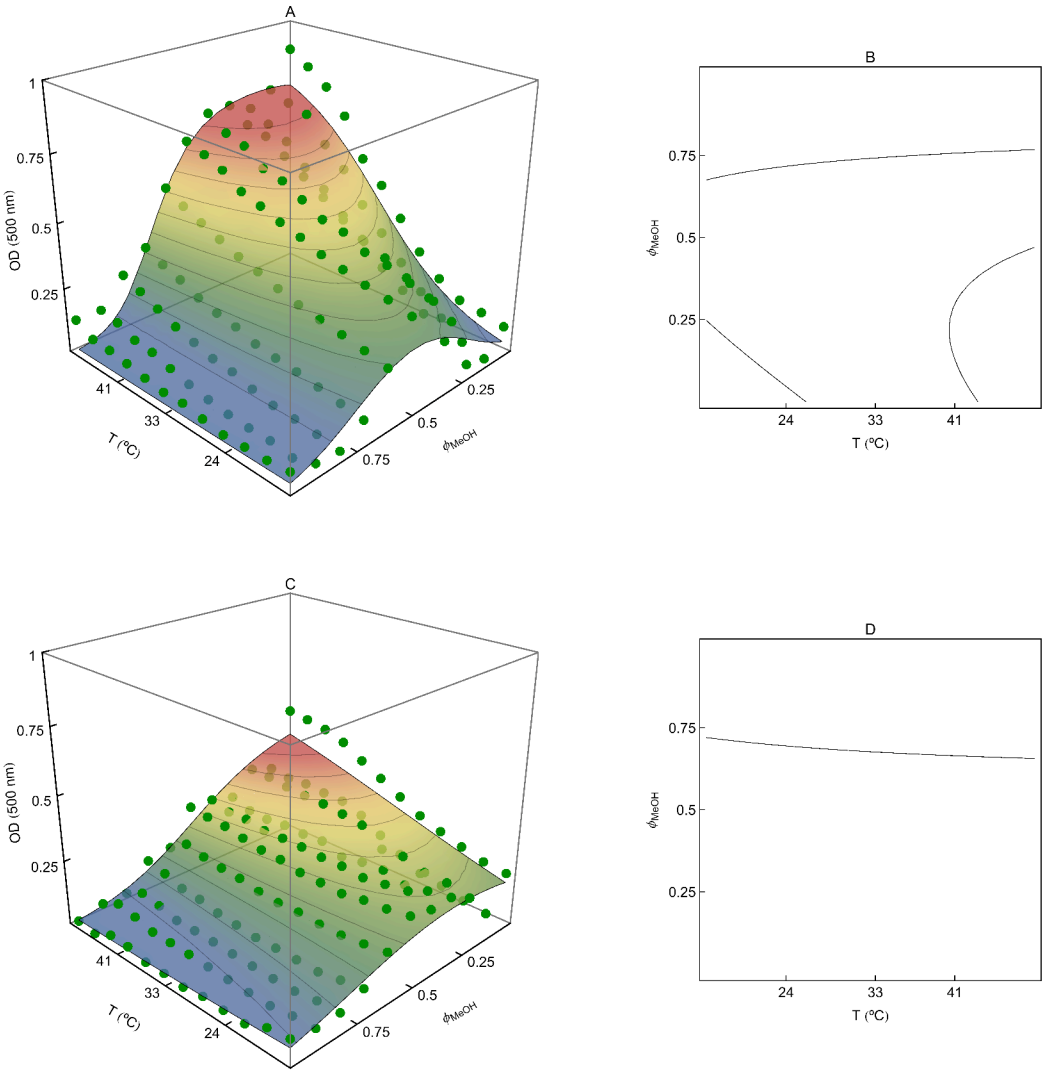


FIGURE 10. Variation of the mean molar absortivity (ε, $M^{-1}$ $cm^{-1}$) of the structural unit of PNIPA/AA nanohydrogel aqueous solutions (12.5 mg $mL^{-1}$), synthesized with 5% of cross-linking agent (CL), as function of volume fraction methanol (v/v) and temperature. The surface represents the fitting of the experimental data with the Equation 18 on the preceding page.

encapsulate alcohol molecules due to local ordering of the water structure [225, 161]. This clathrate structures are stable up to a critical ratio of alcohol to water (allways in the water-rich region) from which there is no longer water to provide clathrate structures and therefore the alcohol molecules may contact with another one [225], allowing the PNIPA nanohydrogel swelling.

CHAPTER 3

# Functional characterization of poly (*N*-isopropylacrylamide) nanohydrogels for the pimaricin controlled release

Once studied the physicochemical characteristics of the poly (*N*-isopropylacrylamide) (PNIPA) nanohydrogels synthesized with different grades of hydrophilicity by adding acrylic acid (AA) as comonomer (Chapter 2 on page 47), in the present chapter we are going to study their ability to transport and release pimaricin as function of nanohydrogel composition and ambient conditions in order to evaluate their possible applications in food packaging.

## 3.1. Materials and Methods

**3.1.1. Materials.** Commercial pimaricin (50% pure pimaricin, 50% lactose) was from VGP Pharmachem (Barcelona, Spain). Dialysis bags (SnakeSkin$^{TM}$ pleated dialysis tubing) with a molar mass cut-off of 3500 g mol$^{-1}$ were from Pierce (Rockford, IL, USA). The nanohydrogels employed inthis work were the same as those employed in Chapter 2 on page 47 (Table 5 on page 48).

**3.1.2. Preparation of pimaricin-loaded PNIPA/AA nanohydrogels.** PNIPA/AA nanohydrogel powder was dispersed in distilled water by agitation for 3 hours at ambient temperature to allow the nanoparticles to swell properly. This suspension was then mixed with a pimaricin water solution to obtain final concentrations of 12.5 mg of nanohydrogel per mL and 0.4 mg of commercial pimaricin per mL. The mixture was stirred overnight at 25 °C (below the LCST) to guarantee that the pimaricin was incorporated

into the nanohydrogel particles. This mixture was used in further release studies. A nanohydrogel sample without pimaricin was processed in the same conditions and used as a control.

For the studies of pimaricin loading efficiency in PNIPA/AA nanohydrogels employing methanol, pimaricin-loaded PNIPA/AA nanohydrogels were prepared in the same way as explained above but replacing distilled water by methanol as the solvent to swell the nanohydrogels and dissolve the pimaricin. After overnight incubation at 25 °C methanol was removed from pimaricin-loaded PNIPA/AA nanohydrogels sample by evaporation at 25 °C in a rotavapor until dryness. Dryed samples were resuspended in 3 mL of distilled water for subsequent loading efficiency studies.

**3.1.3. Pimaricin loading efficiency in PNIPA/AA nanohydrogels.** We evaluate pimaricin loading efficiency (E) in PNIPA/AA nanohydrogels employing different nanoparticle carriers: distilled water and methanol.

For loading efficiency studies, 3 mL of pimaricin-loaded nanohydrogel samples, obtained as explained in Section 3.1.2 on the previous page, were placed in a dialysis tube (3500 g $mol^{-1}$ MWCO) and dialyzed against 12 mL of distilled water at 25 °C under shaking. At intervals, 1 mL samples were withdrawn from the solution in order to follow the change in pimaricin concentration. The volume removed from the probe was returned after measurement. A nanohydrogel sample without pimaricin was processed in the same conditions as above and then used as control. The experiment was carried out in duplicate.

The amount of entrapped pimaricin was calculated following the method proposed by Chen et al. [39]. So E was defined as:

$$E = \frac{C_i - C_{max\,PNIPA-Pim\,25\,ºC}}{C_i} \tag{19}$$

where, $C_i$ is the pimaricin amount (μg) initially added to the nanohydrogel solution and $C_{max\ PNIPA\text{-}Pim\ 25\ ºC}$ is the maximum amount of pimaricin (μg) released from nanohydrogels at 25 °C.

To calculate $C_{max\ PNIPA\text{-}Pim\ 25\ ºC}$, experimental data were fitted according to the following equation, adapted from López et al. [111]:

(20)

$$C_{t\ PNIPA-Pim\ 25\,ºC} = C_{max\ PNIPA-Pim\ 25\,ºC} + (C_{0\ PNIPA-Pim\ 25\,ºC} - C_{max\ PNIPA-Pim\ 25\,ºC}) \cdot e^{-m \cdot t}$$

where, $C_{t\ PNIPA\text{-}Pim\ 25\ ºC}$ and $C_{0\ PNIPA\text{-}Pim\ 25\ ºC}$ are the pimaricin amount (μg) at time $t$ and $0$ respectively, released from the nanohydrogels through the dialysis membrane at 25 °C. The parameter $m$ ($min^{-1}$) is the maximum release rate and $t$ (min) is the sampling time.

Equation 20 is valid in the entire experimental domain, i.e., it is able to fit the pimaricin released at 25 °C in a time interval from $t_0$ (initial time) to $t_{eq}$ (equilibrium dialysis time).

**3.1.4. Pimaricin release from PNIPA/AA nanohydrogels.** For the release studies, 3 mL of pimaricin-loaded nanohydrogel samples, obtained as explained in Section 3.1.2 on page 65, were placed in a dialysis bag and dialyzed against 12 mL of distilled water at a constant temperature while agitating constantly. Samples of 1 mL were taken at intervals from the solution in order to determine the pimaricin concentration. The volume removed from the probe was returned after measurements had been made. A nanohydrogel sample without pimaricin was processed under the same conditions and used as a control. All experiments were carried out in duplicate. In order to determine the time required to reach dialysis equilibrium, a pimaricin solution (3 mL) with the same concentration loaded into the nanohydrogels (0.4 mg powder per mL) was dialyzed against 12 mL of distilled water, as indicated above.

**3.1.5. Pimaricin detection and quantification.** The pimaricin concentration in the dialysis media was determined spectrophotometrically at 319 nm (Beckman Coulter Inc., Brea, CA, USA). Pimaricin has maximum absorption at 304 nm; however, the suboptimal peak (90% of the maximum) observed at 319 nm showed the highest value for the pimaricin/dialyzed PNIPA absorbance ratio.

The molar absorption coefficient ($\varepsilon$) for pimaricin was extrapolated from the linear fit of the absorbance measurements of pure aqueous pimaricin solutions with known concentrations from 0.3 to 30 ppm (within the solubility limit). A value of 0.077±0.006 L $\mu g^{-1}$ $cm^{-1}$ was obtained.

**3.1.6. Statistical analysis.** Student's t-test ($\alpha$ = 0.05) was used to analise differences between two samples for a single variable. Two way analysis of variance (ANOVA) followed by Bonferroni post-tests was performed for multiple comparisons. Both analysis were performed by using GraphPad Prism™ 5 (GraphPad Software Inc., San Diego, CA, USA).

Fitting data were performed by using GraphPad Prism™ 5 (GraphPad Software Inc., San Diego, CA, USA). The significance of the model parameters was assessed with Mathematica 7 (Wolfram Research, Inc., Champaign, IL, USA).

## 3.2. Results and Discussion

**3.2.1. Pimaricin loading efficiency in PNIPA/AA nanohydrogels.** In order to asses the suitability of nanohydrogels as deliver device in active packaging it is relevant to determine their loading efficiency of the biomolecule. This functional property is influenced by the chemical composition of particles but also by the way (environmental variables) of performing the loading process, i.e., the contact time between the nanoparticles and the biomolecule.

3.2.1.1. *Effect of the cross-linking agent content, the incorporation time and the acrylic acid content.* Figure 11 on the facing page shows that E increases when we reduce the cross-linking agent (CL) content and increase the incorporation time (IT). Also the effect

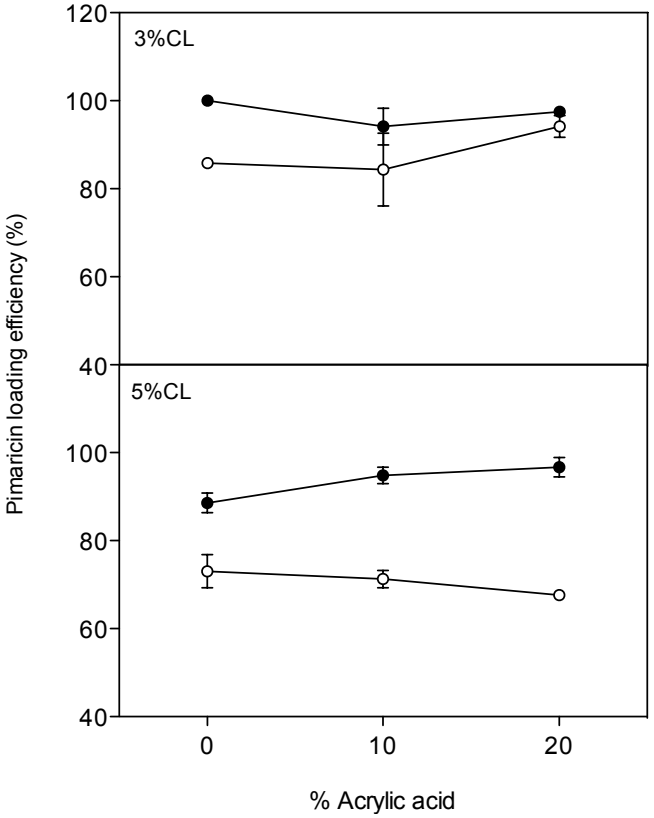


FIGURE 11. Pimaricin loading efficiency (E) in the PNIPA/AA nanohydrogels at 25 °C as function of the cross-linking agent (CL) content and the acrylic acid (AA) content, after 12 h (○) and 60h (●) of incorporation time (IT).

of IT in E seems to be more intense when we increase the CL-content. The ANOVA analysis at 95% confidence level of E shows that the interaction of the CL-percentage and the IT is significant ($p$ = 0.0004), not significant ($p$ = 0.1137) and significant ($p$ = 0.0033), for 0%AA, 10%AA and 20%AA, respectively. The absence of significance with 10% AA could be due to a high error in the experimental data with 3% CL.

In Chapter 2 on page 47 (Section 2.2.1 on page 49) we explained how the increase in the CL-content causes a decrease in the particle size (Z-average) for all the nanohydrogels studied. As the reduction in the Z-average cause a denser nanohydrogel matrix it could

prevent the pimaricin incorporation into the nanohydrogel. These results were consistent with those observed in another works with PNIPA hydrogels [208, 60].

Moreover the increase of the IT provides more time for the biomolecule to diffuse into the polymer matrix so the E increases. On the contrary, with 3% CL nanohydrogel matrix would be expected to be less dense. So the differences varying the IT are less pronounced and, therefore, 12 h re enough to obtain good values of E.

However the AA-content practically does not effect the E for both IT tested, suggesting that weak chemical interactions between pimaricin and nanohydrogel occurs. Only after 60 h of IT the AA-content influences the effect of CL-content in the E, leading to significant ($p < 0.05$) differences between nanohydrogels with 3% and 5% CL.

The ANOVA analysis supports the results above mentioned. Thus, at 95% confidence level of E shows that the effect of the AA-content is not significant ($p > 0.05$) for both 3% and 5% CL and also for 12 h and 60 h of IT. In contrast, the effect of CL-grade and IT in the E remains significant ($p < 0.05$) during all the analysis.

3.2.1.2. *Effect of solvent.* As observed in Chapter 2 on page 47 (Section 2.2.2.3 on page 62), the use methanol as solvent varies the swelling extent of the PNIPA nanohydrogel depending on the volume fraction of the alcohol employed. Accordingly, the presence of methanol should also influence the E.

However, although the E in methanol is lower than in water, there are no significative ($p > 0.05$) differences employing both solvents (Figure 12 on the next page). This results agrees with the fact that PNIPA nanohydrogel is always swelled in pure solvent, water or methanol (Figure 10 on page 63).

In the same way the ANOVA analysis at 95% confidence level of E shows that the effect of the solvent is not quite significant ($p = 0.0731$) and the effect of the AA-content is not significant ($p = 0.4020$). Also the interaction of these two factors is not significant ($p = 0.7775$), i.e., the type of solvent influenced the E independently from the AA-content.

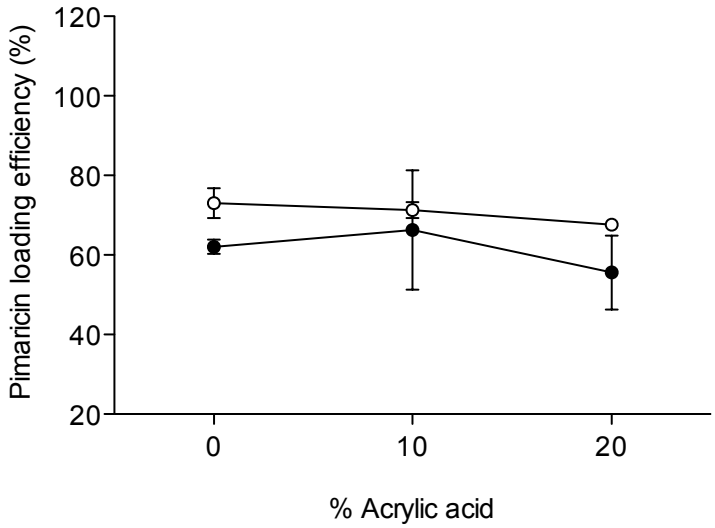


FIGURE 12. Pimaricin loading efficiency (E) in the PNIPA/AA nanohydrogels with 5% CL at 25 °C as function of the AA-content, in distilled water (○) and methanol (●).

**3.2.2. Pimaricin release from PNIPA/AA nanohydrogels.** Due to the experimental difficulties in separating the nanohydrogel from free pimaricin, we placed the loaded nanohydrogel in dialysis bags and determined the free pimaricin concentration over time in the dialysis media (distilled water). Therefore, during the release process, the pimaricin needed to diffuse through two release layers: the nanohydrogel matrix and the dialysis bag (Figure 13 on the next page).

The membrane of the dialysis bag could become a barrier to pimaricin molecules, either because they adhere to the membrane or because they form aggregates [183] that are larger than the pores of the dialysis bag. Therefore, we study the diffusion of free pimaricin through the dialysis bag. The results obtained (data not shown) indicate that diffusion continued until equilibrium was reached and that the dialysis bag did not influence the release of pimaricin. Hence, the free pimaricin transition to the release media would only be governed by the capacity of the molecule to diffuse at the tested temperature. However, all of the pimaricin that has been loaded could not be released

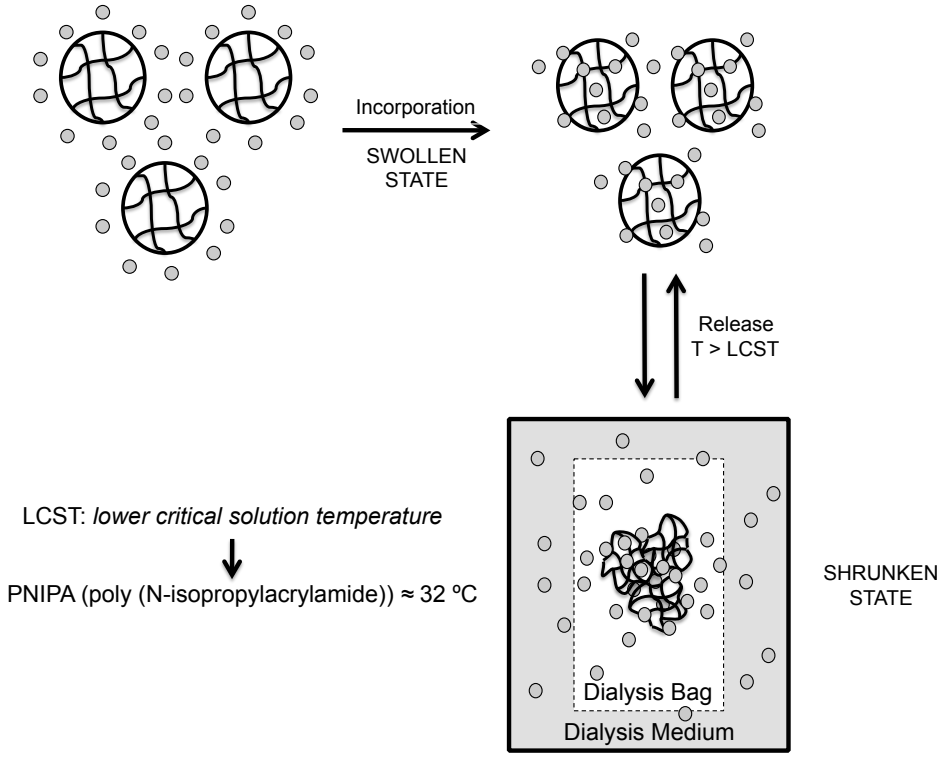


FIGURE 13. Scheme of pimaricin incorporation into PNIPA/AA nanohydrogels and release through the dialysis bag in distilled water.

in the dialysis process because the process stops when it reaches the equilibrium concentration. Thus, the amount of pimaricin released in the dialysis experiments with free pimaricin is considered to be the maximum amount of pimaricin released from the nanohydrogels.

Thus, the relative fraction of pimaricin released ($\gamma F_t$) is defined by the following expression:

$$\gamma F_t = \frac{C_{t\,PNIPA-Pim}}{C_{max\,Pim}} \tag{21}$$

where $C_{t\ PNIPA\text{-}Pim}$ is the amount of pimaricin (μg) released from the nanohydrogel to the dialysis medium (passing through the dialysis membrane) and $C_{max\ Pim}$ is the amount of pimaricin (μg) under the steady-state conditions determined in the dialysis experiments with free pimaricin (without nanohydrogel).

To calculate the maximum relative amount of pimaricin released ($\gamma F_{\max}$), experimental data are fitted according to the following equation, adapted from López et al. [111], in the same way that Equation 20 on page 67:

$$\gamma F_t = \gamma F_{max} + (\gamma F_0 - \gamma F_{max}) \cdot e^{(-m \cdot t)} \tag{22}$$

where $\gamma F_{\max}$ and $\gamma F_0$ are the maximum relative amount of pimaricin and initial relative amount of pimaricin respectively, released from the nanohydrogels through the dialysis membrane. The parameter $m$ ($min^{-1}$) is the maximum release rate and $t$ (min) is the sampling time.

Equation 22 is valid in the entire experimental domain, i.e., it is able to fit the pimaricin released in a time interval from $t_0$ (initial time) to $t_{eq}$ (equilibrium dialysis time). Considering that $\gamma F_{max} = \lim \gamma F_t$ when $t$ tends to infinity, the time needed to reach $\gamma F_{\max}$ would be infinity. For the sake of practicality, we decided to calculate $t_{eq}$ as the time to reach 99% of $\gamma F_{\max}$.

3.2.2.1. *Effect of the cross-linking agent content, the incorporation time and the acrylic acid content.* Figure 14 on the following page shows the effect of nanohydrogel composition on $\gamma F_{max}$ after different IT. The increasing of the IT resultes in the $\gamma F_{max}$ decrease for both 3% and 5% CL. These results are consistent with those obtained for pimaricin loading efficiency. They suggest that the increasing of E as consequence of higher IT (Figure 11 on page 69) will cause a deeper inclusion of pimaricin. So pimaricin remains more entrapped after 60 h of IT preventing its subsequent release. The ANOVA analysis at 95% confidence level of $\gamma F_{max}$ shows that the effect and the IT are extremely significant ($p < 0.0002$), for both 3 and 5% CL. Unlike the results obtained in the study of E the

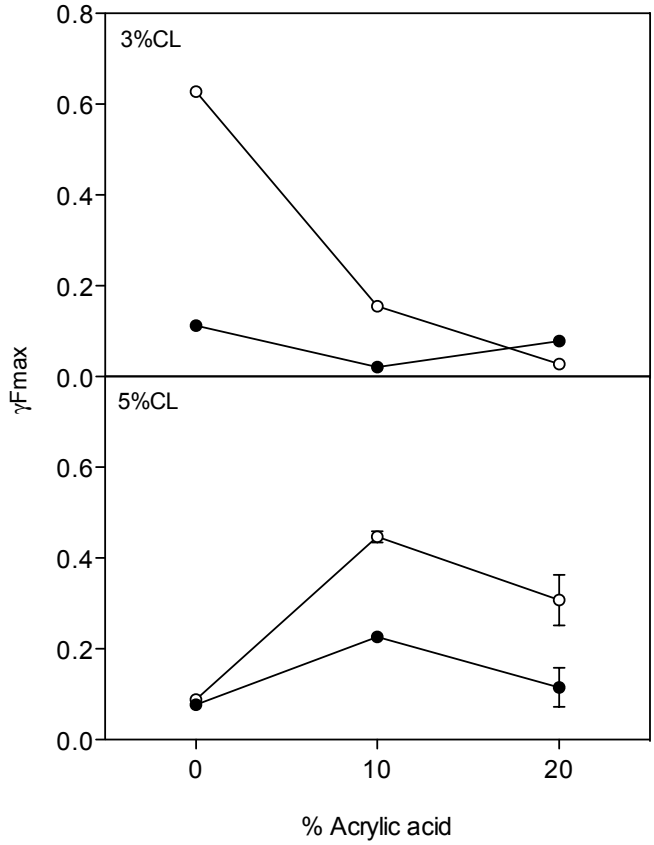


FIGURE 14. Variation of the maximum relative fraction of pimaricin released ($\gamma F_{max}$) from PNIPA/AA nanohydrogels through the dialysis bag of 3500 g $mol^{-1}$ in distilled water at 37 °C as function of the cross-linking agent (CL) content and the acrylic acid (AA) content, after 12 h (○) and 60 h (●) of incorporation time (IT).

ANOVA analysis at 95% confidence level of $\gamma F_{max}$ shows that the effect of the AA-content is now significant ($p < 0.0001$) for both 3 and 5% CL. It has been demonstrated that the introduction of AA in the PNIPA nanohydrogel can modulate the collapse grade (Figure 7 on page 58, Chapter 2). This fact greatly affects the biomolecule release.

Otherwise, the effect of the AA-content is very different depending on the CL-content in the PNIPA/AA nanohydrogel. $\gamma F_{max}$ decreases when the AA-content increases with 3% CL but the results obtained with 5% CL are just the opposite (Figure 14). Additionally,

the analysis of the effect of AA-content and the CL-grade together, at 12h of IT, shows that AA-content is extremely significant ($p < 0.0001$) and the effect of the CL-content is not significant ($p = 0.4735$). When we increased the IT the effect of the CL-content is now significant ($p = 0.0006$) and the effect of AA-content is not significant ($p = 0.1214$). However the interaction of these two factors (CL-content and AA-content) is extremely significant ($p < 0.0001$), i.e., the CL-grade influenced extremely the effect of AA-content in the $\gamma F_{max}$. Hence pimaricin release could be prevented by a greater degree of collapse due to a decrease in the CL-grade. In addition, AA-content and IT will play an important role in the collapse degree and loading efficiency, respectively, and consequently in the release.

The following sections will study in more detail the release profiles of pimaricin from nanohydrogels with different degrees of hydrophilicity.

**3.2.3. Pimaricin release from the PNIPA(5) nanohydrogel.** The most characteristic features of the release of pimaricin from PNIPA(5) were the strong burst effect associated with the pimaricin release curve of the pimaricin-loaded PNIPA(5) nanohydrogel and the plateau observed at around 10% release (Figure 15 on the following page).

Data derived from Equation 22 on page 73 (Table 6 on the following page) indicate that the maximum relative fraction of pimaricin released ($\gamma F_{\max}$) from the PNIPA(5) nanohydrogel at 37 °C was only 9%, and most of the antifungal remained trapped in the collapsed nanogel. The maximum release rate ($m$) was significantly higher ($p = 0.0335$) than that obtained in the dialysis experiments with free pimaricin (data not shown), and the time necessary to reach equilibrium was 0.13 times shorter.

It is well documented that at 37 °C (above the LCST) hydrophobic interactions among PNIPA chains strengthen dramatically (Section 1.4 on page 40, Chapter 1), which leads to the collapse of the polymer and the release of significant amounts of water [222, 87].

It has been reported that loaded molecules can become entrapped in the external part of PNIPA xerogels. Blanco et al. [13] found that methotrexate was released from PNIPA over 25 h with a burst effect of 71% at 15 min. It has been suggested that the

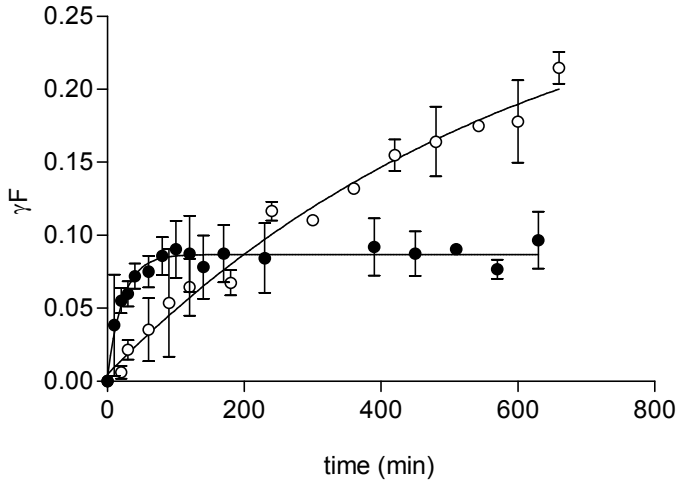


FIGURE 15. Relative fraction of pimaricin released ($\gamma F_t$) from the PNIPA(5) (●) and PNIPA-20AA(5) (○) nanohydrogels through the dialysis bag of 3500 g $mol^{-1}$ in distilled water at 37 °C. The lines are the fitting curves generated from Equation 22 on page 73 ($r^2_{PNIPA(5)}$ = 0.9693; $r^2_{PNIPA\text{-}20AA(5)}$ = 0.9833).

TABLE 6. Maximum relative fraction of pimaricin released ($\gamma F_{max}$) from the nanohydrogels, maximum release rate ($m$) and equilibrium dialysis time ($t_{eq}$) at 37 °C

| Nanohydrogel | $\gamma F_{max\ 37\ °C}$ | $m_{37\ °C}$ ($min^{-1}$) | $t_{eq\ 37\ °C}$ (h) |
|---|---|---|---|
| PNIPA(5) | 0.09±0.002[a] | 44.27x$10^{-3}$±5.76x$10^{-3}$[a] | 1.72 |
| PNIPA-20AA(5) | 0.31±0.06[b] | 1.62x$10^{-3}$±0.48x$10^{-3}$[b] | 47.31 |

Values reported are the means±standard deviation ($n$ = 2).

Different lower case letters in the same column indicate a statistically significant difference ($p$ < 0.05).

fast release of the externally entrapped methotrexate is the cause of the burst effect. The large size and hydrophobicity of the methotrexate incorporated into the nanohydrogel structure might contribute to slowing down their release at 37 °C. Zhang et al. [222]

have described similar effects with 5-Fluorouracil entrapped in PNIPA hydrogels. In this case, some of the drug became entrapped in the shrunken matrix due to the collapse of the polymer chains and gel volume shrinkage, which slowed down the drug release.

In addiction, pimaricin release from PNIPA nanohydrogels are greatly influenced by its high molecular weight following the same behaviour observed previously in the literature for the use of stimuli-sensitive hydrogels for the release of molecules with high molecular weight, as is the case of peptides and proteins [3, 208]. This behaviour is based on the assumption that in collapsed state, biomolecules can not be released to the release media, because they are trapped and could only be released by diffusion through the polymer in glassy state, which is a very slow process. In contrast, when the polymer matrix expands passes a rubbery state and takes place the biomolecule release that diffuses into the system formed by the solvent and the polymer [54].

We suggest that because pimaricin is larger (665.725 g $mol^{-1}$) than methotrexate (454.46 g $mol^{-1}$) and 5-Fluorouracil (130.08 g $mL^{-1}$) and also due to its amphiphilic nature, pimaricin could not be released from the PNIPA nanohydrogel (and/or the pimaricin was entrapped in the shrunken matrix). The burst effect at the beginning could be because the pimaricin was in a very exposed location within the nanohydrogel structure and so it could be released quickly when the water was expelled from the inside, coinciding with the collapse of the nanogel network.

**3.2.4. Pimaricin release from the PNIPA-20AA(5) nanohydrogel.** As explained in Section 1.4 on page 40 (Chapter 1), the physical properties (LCST) of PNIPA nanohydrogels can be modulated by copolymerization with hydrophilic monomers [164, 57, 124]. It is expected that adding AA will promote the formation of new hydrogen bonds with water. As explained above, PNIPA-20AA(5) nanoparticles are larger than PNIPA(5) nanoparticles because they are able to capture more water.

The release kinetic from the PNIPA-20AA(5) nanohydrogel showed a very different profile from that of the PNIPA(5) nanohydrogel (Figure 15 on the preceding page). There

was no burst effect, but rather the pimaricin was released steadily. According to Milašinović et al. [124], the absence of the initial burst suggests that the pimaricin is trapped in the nanogel structure, unlike the previous assayed nanogel in which significant amounts of pimaricin seem to remain exposed on the surface of the nanogel particles.

The maximum amount of pimaricin released from the PNIPA-20AA(5) nanohydrogel was also significantly higher ($p$ = 0.0309) than that released from the PNIPA(5) nanohydrogel (Table 6 on page 76), although it took a very long time to reach the steady state. The $m$ value was significantly lower than that obtained for the PNIPA(5) nanohydrogel ($p$ = 0.0272) and the dialysis experiments with free pimaricin ($p$ = 0.0087). This continuous efflux of pimaricin to the medium indicates that the PNIPA-20AA(5) nanohydrogel imposed less diffusional restrictions than PNIPA(5).

**3.2.5. Release modelling.** To describe the release profile and choose the parameters that help to describe and characterize the type of release, the early-time release data were fitted with different well-known mathematical models [13, 1, 73] as follows:

Zero-order kinetic model

$$\gamma F_t = k_0 \cdot t \tag{23}$$

First-order model

$$\gamma F_t = 1 - e^{k_1 \cdot t} \tag{24}$$

Higuchi model

$$\gamma F_t = k_H \cdot t^{1/2} \tag{25}$$

Hixson-Crowell cube root model

$$\gamma F_t = 1 - (1 - k_{H-C} \cdot t)^3 \tag{26}$$

Korsmeyer–Peppas model

$$\gamma F_t = k_{K-P} \cdot t^n \tag{27}$$

where, $\gamma F_t$ is the fraction of pimaricin released as already explained in Equation 3 on page 55. The terms $k_0$, $k_1$, $k_H$, $k_{H\text{-}C}$ and $k_{K\text{-}P}$ refer to the release kinetic constants obtained after fitting with zero-order, first-order, Higuchi, Hixson-Crowell cube root and Korsmeyer–Peppas models, respectively.

In all equations, $k$ is a constant that depends on the drug-polymer system characteristics, and $n$ is the diffusional exponent that depends on both the geometry of the delivery system and the physical mechanisms involved [152]. Thus, according to the $n$ value the release from a spherical particle can be catalogued into one of the following diffusion mechanisms [73]:

- $n \leq 0.43$: Fickian diffusion (Case I). Drug release is controlled only by diffusion into the release media.

- $n \geq 0.85$: Case II transport. Drug release is controlled by the collapse and swelling mechanism.

- $0.43 < n < 0.85$: Non-Fickian transport or anomalous transport. Drug release is controlled by both mechanism.

In general, the goodness of fit for the models investigated ranked in the following order: Korsmeyer-Peppas > Higuchi > first-order > Hixson-Crowell > zero-order (Table 7 on the following page). Thus, Korsmeyer-Peppas model was that best described the pimaricin release kinetics from nanohydrogels studied.

TABLE 7. Best-fit parameters of the kinetic models proposed (Equations 23- 10 on page 56) for pimaricin release from PNIPA nanohydrogels at 37 ºC

| Kinetic model | | PNIPA(5) | PNIPA-20AA(5) |
|---|---|---|---|
| zero-order | $k_0$ | $23.80\text{x}10^{-4}\pm3.14\text{x}10^{-4}$ ** | $3.50\text{x}10^{-4}\pm0.15\text{x}10^{-4}$ *** |
| | $r^2$ | 0.8186 | 0.9288 |
| first-order | $k_1$ | $24.64\text{x}10^{-4}\pm3.23\text{x}10^{-4}$ ** | $3.84\text{x}10^{-4}\pm0.15\text{x}10^{-4}$ *** |
| | $r^2$ | 0.8305 | 0.9469 |
| Higuchi | $k_H$ | $117.70\text{x}10^{-4}\pm3.98\text{x}10^{-4}$ *** | $70.64\text{x}10^{-4}\pm2.58\text{x}10^{-4}$ *** |
| | $r^2$ | 0.9875 | 0.9452 |
| Hixson-Crowell cube root | $k_{H\text{-}C}$ | $8.12\text{x}10^{-4}\pm1.07\text{x}10^{-4}$ ** | $1.24\text{x}10^{-4}\pm2.58\text{x}10^{-4}$ *** |
| | $r^2$ | 0.8266 | 0.9413 |
| Korsmeyer–Peppas | $k_{K\text{-}P}$ | $162.40\text{x}10^{-4}\pm34.60\text{x}10^{-4}$ * | $22.25\text{x}10^{-4}\pm5.65\text{x}10^{-4}$ ** |
| | $n$ | 0.40±0.07 * | 0.70±0.04 *** |
| | $r^2$ | 0.9941 | 0.9837 |

Values reported are the means±standard deviation ($n$ = 2).

n.s. ($p > 0.05$): not significant.

* ($p < 0.05$): significant.

** ($p < 0.01$): very significant.

*** ($p < 0.001$): extremely significant.

The values of diffusion exponent $n$ were very different for each drug-polymer system. The release mechanism from PNIPA(5) nanohydrogel was Fickian diffusion (Case I) and otherwise from PNIPA-20AA(5) nanohydrogel the release was classified as Non-Fickian transport. From these results, it can be assumed that the pimaricin released from the most hydrophobic nanohydrogel probably only corresponds to that encapsulated on the nanogel particle surface, which probably was thrown out by convective forces generated by the nanogel collapse and then was released by diffusion through the dialysis tube. In case of the hydrophilic nanohydrogel, as explained in as explained in the previous section, the pimaricin was released by diffusion from inside the polymer matrix, apparently with greater difficulty than when it remained in the polymer surface, leading to an increase in the diffusion coefficient value.

**3.2.6. Effect of temperature and pH on the release of pimaricin from nanohydrogels.** To clarify the processes involved in the release of pimaricin from nanohydrogels with and without AA, we conducted a new experiment in which the nanohydrogels were loaded with pimaricin at 25°C as in the previous assays and then used to obtain the different kinetic profiles by dialysis at 15, 25, 37 and 47 °C (Figure 16). In the same way, the effect of the pH was evaluated varying the pH of the release medium from 3 to 8 (Figure 17 on the next page). The effect of the pH was only evaluated in the release of pimaricin from nanohydrogels with AA since, as we saw in Section 2.2.2.2 on page 59 (Chapter 2).

As the temperature increased, the $\gamma F_{\max}$ value of the PNIPA-20AA(5) nanohydrogel increased up to a maximum and then decreased slightly. However, significantly less pimaricin was released from the PNIPA(5) nanohydrogel as the temperature increased (Figure 16 on the next page). Therefore, by plotting the maximum relative fractional release ($\gamma F_{\max}$) against temperature ($T$), it was possible to observe a well-defined optima, and thus the following second-order polynomial function was fitted with the experimental data:

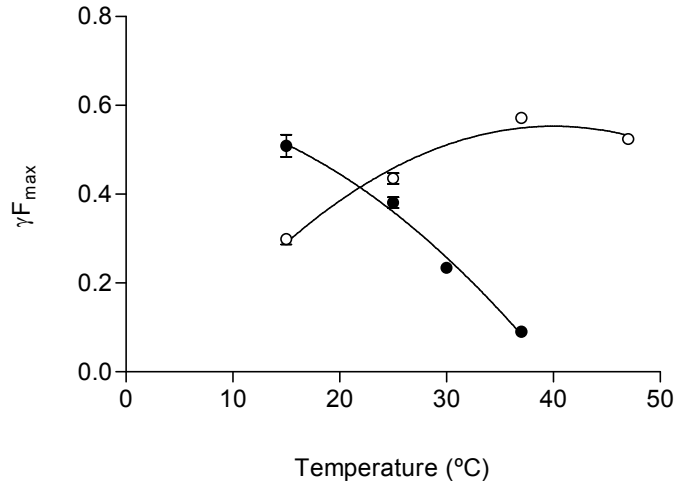


FIGURE 16. Variation of the maximum relative fraction of pimaricin released ($\gamma F_{max}$) from the PNIPA(5) (●) and PNIPA-20AA(5) (○) nanohydrogels through the dialysis bag of 3500 g mol$^{-1}$ in distilled water in relation to temperature. The lines are the fitting curves generated from Equation 28 on the facing page ($r^2_{PNIPA(5)}$ = 0.9896; $r^2_{PNIPA\text{-}20AA(5)}$ = 0.9725).

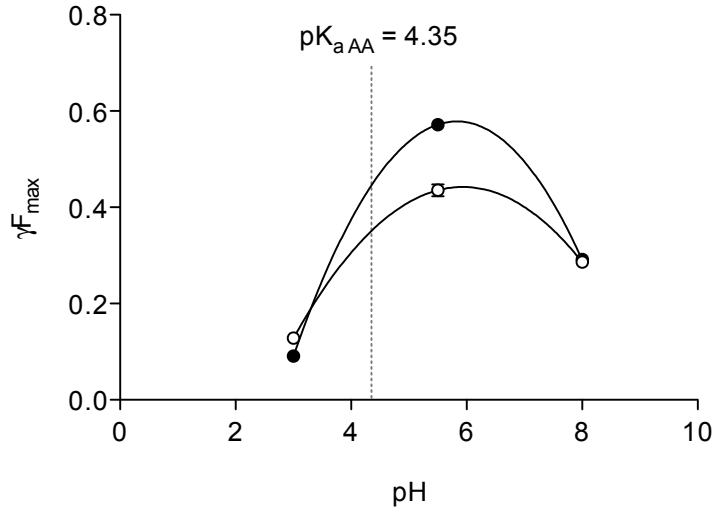


FIGURE 17. Variation of the maximum relative fraction of pimaricin released ($\gamma F_{max}$) from the PNIPA-20AA(5) nanohydrogels through the dialysis bag of 3500 g mol$^{-1}$ in distilled water at 25 ºC (○) and 37ºC (●) in relation to pH. The lines are the fitting curves generated from Equation 28 on the facing page ($r^2_{PNIPA(5)}$ = 1.0000; $r^2_{PNIPA\text{-}20AA(5)}$ = 1.0000).

(28) $$\gamma F_{max} = a_0 + a_1 \cdot T + a_2 \cdot T^2$$

By deriving the functions obtained in relation to the temperature and solving the roots of the resulting functions, the optimal temperature at which the largest amount of pimaricin was released was calculated to be 40.04 °C for the PNIPA-20AA(5) nanohydrogel and -1.25 °C for the PNIPA(5) nanohydrogel. This latter optimum temperature value is obviously located outside the experimental domain. Even so, the trend predicted by the model clearly indicates that for the PNIPA(5) nanohydrogel a decrease in temperature would lead to an increase in the amount of pimaricin released (Figure 16 on the facing page).

The observed behaviour could be interpreted as resulting from the temperature causing the nanohydrogel collapse in acordance with the nanohydrogel behaviour observed in Section 2.2.2 on page 53 (Chapter 2). Hydrophobic interactions are one of the main factors leading to the collapse of a nanohydrogel above the LCST [57]. The presence of AA might also affect the deswelling rate, and give rise to a more hydrated collapse state that facilitates the continuous diffusion of pimaricin to the medium. However, the collapse of the less hydrated PNIPA(5) nanohydrogel would be more intense, trapping pimaricin molecules within the shrunken matrix and aborting their release (Figure 16 on the facing page).

Respect to the pimaricin release from PNIPA-20AA(5) nanohydrogel was very different above and below the pKa of AA (Figure 17 on the preceding page). The effect is similar to that explained in the preceding paragraphs when we analysed the effect of temperature in the pimaricin release from PNIPA/AA nanohydrogels. As we saw in Section 2.2.2.2 on page 59 (Chapter 2), when we decrease the pH of the release medium the collapse of the PNIPA-co-AA was increased and therefore the pimaricin release was also increased. However above the $pK_a$ of the AA the nanohydrogel collase was too intense avoiding the pimaricin relase that remain trapped in its matrix. In the same way as in the study

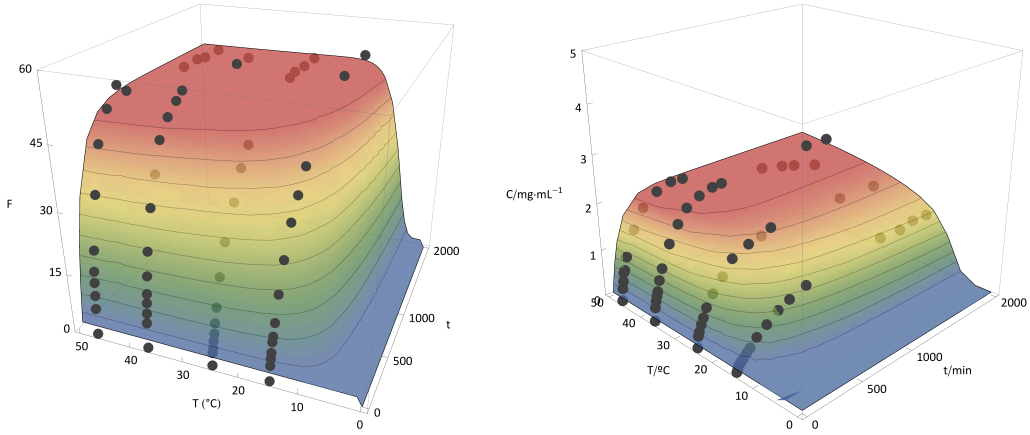


FIGURE 18. Variation of the concentration of pimaricin released ($C_t$) from a free pimaricin solution (A) and a pimaricin-loaded PNIPA-20AA(5) nanohydrogel supension (B) through the dialysis bag of 3500 g mol$^{-1}$ in distilled water in relation to temperature. The experimental data are represented as ●. The responsive surface are the fitting generated from Equation 30 on page 86 ($r^2_{\text{Pim (A)}}$ = 0.9940; $r^2_{\text{PNIPA-20AA(5)-Pim (B)}}$ = 0.9796).

of the effect of temperature, by plotting the maximum relative fractional release ($\gamma F_{\max}$) against pH ($T$), it was possible to observe a well-defined optima, and thus the following second-order polynomial function was fitted with the experimental data:

(29) $$\gamma F_{max} = a_0 + a_1 \cdot pH + a_2 \cdot pH^2$$

By deriving the functions obtained in relation to the pH and solving the roots of the resulting functions, the optimal pH at which the largest amount of pimaricin was released was calculated to be 5 for the PNIPA-20AA(5) nanohydrogel for both, 25 ºC and 37 ºC (Figure 17 on page 82).

In order to conduct a more complete study, we evaluated the combined effect of temperature and pH on the pimaricin release from the nanohydrogel with acrylic (PNIPA-20AA(5) throughout the time. That is why we developed an equation that allowed calculate the concentration of pimaricin ($C_t$) as function of time released through the dialysis

TABLE 8. Variation of the fitting parameters calculated with Equation 30 on the next page that allow calculate the concentration of pimaricin released ($C_t$) from a free pimaricin solution (Pim) and a pimaricin-loaded PNIPA-20AA(5) nanohydrogel supension (PNIPA-20AA(5)-Pim) through the dialysis bag of 3500 g mol$^{-1}$ in distilled water in relation to temperature

| Treatment | Pim | PNIPA-20AA(5)-Pim |
|---|---|---|
| $C_0$ | 0.179±0.058$^{**}$ | 0.063±0.055$^{n.s.}$ |
| $C_{max}$ | 4.110±0.136$^{***}$ | 2.445±0.153$^{***}$ |
| $m$ | 0.011±0.001$^{***}$ | 0.021±0.005$^{***}$ |
| $\alpha$ | -0.343±0.893$^{n.s.}$ | 7.957±1.935$^{***}$ |
| $\beta$ | 24.074±2.809$^{***}$ | 35.578±6.322$^{***}$ |

Values reported are the means±standard deviation ($n$ = 2).

$^{n.s.}$($p > 0.05$): not significant.

$^{*}$($p < 0.05$): significant.

$^{**}$($p < 0.01$): very significant.

$^{***}$($p < 0.001$): extremely significant.

tube from a free pimaricin solution and from a pimaricin-loaded nanohydrogel suspension. In this same work we also evaluated the maximum pimaricin released as function of the temperature of the release media. As the maximum concentration of pimaricin reached in the release media ($C_{max}$) and the release rate ($m$) is highly dependent of the temperature, we could calculate the $C_t$ at each sampling time and temperature in the grape juice in order to evaluate the specific inhibition:

$$C_t = C_{max} \cdot e^{-\frac{\alpha}{T}} + \left(C_0 - C_{max} \cdot e^{\frac{\alpha}{T}}\right) \cdot e^{-m \cdot e^{-\frac{\beta}{T}} \cdot t} \tag{30}$$

where $C_0$ is the initial concentration of pimaricin (μg $mL^{-1}$) in the release media. $t$ is the sampling time and $T$ the temperature.

The variation of the concentration of pimaricin in the release media with time as function of temperature in samples treated with free pimaricin and pimaricin-loaded PNIPA-20AA(5) nanohydrogel are represented in Figure 18 on page 84. When the pimaricin was free the $C_{max}$ achieved in the release media was the same for all temperatures as there was nothing that interfere in the pimaricin release this is why α is not significant ($p > 0.05$) (Table 8 on the previous page). However the parameter m is significant ($p < 0.001$) (Table 8 on the preceding page) as the release rate should change as funtion of the temperature as the diffusion of the molecules increased when the temperature increase. On the other hand, the $C_{max}$ is highly afected by the temperature (Table 8 on the previous page) as we saw in Section 2.2.2 on page 53 (Chapter 2) because of the effect of the nanohydrogel collapse. In any case the Equation 5 on page 55 provides a high degree of fit (Figure 18 on page 84) to experimental data that allows us to calculate the $C_t$ in the grape juice over bioassay taking into account the temperature change from 8 °C to 25 °C.

**3.2.7. Sustained Controlled Release.** After studying the different capacities of P-NIPA nanohydrogels to transport and release pimaricin when the temperature is increased above its LCST, we then alternated temperature cycles to determine whether or not this release is sustained over time. This is important because in the food industry it may be necessary to release the antifungal in various cycles.

Therefore, we analysed pimaricin release from nanohydrogels with stepwise temperature changes between 15 and 37 °C. The cumulative pimaricin release profiles as well as

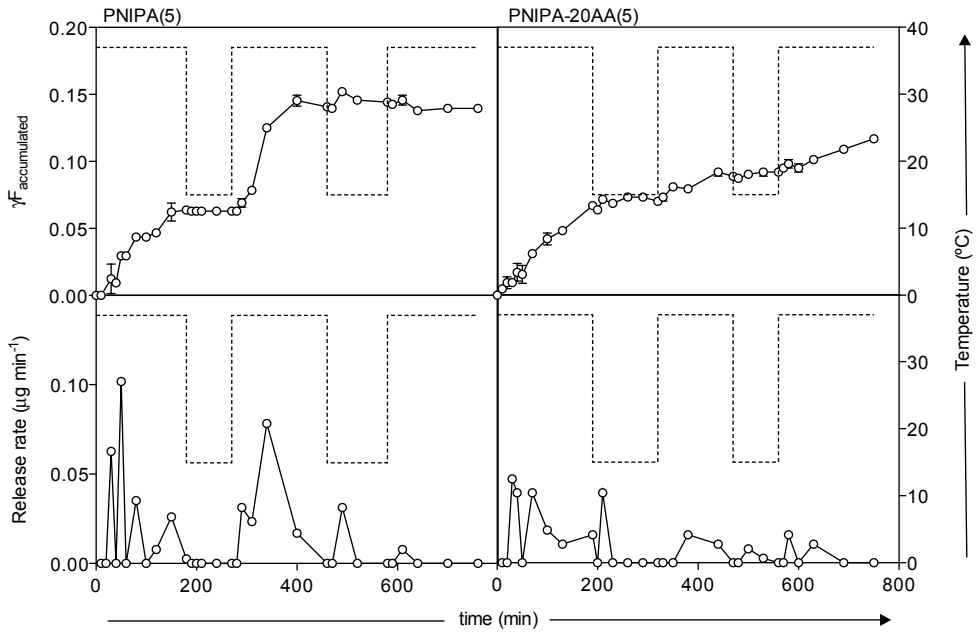


FIGURE 19. Relative fraction of accumulated pimaricin released and the release rate of pimaricin from the PNIPA(5) and PNIPA-20AA(5) nanohydrogels through the dialysis bag of 3500 g mol$^{-1}$ in distilled water. The dashed line shows the temperature cycling of the release medium between 37 °C and 15 °C.

the pimaricin release rate as a function of pulsatile temperature are shown in Figure 19 on the next page.

The results for the PNIPA(5) nanohydrogel were consistent with the positive squeezing mechanism reported in the literature [23, 172, 208]. When the temperature was increased, the release rate peaked rapidly followed by a very slow release process. Pimaricin release stopped after two temperature pulses and during these cycles 15% was released, which indicates that the deswelling process did not help to squeeze more pimaricin out of the gel matrix.

However, when AA was added to the PNIPA-20AA(5) nanohydrogel, the temperature changes did not affect the release rate as dramatically. Although the biggest release peak

occurred in the first cycle at 37 °C, after the third cycle at this temperature the release rate still remained apparently constant.

Therefore, higher releases were obtained by alternating on/off cycles, and consequently there were larger amounts of pimaricin in the release medium than in a single cycle at 37 °C, although with the PNIPA-20AA(5) nanohydrogel a more sustained release over time was achieved.

CHAPTER 4

# Evaluation of antimicrobial effectiveness of pimaricin-loaded thermosensitive nanohydrogels in cheeses from Arzúa-Ulloa DOP

In Chapter 3 on page 65 we have demonstrate the validity of poly (*N*-isopropylacrylamide) (PNIPA) nanohydrogels to transport and release pimaricin, being able to modulate its release patterns by varying the nanoparticle hydrophilicity and the temperature. Thus, the more hydrophilic nanohydrogels -PNIPA nanohydrogel copolymerized with acrylic acid (AA)- lead to a sustained pimaricin controlled release over time.

Taking into account the potential application of the pimaricin-nanohydrogel system for antimicrobial active packaging, in this Chapter we aimed to evaluate the effectiveness of the pimaricin-loaded PNIPA nanodevices in controlling mould spoilage employing a food model system consisting in Potato Dextrose Agar (PDA) plates. In order to assess the protective effect of nanohydrogels, mould spoilage was evaluated under favourable and unfavourable conditions for the chemical stability of pimaricin. In addition we evaluate the ability of pimaricin-loaded PNIPA nanohydrogels to avoid the growth of microbial spoilage in a real food. For this purpose we assayed the pimaricin-loaded PNIPA-20AA(5) nanohydrogel system to prevent natural and artificial contamination in cheese samples from Arzúa-Ulloa DOP stored under different thermal conditions simulating a break in the cold chain.

## 4.1. Material and Methods

**4.1.1. Preparation of pimaricin-loaded nanohydrogel.** Commercial pimaricin (50% pure pimaricin, 50% lactose) was from VGP Pharmachem (Barcelona, Spain) and the nanohydrogel employed in this work was NIPA copolymerized with 20% AA (PNIPA-20AA(5)). The nanohydrogel synthesis and preparation of pimaricin-loaded nanohydrogel were performed as previously described (Section 2.1.2 on page 47, Chapter 2).

**4.1.2. Inhibition studies employing a food model system.** We designed a food model system consisting of Petri dishes with 5 mL of PDA (Difco$^{TM}$, Detroit, MI, USA). In order to simulate favourable (A) and unfavourable (B) conditions for the chemical stability of pimaricin, we considered the following conditions:

**A:** PDA agar without acidification and plate storage under dark conditions.

**B:** Acidified PDA agar (pH = 3) with 10% (w/v) L(+)-tartaric acid (Panreac, Barcelona, Spain) and plate storage under fluorescent lighting.

The antimicrobial effectiveness of the nanohydrogel-pimaricin system (NP) was evaluated together with control treatments in which the nanohydrogel-pimaricin system was substituted by distilled water (C), the nanohydrogel (N) and free pimaricin (P). The nanohydrogel and pimaricin concentrations and ratios were the same as those used for the release studies.

An aliquot of 25 μL of a 12 h-culture of *Saccharomyces cerevisiae* (Sc 1.02) ($30x10^7$ UFC $mL^{-1}$) was inoculated in triplicate into the Petri dishes. After 1 hour in the fridge to allow the inoculated culture to be absorbed properly, 100 μL of each antimicrobial sample (NP, N, C and P) was spread over the plate surface. All plates were incubated at 4 °C for 7 days and then at 25 °C until the end of the experiment (15 days).

**4.1.3. Preparation of Arzúa-Ulloa DOP cheeses coated with pimaricin-loaded PNIPA nanohydrogels.** The antimicrobial effectiveness of the pimaricin-loaded PNIPA-20AA(5) nanohydrogel system, was assayed both against endogenous and artificial contamination in cheese samples from Arzúa-Ulloa DOP stored under conditions of thermal abuse, in two different bioassays.

For the first bioassay (cheeses with natutal contamination), 80 pieces of fresh cheese from Arzúa-Ulloa DOP (3 days of ripening after manufacture) with similar dimensions and an average weight of 13 g, were randomly distributed among four treatments: untreated cheese (C), cheese treated with a 12.5 mg $mL^{-1}$ nanohydrogel suspension (N), cheese treated with a 0.4 mg $mL^{-1}$ commercial pimaricin solutio (P), and cheese treated with pimaricin-loaded nanohydrogel suspension (at the same concentrations). To apply the treatments 0.5 mL of each suspension was spread over the cheese surface using a sterile inoculating loop. Cheeses were incubated at 8 ºC for 7 days in order to ensure a proper temperature for cheese ripening. After this period, the incubation temperature was lowered to 4 ºC (typical storage conditions) during 64 days. Then to simulate a break in the cold chain the temperature was raised to 37 ºC for 12 h on day 16 of storage. Four cheese samples per treatment were analyzed at 7, 16, 30, 43 and 64 days after cheese manufacture. Four cheese samples were analyzed at initial time before applying any treatment.

For the second bioassay (cheeses with artificial contamination), 102 pieces of fresh cheeses from Arzúa-Ulloa DOP (2 days of ripening after manufacture) were prepared. After 8 days of storage (after cheese sampling), cheeses were inoculated with a 12-hour culture (260x105 CFU $g^{-1}$) of Sc 1.02, obtained after growth in yeast extract-peptone-glucose (YPD) medium (Panreac, Barcelona, Spain) at 30 ºC. Cheeses were of similar dimensions and an average weight of 13 g and were distributed and treated in the same way as in the previous bioassay. However, the total assay duration was 30 days and the simulation in the broken cold chain was carried out increasing the temperature at various points of storage time: at 8 (after cheese sampling) and 14 days of storage from 4

to 37 ºC during 80 min and at 17, 21 and 29 days of storage from 4 to 25 ºC during 180 min. Cheese samples were analyzed at 8, 15, 22 and 30 days after cheese manufacture. At each sampling time, six samples per treatment were analyzed, of which two were used for water activity analysis and four for the remaining analysis. Six samples of cheese were analyzed at initial time, before applying any treatment.

**4.1.4. Physico-chemical cheese analysis.** Weight loss of cheese samples was calculated as the percentage of weight loss from the initial cheese weight after treatment application.

For determination of the water activity ($a_w$) cheese samples were previously cut into a grinder. The $a_w$ values were obtained at 25 °C using a LabMaster-$a_w$ (Novasina, Switzerland).

The colour of surface cheese samples was measured with a colorimeter Chroma CR-400/410 (Konica Minolta, Japan), using CIE *L*a*b** coordinates, where *L** corresponds to lightness, *a** to red/green chromaticity and *b** to yellow/blue chromaticity. The instrument was calibrated with a white standard plate. The cheese colour was expressed by the total colour difference ($\Delta E^*$), which was calculated according to the following equation reported by MacDougall [112]:

$$\triangle E^* = \left(\triangle L^{*2} + \triangle a^{*2} + \triangle b^{*2}\right)^{1/2} \tag{31}$$

where, $\Delta L^*$, $\Delta a^*$ and $\Delta b^*$ are the differences in *L*a*b** coordinates between the initial values (before coating) and the values measured during the experiment.

The pH of cheese samples was measured after homogenizing the samples in a Stomacher® 3500 (Seward Medical, UK).

**4.1.5. Microbiological analysis.** Total fungal and mesophilic counts were determined using standard plate count (SPC), with PDA acidified to pH 3.5 with 10% (w/v) L(+)-tartaric acid and Plate Count Agar (PCA, Difco™, Detroit, MI, USA) respectively.

Each sample was homogenized with 100 mL of 0.8% (w/v) sterile saline solution (Panreac, Barcelona, Spain) for 1 minute in a Stomacher® 3500. Tenfold serial dilutions were performed for each sample and aliquots (100 µL) of the appropriate dilutions were inoculated in PDA and PCA and incubated at 25 °C for 7 days and 30 ºC for 48 hours to enumerate total fungal counts and mesophilic counts, respectively. To ensure the reproducibility of fungal counts, an aliquot of homogenized samples was resuspended in Tryptic Soy Broth (TSB, Cultimed, Panreac, Barcelona, Spain) for 2 h (0.5 mL/4.5 mL) to revive the propagules and 10-fold serial dilutions were obtained in 0.8%, w/v sterile saline solution with 0.01% (w/v) Tween® 80 (Panreac, Barcelona, Spain).

Total fungal counts were also determined by quantitative polymerase chain reaction (qPCR) whose procedure is described in the following sections.

4.1.5.1. *DNA extraction.* 10 mL from from the homogenates used for microbiological analysis were centrifuged (4000 rpm, 10 min) and washed twice with 10 mL and 1 mL of sterile phosphate buffered saline (PBS, Panreac, Barcelona, Spain), respectively. Pellets were resuspended in 550 µL Buffer BCF from Speedtools Food DNA extraction Kit (Biotools, B&M Labs. S.A.) and incubated overnight at 65 ºC. Samples were transferred to a 2-mL sterile tubes containing 0.25 g of 425-600 µm-diameter and 0.25 g of $\leq$ 106 µm-diameter glass beads acid washed from Sigma-Aldrich (Munich, Germany). Tubes were shaken in a Tissuelyser® LT (Qiagen, Venlo, The Netherlands) for 3 min at 50 Hz and then centrifuged at 10,000 rpm for 10 min. Supernatants were transferred to a new sterile tube and Genomic DNA extracted with the Speedtools Food DNA extraction Kit (Biotools, B&M Labs. S.A.). Then DNA was purified with StrataPrep PCR Purification Kit (Stratagene, Agilent Technologies España, S.L., Madrid).

The concentration and purity of DNA were determined using a Nanodrop 2000c (ThermoFisher Scientific, Spain).

4.1.5.2. *Sensitivity, detection limit and linearity of the qPCR assay.* The sensitivity, detection limit and linearity of the qPCR assay for the total fungal count, was determined using a 12-hour pure culture of Sc 1.02. Genomic DNA was extracted from as explained

in Section 4.1.5.1 on the preceding page for the cheese samples. A standard curve from Sc 1.02 genomic DNA was obtained by plotting the cycle threshold ($C_T$) against the Sc 1.02 cell quantity expressed as log (CFU $mL^{-1}$). Counts were obtained by plating tenfold serial dilutions of the Sc 1.02 culture in PDA.

The amplification efficiency ($E$) was estimated from the slope ($k$) of the standard curve, using the formula $E = \left(10 - \frac{1}{k}\right) - 1$. A reaction with $E$ = 1 generated a slope of -3.32.

Additionally we performed another standard curve employing Arzúa-Ulloa cheese to evaluate the quantification range, linearity and sensitivity in this food matrix. Sliced commercial cheese samples (10 g per sample) were sterilized under UV exposure during 75 min. Cheese samples were inoculated with 1 mL of a batch of 10-fold serial dilutions from a 12-hour culture. Then cheese samples were homogenized for 1 min in a Stomacher® 3500. and the CFU $mL^{-1}$ determined in PDA plates. The standard curve in cheese was obtained plotting $C_T$ values against the log (CFU $mL^{-1}$) of Sc 1.02. Four replicates for each curve were obtained.

4.1.5.3. *qPCR assay.* Primers NL1, (5'-GCC ATA TCA ATA AGC GGA GGA AAA G-3') and LS2 (5'-ATT CCC AAA CAA CTC GAC TC-3'), corresponding to nucleotide positions 266 to 285 on the *Saccharomyces cerevisiae* 26S RNA gene [44], were used to amplify a region of approximately 250 nucleotides. qPCR was performed in a final volume of 25 µL employing Brilliant II SYBR® Green QPCR Master Mix (Stratagene, Agilent Technologies S.L., Spain), ROX dye reference (final concentration, 30 nM), primers (final concentration, 400 nM), and 3 µL of template DNA. Thermal cycling conditions were as follows: 95 ºC for 10 min, 40 cycles of 95 ºC for 30 s, 55 ºC for 1 min and 72 ºC for 1 min. Thermal cycling, fluorescent data collection, and data analysis were carried out with Mx3000P QPCR system with MxPro™ QPCR Software (Stratagene, Agilent Technologies S.L., Spain).

**4.1.6. Statistical analysis.** Differences in antimicrobial effectiveness amongst treatments were evaluated by analysis of variance (ANOVA) followed by Bonferroni post-tests

for multiple comparisons by using GraphPad Prism™ 5 (GraphPad Software Inc., San Diego, CA, USA).

## 4.2. Results and Discussion

**4.2.1. Inhibition studies employing food model systems.** To evaluate the antimicrobial effectiveness of the pimaricin-nanohydrogel system proposed, we conduct experiments using a food model system consisting of PDA plates. In addition, this assay is used to assess the capacity of nanohydrogels to protect the pimaricin by keeping it chemically stable under favourable (A) and unfavourable (B) conditions since critical amounts of pimaricin could be degraded under acidic conditions [183] and fluorescent lighting. Koontz et al. [99] addressed this problem and studied how forming inclusion complexes of pimaricin and cyclodextrins increased the stability of pimaricin compared to free pimaricin in cheese products stored under high-intensity fluorescent lighting in supermarket freezer showcases.

No growth is observed at 4 °C (Table 9 on the next page) in any of the plates or storage conditions (A or B) assayed. When the temperature increases up to 25 °C and under favourable conditions for pimaricin stability (A), growth peaked rapidly and counts are above the limit (CFU > 75, in 5 mL of medium) for controls without pimaricin (C and N). Nonetheless, when pimaricin is present, there is much less growth, especially in those plates containing pimaricin in the nanohydrogel (Table 9 on the following page).

In plates under unfavourable conditions (B: acidic medium and storage under fluorescent lighting), counts are low for all treatments because yeast grows more slowly in acidic media; however, the poorest growth is again observed on plates with the pimaricin-loaded nanohydrogel (Table 9 on the next page).

In order to quantify these effects, we calculate the percentage reduction in microbial growth as follows:

TABLE 9. Counts (CFU) of *Saccharomyces cerevisiae* (Sc 1.02) on PDA agar plates without acidification stored under dark conditions (A), and acidified PDA agar plates stored under fluorescent lighting (B), treated with distilled water (C), nanohydrogel (N), free pimaricin (P) and the nanohydrogel-pimaricin system (NP)

| | 4 ºC | | | | 25 ºC | | | |
|---|---|---|---|---|---|---|---|---|
| | 2 days | | 7 days | | 9 days | | 15 days | |
| | A | B | A | B | A | B | A | B |
| C | - | - | - | - | 347.0±33.1 | 11.7±12.6 | 327.3±23.8 | 19.7±13.5 |
| N | - | - | - | - | 405.7±46.5 | 54.0±26.1 | 346.7±37.3 | 57.0±22.7 |
| P | - | - | - | - | 65.7±3.8 | 0.3±0.6 | 64.0±7.8 | 4.7±2.1 |
| NP | - | - | - | - | 29.3±10.0 | - | 26.3±9.1 | 0.3±0.6 |

Values reported are the means±standard deviation (n = 3).

$$\%R = \left(\frac{N_0 - N}{N_0}\right) \cdot 100 \tag{32}$$

where, $N_0$ is the mean count on control plates (C) and $N$ is the mean count on plates with pimaricin (P) and pimaricin-loaded nanohydrogel (NP), both expressed as Log (CFU $mL^{-1}$ ).

For plates under (A) conditions, the NP treatment shows a reduction of 27.07±4.15%, which is higher than that observed on plates with the P treatment, which shows a reduction of 17.26±1.34%, although the difference between the two treatments is not significant ($p > 0.05$). However, under (B) conditions, there is a larger difference between the

NP and P treatments. The reduction on plates with the NP treatment is 80.94±33.02%, which is significantly higher ($p < 0.01$) than that observed on plates with the P treatment, 19.91±6.68%. In any case, the ANOVA analysis at a 95% level of confidence the percentage reduction (%$R$) shows that the effect of the treatment is very significant ($p = 0.0069$) and the effect of growth conditions (pH, light) is significant ($p = 0.0205$). The interaction between these two factors is also significant ($p = 0.0311$), i.e., the treatment does not have the same effect under the two growth conditions assayed.

Therefore, the antifungal effect of pimaricin is potentiated when it is applied loaded into the PNIPA-20AA(5) nanohydrogel probably because pimaricin is released slowly when environmental conditions required it. This seems to indicate that the nanohydrogel has a protective effect against degrading conditions (pH, light), which thus make the antifungal effect of pimaricin more intense.

Therefore, the nanohydrogel-pimaricin system proposed in this work would be useful in packaging for food products that are easily spoiled by fungal growth (i.e., which have low pH and a high moisture content) and that are normally exposed to changes in storage temperature due to transport and shelf time. As pimaricin is usually used to prevent moulds and yeasts growing on the surface of cheese we are currently performing experiments with cheese samples to test PNIPA-nanohydrogel systems. The controlled release of pimaricin from PNIPA nanohydrogels could reduce the amount of pimaricin on the surface of the cheese, and therefore reduce the amount that migrates to the cheese bulk.

**4.2.2. Effect of nanohydrogel coating on cheeses from Arzúa-Ulloa DOP.** During cheese ripening microbiological, enzymatic and physico-chemical changes determine the cheese texture, taste and flavour and, consequently, the final consumer acceptance. The main physico-chemical changes of cheese ripening, such as weight loss and surface colour, are related with mass transfer process both inside the cheese and between the cheese and the atmospheric environment. Thus, properties of cheese out-layer have a great influence in these physico-chemical changes and can be easily modified by surface

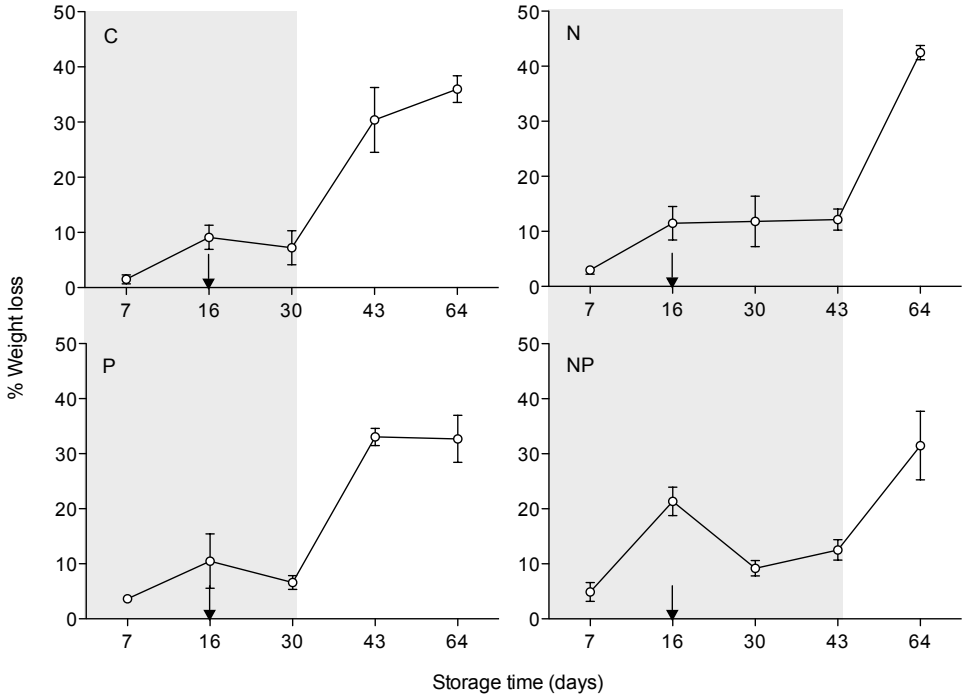


FIGURE 20. Percentage of weight loss throughout storage time for cheese samples with natural contamination: cheeses without treatment (C), treated with pimaricin solution (P), treated with nanohydrogel suspension (N) and treated with pimaricin-loaded nanohydrogel suspension (NP). Arrows represent the change in the storage temperature from 4 to 37 ºC during 12 h.

coating with impermeable (wax) or permeable (hydrogel) substances. For these reasons the effect of nanohydrogel coating in some cheese ripening parameters was studied.

**4.2.3. Weight loss studies.** Figures 20 and 21 on page 100 show the weight loss of cheeses treated and stored as explained in Section 4.1.3 on page 91 for the bioassays with natural and artificial contamination respectively.

In the bioassay with natural contamination (Figure 20), weight loss increases in all cases until 16 days of storage. Weight loss reaches values of around 10% with no significant ($p < 0.05$) differences between treatments except for cheeses treated with a pimaricin-loaded nanohydrogel suspension (NP), which leads to the highest mean weight

loss (21%; $p < 0.05$) at this point. This difference may be due to the fact that each cheese sample constitutes an experimental unit and therefore minor differences in porosity between them can occur. At 30 days, weight loss practically stops and differences between treatments are not significant ($p > 0.05$). From this point, cheeses treated with and without nanohydrogel present two well-differentiated behaviours. Thus, at 43 days of storage, cheeses without nanohydrogel treatment (C and P) leads to a mean weight loss (30-33%) significantly higher ($p < 0.05$) than that found for nanohydrogel treated cheeses (12%). Finally after 64 days of storage, cheese weight losses are similar between treatments (30-40%) and only N-treated cheeses show significantly ($p < 0.05$) higher weight losses with respect to the P and NP treatments.

With regard to the bioassay with artificial contamination (Figure 21 on the following page), there are not significant ($p > 0.05$) differences between cheese weight losses after 8 days of storage. However, after 15 days of storage, NP-treated cheeses lose significantly ($p < 0.001$) more weight than the other treatments. At 22 days of storage P-treated cheeses lose significantly ($p < 0.001$) less weight than cheeses with nanohydrogel (N and NP). At the end of the experiment (30 days of storage), the only significant ($p < 0.05$) differences appear between cheeses with N and P treatment. In this case, no different behaviours between cheeses treated with and without nanohydrogel are observed as do it in the bioassay with natural contamination. Overall, weight loss increases linearly along sampling time, showing a 35% average weight loss after 30 days of storage. Weight losses are higher than those previously reported for this type of cheeses. However we have to take into account that the small size (around 10 g) of cheese samples, favours higher water losses than in cheeses used in Rodriguez-Alonso et al. [155], with 100-150 g.

On the other hand, we also have to take into account the significant ($p < 0.001$) differences between weight losses in bioassays with natural and artificial contamination. This behaviour could be due to the cheese melting that occurred in the bioassay with natural contamination during the temperature rise at 16 days of storage. Cheese from

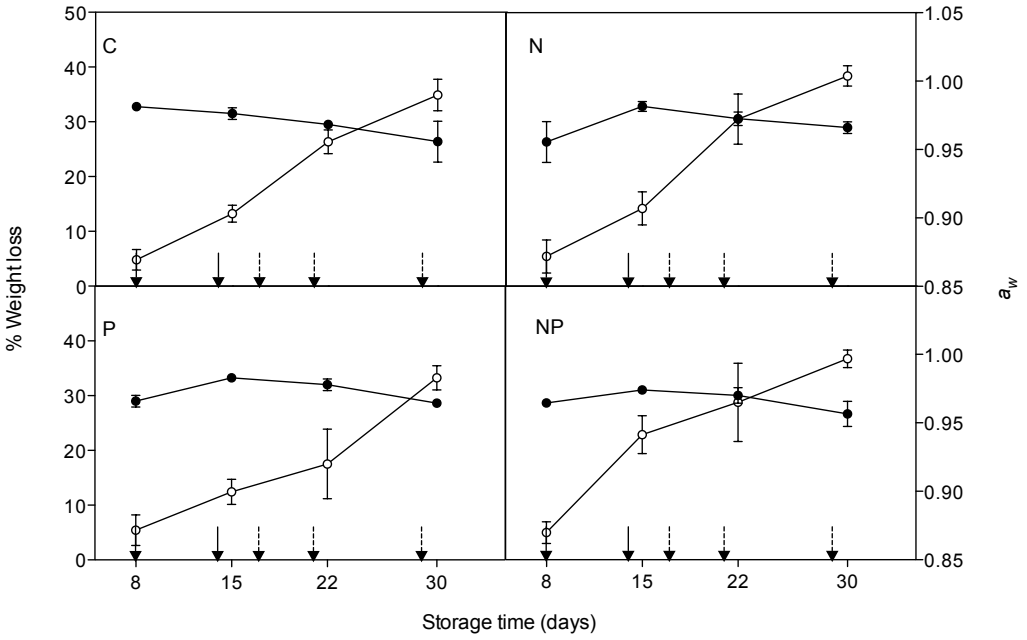


FIGURE 21. Percentage of weight loss (○) and water activity ($a_w$) (●) throughout storage time for cheese samples with artificial contamination: cheeses without treatment (C), treated with pimaricin solution (P), treated with nanohydrogel suspension (N) and treated with pimaricin-loaded nanohydrogel suspension (NP). Arrows with continuous line represent the change in the storage temperature from 4 to 37 ºC during 80 min and arrows with dashed line represent the change in the storage temperature from 4 to 25 ºC during 180 min.

Arzúa-Ulloa DOP has $\geq$ 45% of fat/dry matter content [155] and can be considered a full-fat cheese. Kim et al. [98] appointed that moisture loss is lower in full-fat cheese samples due to the fact that large amount of fat inhibit moisture loss by covering the melted cheese surface. Once the water reaches the surface it can be released again leading to the rapid increase in weight loss in the last sampling times.

For both bioassays, the ANOVA analysis at 95% confidence level for weight loss shows that the effect of the interaction between the storage time and the treatment is significant ($p < 0.0001$), i.e., treatment does not have the same effect on weight loss during all storage time.

**4.2.4. Water activity studies.** The water activity ($a_w$) of cheese samples with artificial contamination are shown in Figure 21 on the preceding page. $a_w$ is an important physico-chemical parameter which influences the microbiological and the biochemical evolution during the cheese ripening process. The knowledge of this parameter is useful for the control of the ripening process and for the control of the final organoleptic properties and safety standards of cheese [162]. The $a_w$ decreases until 30 days of storage, reaching values around 0.960. However there are no significant ($p > 0.05$) differences between treatments. The ANOVA analysis at 95% confidence level of the $a_w$ variation shows that the effect of time is significant ($p < 0.0001$) although the effect of treatment is not significant ($p = 0.2667$). The interaction of these two factors is considered not quite significant ($p = 0.0524$), i.e., treatment has practically the same effect during all storage time. So it seems that the nanohydrogel coating does not have any negative effect respect to the control samples.

**4.2.5. Colour studies.** Cheeses from Arzúa-Ulloa DOP only can be marketed if they retain the external features of its natural ripening, preserving its appearance and natural colour [27], and therefore the monitoring of colour changes during storage would be an important issue. In Figures 22 on the following page and 23 on page 103 colour variation is represented as colour difference ($\Delta E^*$) and variation profile of the $L^*a^*b^*$ coordinates of cheeses from both bioassays with natural and artificial contamination respectively.

The profiles of $\Delta E^*$ along storage agree with those observed above for the weight loss, presenting two different behaviours in cheeses with and without nanohydrogel coating. In the bioassay with natural contamination, until 30 days of storage no significant ($p > 0.05$) differences are observed between treatments and only significant ($p < 0.05$) differences between N and NP-treated cheeses are found, at 7 and 16 days of storage. However, these differences could be due to the porosity differences between cheese samples, in the same way as explained in Section 4.2.3 on page 98 for the weight loss values. From 30 days of storage, differences between samples with and without nanohydrogel are significant ($p < 0.05$). In addition, differences between C and P treatment and differences

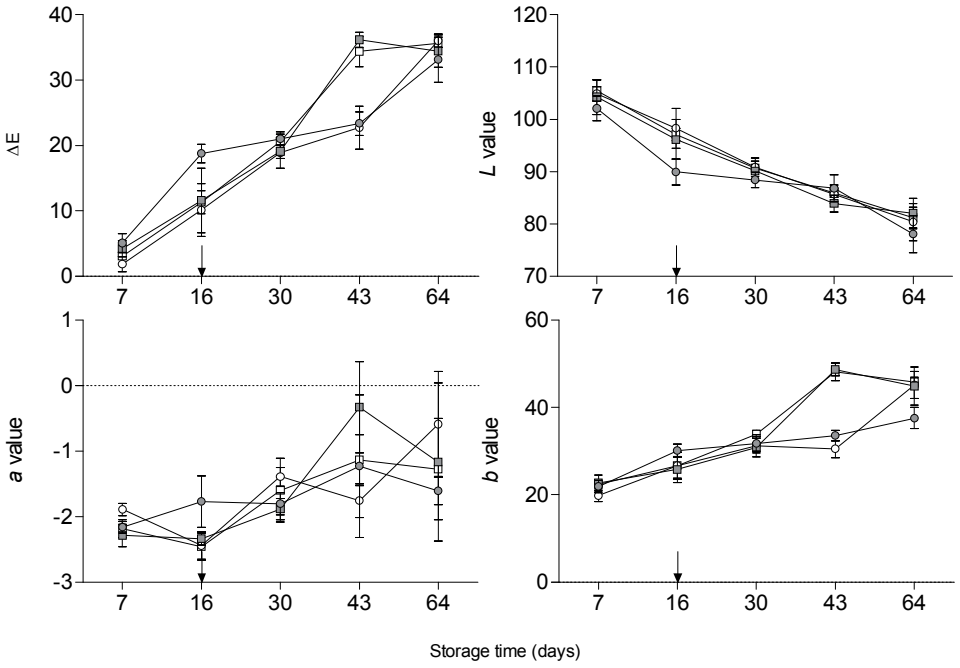


FIGURE 22. Colour difference ($\Delta E^*$) and CIE $L^*a^*b^*$ coordinates during storage time for cheese samples with natural contamination: cheeses without treatment (C, □), treated with pimaricin solution (P, ■), treated with nanohydrogel suspension (N, ○) and treated with pimaricin-loaded nanohydrogel suspension (NP, ●). Arrows represent the change in the storage temperature from 4 to 37 ºC during 12 h.

between N and NP treatment are not significant ($p > 0.05$). At the end of the experiment there are not significant ($p > 0.05$) differences between treatments.

As in previous works [24, 157], $L^*$ value decreased and $b^*$ value increased (Figures 22 and 23 on the facing page) as the cheeses aged. However the parameter that best reflects the colour differences between cheeses with and without nanohydrogel is the yellowness ($b^*$ value). These results agree with visual appreciation of the cheeses. So samples with nanohydrogel coating (N and NP) show fewer yellow surfaces.

As in the bioassay with natural contamination, it seems cheese colour differences in the bioassay with artificial are mainly due to yellowness ($b^*$ value) changes (Figure 23 on the next page). The $b^*$ values are significantly ($p < 0.05$) higher in NP-treated cheeses

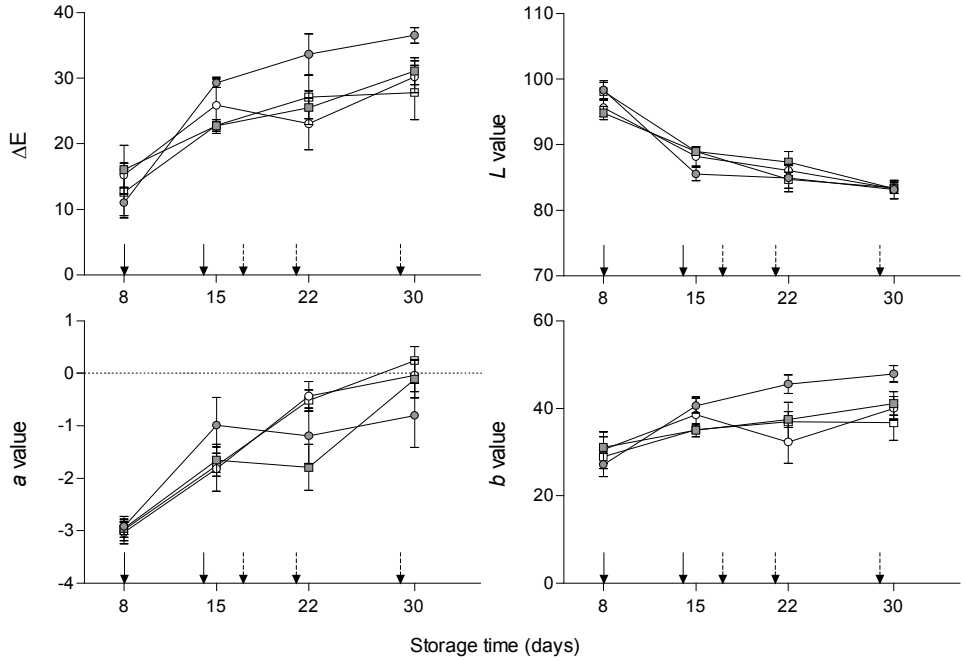


FIGURE 23. Colour difference ($\Delta E^*$) and CIE $L^*a^*b^*$ coordinates during storage time for cheese samples with artificial contamination: cheeses without treatment (C, □), treated with pimaricin solution (P, ■), treated with nanohydrogel suspension (N, ○) and treated with pimaricin-loaded nanohydrogel suspension (NP, ●). Arrows with continuous line represent the change in the storage temperature from 4 to 37 ºC during 80 min and arrows with dashed line represent the change in the storage temperature and from 4 to 25 ºC during 180 min.

respect to the other, after 22 days of storage. As discussed above, NP-treated cheeses begin to lose weight, i.e. water, earlier than the other and therefore, the yellowness begins to develop before, although these differences are non visually perceptible, in contrast to the differences that we observe in the bioassay with natural contamination. In general, the $L^*$ value decreases with time and the $b^*$ value increases during all the storage time.

In the same manner as the weight losses (Section 4.2.3 on page 98), the ANOVA analysis at 95% confidence level of the colour difference ($\Delta E^*$) studied for both bioassays shows that the interaction of the effect of storage time and the effect of treatment is

significant ($p < 0.0001$), i.e., treatment does not have the same effect during all storage time.

**4.2.6. pH evolution.** During 64 days of storage, pH values in cheeses with natural contamination do not show significant ($p > 0.05$) differences between treatments (Table 10 on the next page). The ANOVA analysis at 95% confidence level of the pH variation shows that the effect of time is significant ($p < 0.0001$) whereas the effect of treatment is not significant ($p = 0.6500$). The interaction of these two factors is not significant ($p = 0.1717$), i.e., the treatments have the same effect during all storage time.

In the bioassay with artificial contamination, the pH values are slightly higher ($p > 0.05$) in untreated cheeses (Table 11 on page 107) at 8 days of storage respect to the all treatments and at 22 days only respect to the N treatment. Overall, the variation of pH during the experiment is not very high. The ANOVA analysis at 95% confidence level of the pH variation studied shows that the effect of time and the treatment is significant ($p < 0.0001$). However, the interaction of these two factors is considered not quite significant ($p = 0.0764$), i.e., the treatments have practically the same effect during all storage time.

The results suggest that nanohydrogel coating does not influence the cheese natural ripening.

**4.2.7. Microbiological control of pimaricin-loaded nanohydrogel coating during cheese storage.** During storage a risk of an external contamination of cheese by spoilage microorganisms exists. This risk is higher when a breakdown in the cool chain occurs, but can be avoided or reduced by using pimaricin-loaded nanohydrogel coatings.

During the first bioassay with natural contamination, mesophilic counts practically did not show significant ($p > 0.05$) differences between treatments, which agrees with the results of the pH variation (Section 4.2.6). Since the main contributor to mesophilic counts in cheese are lactic acid bacteria it seems that nanohydrogel does not influence the cheese natural ripening. Only significant ($p < 0.05$) differences appear between treatments at 43 days of storage in cheeses from the bioassay with natural contamination

TABLE 10. Changes of pH, total mesophiles and fungal counts log (CFU $g^{-1}$) during storage time for cheese samples with natural contamination (temperature was raised at 16 days of storage after sampling from 4 to 37 ºC during 12 h)

| Storage time (days) | pH | | | |
|---|---|---|---|---|
| | C | N | P | NP |
| 3 | 5.84±0.11[a] | 5.84±0.11[a] | 5.84±0.11[a] | 5.84±0.11[a] |
| 7 | 5.82±0.09[a] | 5.89±0.05[a] | 5.92±0.04[a] | 5.84±0.02[a] |
| 16 | 5.87±0.06[a] | 5.85±0.10[a] | 5.90±0.08[a] | 5.84±0.06[a] |
| 30 | 5.53±0.12[a] | 5.45±0.07[a] | 5.37±0.08[a] | 5.42±0.11[a] |
| 43 | 5.72±0.16[a] | 5.58±0.11[a] | 5.54±0.04[a] | 5.63±0.10[a] |
| 64 | 5.96±0.29[a] | 6.21±0.18[a] | 6.11±0.19[a] | 6.02±0.06[a] |
| | Log (Mesophilic CFU/g of cheese) | | | |
| 3 | 9.10±0.14[a] | 9.10±0.14[a] | 9.10±0.14[a] | 9.10±0.14[a] |
| 7 | 9.31±0.10[a] | 9.18±0.17[a] | 9.24±0.06[a] | 9.38±0.06[a] |
| 16 | 9.35±0.09[a] | 9.31±0.10[a] | 9.26±0.07[a] | 9.28±0.09[a] |
| 30 | 7.69±0.38[a] | 7.44±0.36[a] | 7.76±0.45[a] | 7.67±0.37[a] |
| 43 | 6.80±0.51[a] | 7.92±0.12[b] | 7.59±0.34[ab] | 8.15±0.41[b] |
| 64 | 7.04±0.62[a] | 7.05±0.57[a] | 7.90±0.66[a] | 7.63±0.33[a] |
| | Log (Fungal CFU/g of cheese) | | | |
| 3 | <1.90 | <1.90 | <1.90 | <1.90 |
| 7 | <1.90 | <1.90 | <1.90 | <1.90 |
| 16 | <1.90 | <1.90 | <1.90 | <1.90 |
| 30 | 4.58±0.51[a] | 3.65±0.53[a] | 3.62±0.18[a] | 4.57±0.65[a] |

Values reported are the means±standard deviation ($n$ = 4).

[a-b]Different lower case letters in the same row indicate a statiscally significant difference ($p < 0.05$).

C: cheeses without treatment.

P: cheeses treated with pimaricin solution.

N: cheeses treated with nanohydrogel suspension.

NP: cheeses treated with pimaricin-loaded nanohydrogel suspension.

(Table 10 on the preceding page) and at 8 days of storage in cheeses from the bioassay with artificial contamination (Table 11 on the next page). The ANOVA analysis at 95% confidence level of the variation in mesophilic counts shows that the effect of time is significant ($p < 0.0001$), however the effect of treatment is not significant ($p = 0.1980$). The interaction of these two factors is significant ($p = 0.0258$), i.e., treatment doe not have the same effect during all storage time.

For both bioassays, mesophilic counts are above 9 log units during ripening (Table 10 on the preceding page and 11 on the next page), with similar values to those obtained in other studies with cheeses from Arzúa-Ulloa DOP [155, 32]. There is a slight increase in mesophilic counts until 16 and 8 days of storage for the bioassay with natural and artificial contamination respectively. From this point, in general there is a decrease in mesohilic counts.

The results agree with the pH variation (Table 10 on the preceding page and 11 on the next page). Most mesophilic organisms present in the cheese are lactic acid bacteria that low the pH by producing lactic acid [182]. At the time yeast and mould became to growth in the cheese surface, they could use the lactic acid [32] increasing the cheese pH. As the fungal growth begin earlier in the bioassay with artificial contamination, the pH decrease and the mesophilic growth also stops earlier.

The minimum shelf life for Arzúa-Ulloa cheese is 60 days, but usually sold within one month, as from this moment the uncoated cheeses begin to show fungal growth at the surface. Then 30 days is reported as the last sampling time for the total fungal counts analysis.

In the bioassay with natural contamination, until 30 days of storage there are no significant ($p > 0.05$) differences between treatments (Table 10 on the preceding page). Fajardo et al. [59] appointed that the absence of differences between Saloio cheeses coated with an edible film containing pimaricin are not to be expected when the counts are performed in the whole cheese samples and not only at their surface and as in this work the results are obtained under no inoculation conditions. In the bioassay with

TABLE 11. Changes of pH, total mesophiles and fungal counts Log (CFU $g^{-1}$) during storage time for cheese samples with artificial contamination (temperature was raised at 8 days of storage after sampling and 14 days of storage from 4 to 37 ºC during 80 min and from 4 to 25 ºC during 180 min at 17, 21 and 29 days of storage)

| | pH | | | |
|---|---|---|---|---|
| Storage time (days) | C | N | P | NP |
| 2 | 5.60±0.05$^{a}$ | 5.60±0.05$^{a}$ | 5.60±0.05$^{a}$ | 5.60±0.05$^{a}$ |
| 8 | 5.64±0.04$^{a}$ | 5.44±0.07$^{b}$ | 5.52±0.04$^{b}$ | 5.54±0.02$^{b}$ |
| 15 | 5.75±0.03$^{a}$ | 5.67±0.10$^{a}$ | 5.72±0.05$^{a}$ | 5.68±0.03$^{a}$ |
| 22 | 5.75±0.13$^{a}$ | 5.59±0.05$^{b}$ | 5.68±0.03$^{ab}$ | 5.64±0.05$^{ab}$ |
| 30 | 5.68±0.12$^{a}$ | 5.65±0.03$^{a}$ | 5.59±0.01$^{a}$ | 5.65±0.06$^{a}$ |
| | Log (Mesophilic CFU/g of cheese) | | | |
| 2 | 9.20±0.13$^{a}$ | 9.20±0.13$^{a}$ | 9.20±0.13$^{a}$ | 9.20±0.13$^{a}$ |
| 8 | 9.28±0.16$^{a}$ | 9.49±0$^{ab}$ | 9.53±0.05$^{b}$ | 9.48±0.11$^{ab}$ |
| 15 | 9.24±0.11$^{a}$ | 9.17±0.12$^{a}$ | 9.19±0.12$^{a}$ | 9.25±0.04$^{a}$ |
| 22 | 9.16±0.13$^{a}$ | 9.00±0.27$^{a}$ | 8.97±0.29$^{a}$ | 8.95±0.26$^{a}$ |
| 30 | 9.01±0.10$^{a}$ | 8.48±0.14$^{a}$ | 8.79±0.30$^{a}$ | 8.45±0.48$^{a}$ |
| | Log (Fungal CFU/g of cheese) | | | |
| 2 | <2.90 | <2.90 | <2.90 | <2.90 |
| 8 | 4.11±0.33$^{a}$ | 3.57±0.16$^{a}$ | 3.24±0.37$^{a}$ | 3.18±0.67$^{a}$ |
| 15 | 6.28±0.15$^{a}$ | 6.11±0.19$^{a}$ | 6.07±0.14$^{a}$ | 5.51±0.21$^{b}$ |
| 22 | 6.13±0.24$^{ab}$ | 6.41±0.17$^{a}$ | 6.40±0.13$^{a}$ | 5.83±0.32$^{b}$ |
| 30 | 5.92±0.14$^{ab}$ | 6.28±0.49$^{a}$ | 5.83±0.25$^{ab}$ | 5.59±0.16$^{b}$ |

Values reported are the means±standard deviation ($n$ = 4).

$^{a-b}$Different lower case letters in the same row indicate a statiscally significant difference ($p < 0.05$).

C: cheeses without treatment.

P: cheeses treated with pimaricin solution.

N: cheeses treated with nanohydrogel suspension.

NP: cheeses treated with pimaricin-loaded nanohydrogel suspension.

artificial contamination the total fungal counts increase from the inoculation at 8 days of storage for all treatments. Counts in cheeses with NP treatment are significantly ($p < 0.05$) lower respect to all other treatments at 15 days of storage, to the N and P treatments at 22 days of storage and to the N treatment at 30 days of storage. The ANOVA analysis at 95% confidence level of the total fungal counts variation shows that the effect of time and the effect of treatment are both significant ($p < 0.0001$). However the interaction of these two factors is not significant ($p = 0.2380$), i.e., treatments have the same effect during all storage time.

Therefore, despite the antimicrobial effect is not maintained for a long time, as initial microbial load is very high ($169x10^7$ UFC $mL^{-1}$), the differences founded with respect to the pimaricin treatment evidence the protective effect of the pimaricin-loaded nanohydrogel system observed in the food model system (Section 4.2.1 on page 95) that will allow maintain an antimicrobial effect of pimaricin for longer.

**4.2.8. Microbiological analysis by quantitative polymerase chain reaction (qPCR) of cheeses from Arzúa-Ulloa DOP coated with pimaricin-loaded nanohydrogel.** In the former paragraphs the suitability of pimaricin-loaded nanohydrogel coating to control the growth of spoilage microorganism was proved using a yeast as indicator in naturally and artificially contaminated cheeses. However, traditional methods based on SPC are most commonly used to quantify CFUs, but often cause confusion, as they depend largely on the physiological state of the organism and its ability to grow. In addition, hyphal filaments cannot be quantified using these techniques for enumeration of viable counts that usually reflect the number of spores rather than mycelia. In young colonies or within the food, mould growth is primarily composed of hyphae and viable counts are generally low. These inconveniences make reasonable contrast the antimicrobial efficacy of pimaricin-loaded nanohydrogel coatings by procedures independent of yeast or fungal cultures.

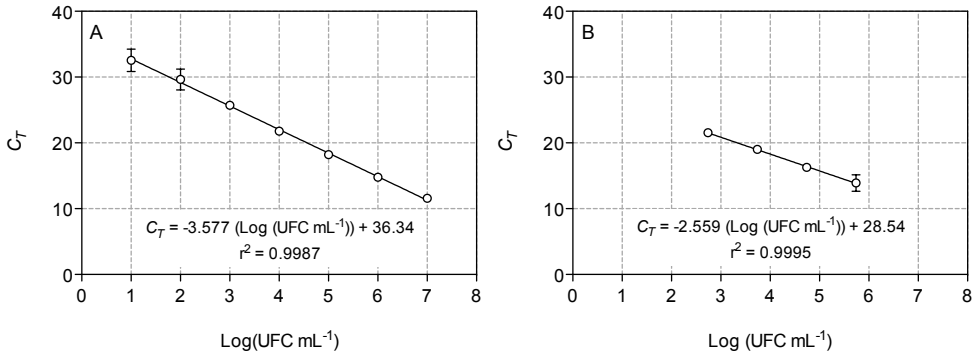


FIGURE 24. DNA standard curve for total fungal quantification by qPCR in two different matrix: culture broth (A) and cheese (B).

In this sense, several authors have developed methods based on the detection and quantification of DNA, which avoids the aforementioned problems [4, 56] but not to quantify the total fungal counts in cheeses so far.

In this paper, we developed a qPCR method that allows quantification of total fungal counts directly from the cheese samples. For this purpose, first we determine the sensitivity and detection limits of the qPCR assay to quantify the total fungal counts in cheeses a standard curve from DNA extracted from pure cultures of Sc 1.02 is determined. The assay is linear over 7 orders of magnitude, being the detection limit of 1 log (CFU mL$^{-1}$) (Figure 24).

The efficiency of the reaction is 0.91±0.08, which means that the amplification rate is very efficient and the qPCR assay is highly linear (r$^2$ = 0.9987). The nontemplate samples used as controls in the qPCR assay shows positive signals ($C_T$ values of 36.06±1.89), probably due to an accumulation of dimers of oligonucleotide primers to which SYBR Green molecules bound [82]. However, the melting curve obtained for this nonspecific product is different from that of the correct amplicon (data not shown). Also these $C_T$ values of the nontemplate controls are far enough from the $C_T$ values obtained for the $10^1$ CFU mL$^{-1}$ (32.56±1.70).

TABLE 12. Accuracy of the qPCR assay for the quantification of total fungal content in cheese

| | % Accuracy | | | |
|---|---|---|---|---|
| Storage time (days) | C | N | P | NP |
| 8 | 98.10±22.95 | 124.20±9.06 | 124.48±26,60 | 129.93±31.91 |
| 15 | 104.24±8.17 | 112.54±5.84 | 110.11±5.93 | 117.41±7.96 |
| 22 | 111.08±9.59 | 107.32±5.68 | 109.23±2.82 | 117.41±7.56 |
| 30 | 109.99±8.34 | 108.12±12.04 | 108.42±8.27 | 122.89±5.07 |

Values reported are the means±standard deviation ($n$ = 4).

C: cheeses without treatment.

P: cheeses treated with pimaricin solution.

N: cheeses treated with nanohydrogel suspension.

NP: cheeses treated with pimaricin-loaded nanohydrogel suspension.

The detection limit of total fungal quantification in cheese is nearly 2 logarithmic units higher (Figure 24 on the previous page) than for pure culture of Sc 1.02. Nevertheless, the assay is linear over 4 orders of magnitude. Even though the amplification in cheese matrix is highly linear ($r^2$ = 0.9995), the efficiency is high (1.47±0.17), probably due to the presence of inhibitors from the cheese matrix that have not been removed during DNA extraction. Another possibility could be that the reaction has too much target, i.e., presence of large amount of nontarget DNA coming from other cheese microorganism, as $C_T$ values of the negative control samples (cheeses without artificial contamination) are too low (23.08±0.59).

Cheese samples artifially contaminated with Sc 1.02 are analyzed by qPCR and results compared with microbiological analysis by SPC (Table 11 on page 107). For comparison of these results we evaluate the accuracy of the qPCR assay for the total fungal quantification in cheeses. The correlation between the enumerations of the bioassay cheese samples by qPCR and by SPC is good, around 100% of accuracy (Table 12 on the preceding page). However, for all treatments and sampling time the enumerations obtained by qPCR are higher than those obtained by SPC as a result of viable but non-culturable fungi or, as indicated by Hierro et al. [82], more likely due to the presence of dead cells in the sample.

CHAPTER 5

# Evaluation of antimicrobial effectiveness of pimaricin-loaded thermosensitive nanohydrogels in grape juice

In previous works we demonstrated the usefulness of PNIPA nanohydrogels with different composition to transport and release pimaricin as response of ambiental triggers like temperature and pH (Chapter 2 on page 47). Additionally the antimicrobial effectiveness of pimaricin-nanohydrogels systems was tested in a solid food model sytem and in cheeses (Chapter 4 on page 89).

In order to extend the shelf life of fresh fruit juices the use of a smart active packaging bassed on nanohidrogels as device for controlled release pimaricin was investigated in this Chapter. Evaluation of the effectiveness to control microbial growth spoilage of these systems is presented in a liquid food model system as well as in grape juice.

## 5.1. Material and Methods

**5.1.1. Materials.** Commercial pimaricin (50% pure pimaricin, 50% lactose) was from VGP Pharmachem (Barcelona, Spain). Pure pimaricin (M = 665.73 g $mol^{-1}$) from *Streptomyces chattanoogensis* ($\geq$95%, HPLC) was from Sigma-Aldrich (Munich, Germany). Dialysis bags (SnakeSkin$^{TM}$ pleated dialysis tubing) with a molar mass cut-off of 3500 g $mol^{-1}$ were from Pierce (Rockford, IL, USA).

D(+)-Glucose anhydrous PA-ACS, bacteriological peptone and yeast extract were all from Panreac (Barcelona, Spain). Acetic acid puriss. *p.a. ACS* reagent ($\geq$99.8%) and

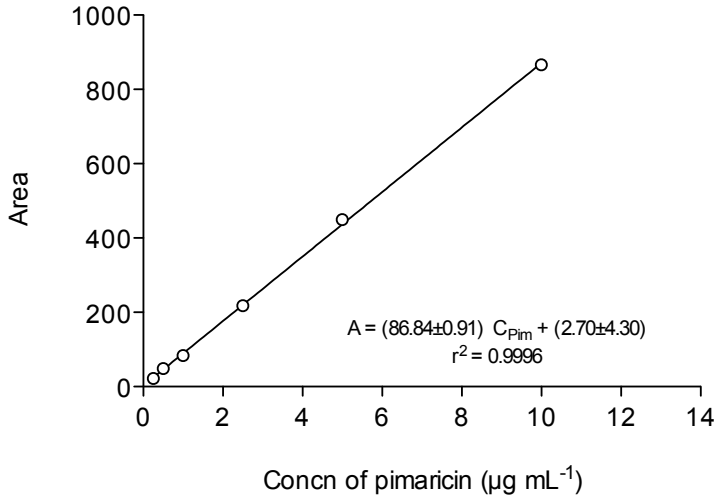


FIGURE 25. Pimaricin standard curve prepared in a standard diluent solution (S.D.) for its quantification by RP-HPLC.

methanol CHROMASOLV®, for HPLC (≥99.9%) were from Sigma-Aldrich (Munich, Germany). Commercial white grape juice was used as received.

**5.1.2. Pimaricin detection by reverse phase high performance liquid chromatography (RP-HPLC).** Pimaricin quantification by RP-HPLC was performed following a modified method from Roberts et al. [153]. RP-HPLC was performed using an Agilent 1200 system (Agilent Technologies, Palo Alto, CA, USA). Separation was performed employing a ACE® $C_{18}$ column (4.6 mm x 150 mm, 5 μm) with the column oven maintained at 30 ºC. The flow rate was 1.0 mL $min^{-1}$, the injection volume was 20 μL and the detection wavelength 319 nm. Mobile phase A consisted in MilliQ water/acetic acid (97:3, v/v) and mobile phase B was methanol/acetic acid (97:3, v/v). Mobile phase A at 90% was maintained for the first 6 min and decreased linearly to 10% over 25 min. Finally, the mobile phase A was increased to 90% and the column was reequilibrated for a further 9 min.

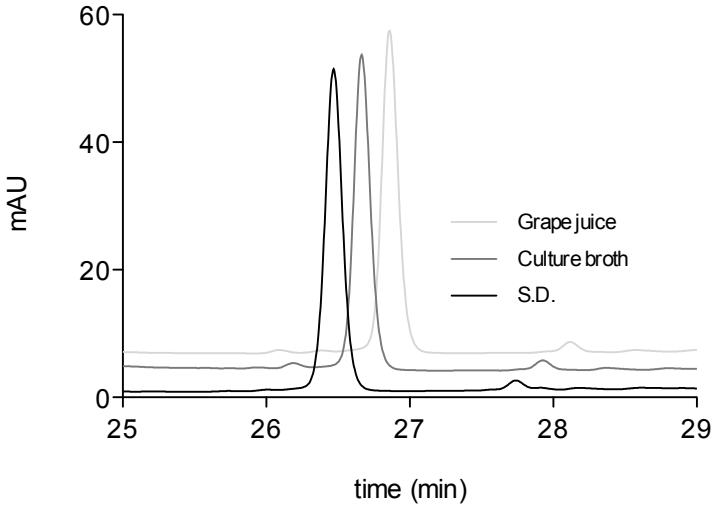


FIGURE 26. HPLC chromatogram at 319 nm of standard diluent solution (SD), YPD broth and grape juice added with pure pimaricin (5 μg $mL^{-1}$).

The assay was highly linear (Figure 25 on the facing page) from 0.05 to 10 μg $mL^{-1}$ of pure pimaricin dissolved in a standard diluent solution (S.D.) of methanol:MilliQ water:acetic acid (50:47:3, v/v/v).

Pimaricin quantification accuracy by RP-HPLC was determined by adding culture broth and grape juice with pure pimaricin solutions in S.D. to obtain final concentrations of 5 μg $mL^{-1}$. Figure 26 shows an HPLC chromatogram at 319 nm of S.D., culture broth and grape juice added with the same amount of pimaricin. The recovery was very high, 98.11% and 97.32% from the culture broth and grape juice respectively. So we can spare a previous step in which we extract the pimaricin from the matrices evaluated in this work.

**5.1.3. Analysis of pimaricin degradation.** We evaluated the pimaricin degradation in two different matrices: culture broth and grape juice. Culture broth was yeast extract-peptone-glucose (YPD) broth (Panreac, Barcelona, Spain). Both matrices, YPD broth and grape juice, were added with a commercial pimaricin aqueous solution (4 μg $mL^{-1}$) and

stored at 37 ºC and 25 ºC, for culture broth and grape juice respectively. The pimaricin concentration was followed daily during 15 days by RP-HPLC.

We also evaluated the pimaricin degradation in grape juice under pasteurization conditions. For these propose grape juice was added with a commercial pimaricin aqueous solution (3 μg $mL^{-1}$) and heated at 80 ºC in a thermostatized bath. Aliquots were removed at different time intervals within 1 h and the pimaricin concentration was also determined by RP-HPLC. All the experiments were carried out in duplicate.

In order to standarise the results, the fraction of pimaricin at each sampling time was calculated as follows:

$$F_t = 1 - \frac{C_0 - C_t}{C_0} \tag{33}$$

where $C_t$ and $C_0$ are the concentration of pimaricin (μg $mL^{-1}$) at time $t$ and at initial time respectively.

**5.1.4. Dose-response curves.** We performed a dose-response assay in two different matrices: culture broth and grape juice. Both matrices were inoculated with 830 μL of a 12-hour culture of the indicator microorganism (6x$10^7$ CFU $mL^{-1}$), *Saccharomyces cerevisiae* (Sc 1.02). This matrices were added with a pimaricin solution prepared under sterile conditions to obtain concentrations of pimaricin ranging from 0 to 10 μg $mL^{-1}$. Then, they were incubated at 120 rpm and 37 ºC and 25 ºC, for the culture broth and grape juice respectively. At selected times, aliquots of 1 mL were removed in duplicate to follow the Sc 1.02 growth spectophotometrically (Beckman Coulter Inc., Brea, CA, USA) by optical density (OD) detection at 600 nm.

**5.1.5. Inhibition studies.**

5.1.5.1. *Preparation of pimaricin-loaded nanohydrogel.* The nanohydrogels employed in this work, NIPA homopolymer (PNIPA(5)) and NIPA copolymerized with AA (PNIPA-20AA(5)), were synthesized as explained in Section 2.1.2 on page 47 (Chapter 2).

For the inhibition studies employing a liquid food model system the nanohydrogels samples loaded with pimaricin were prepared as explained in Section 3.1.2 on page 65 (Chapter 3) but using the YPD broth as a solvent to avoid the growing broth dilution with water in a subsequent step. PNIPA/AA nanohydrogel powder was dispersed in a sterile YPD broth by agitation using a magnetic stirrer during 3 hours at ambient temperature to allow a proper swelling of the nanoparticles. Subsequently, this suspension was mixed with a pimaricin solution prepared also in sterile YPD broth to obtain final concentrations of 12.5 mg of nanohydrogel per mL and 0.4 mg of pimaricin powder per mL (21.93 μg $mL^{-1}$ of solubilized pimaricin). The mixture was stirred overnight at 25 ºC (below LCST) in order to guarantee the incorporation of the pimaricin into the nanohydrogel particles. Nanohydrogel samples without pimaricin and free pimaricin samples were processed in the same conditions as above.

For the inhibition studies employing grape juice we only used the PNIPA-20AA(5) nanohydrogel. Nanohydrogel loaded with pimaricin, nanohydrogel without pimaricin and free pimaricin samples were prepared in the same manner as explained above but replacing the YPD broth by white grape juice. The pH of the grape juice employed at this point was increased to 8 during the loading step in order to guarantee the correct swelling of nanohydrogel particles since at the pH of the grape juice (3.5) the PNIPA-20AA(5) collapses, as we saw in Section 2.2.2 on page 53 (Chapter 2). The experiments were carried out in duplicate under sterile conditions.

5.1.5.2. *Preparation of indicator microoganism suspension.* The culture of the indicator microorganism was prepared by inoculating the 12 mL of the YPD broth with a 12-hour Sc 1.02 culture ($6x10^7$ CFU $mL^{-1}$). Its final OD at 600 nm was adjusted to 0.020 (1 mm path length).

The culture of the indicator microorganism for the inhibition studies in grape juice was prepared in three steps. The stock culture of Sc 1.02 was firstly growth in the YPD broth. After 12 hours this culture was used as inoculum in a new culture with grape juice (pH 3.5). Finally, after 12-hours, this last culture ($6x10^7$ CFU $mL^{-1}$) was used as

inoculum for 12 mL of grape juice. Its final OD at 600 nm was adjusted to 0.010 (1 mm path length). The experiments were carried out in duplicate under sterile conditions.

5.1.5.3. *Growth inhibition assay.* The samples, prepared as explained in Section 5.1.5.1 on page 116, were distributed among the following treatments: PNIPA(5) nanohydrogel suspension without ($N_{PNIPA(5)}$) and loaded with pimaricin ($NP_{PNIPA(5)}$), PNIPA-20AA(5) nanohydrogel suspension without ($N_{PNIPA\text{-}20AA(5)}$) and loaded with pimaricin ($NP_{PNIPA\text{-}20AA(5)}$), samples treated with free pimaricin solution (P) and, finally, untreated samples (C). 3 mL from these treatments were placed in a dialysis tube and dialyzed against 12 mL of the suspension with the indicator microorganism obtained as explained in Section 5.1.5.2 on the preceding page. Incubation temperature was 37 ºC for the bioassay in culture broth. For the bioassay in grape juice it was 8 ºC during 6 hours and was raised to 25 °C till the end of the experiment. The experiments were carried out in duplicate under sterile conditions.

At selected times, aliquots of 2 μL were removed from the dialysate to follow the Sc 1.02 growth by measuring OD at 600 nm using a Thermo Scientific NanoDrop 2000c (Wilmington, DE, USA) to assume a constant dialysis volume since we can not refund the sample withdrawn in order to maintain the sterility of the culture.

**5.1.6. Growth modelling.** Logistic equation is a widely used model to describe microbial growth as well as for predicting inhibition of microbial growth [227, 18, 199, 196]. However the simple formal description of logistic equation presents drawbacks when we try to do statistically significant comparisons between parameters of practical interest, like maximum rate or the lag period. Therefore, Vázquez and Murado [195] defined the following equation:

$$OD_t = \frac{B}{1 + e^{2+\frac{4\cdot\mu_B}{B}\cdot(\lambda_B - t)}} \tag{34}$$

where $B$ is maximum growth (expressed as OD units) of the microorganism. $\mu_B$ is the maximum specific growth rate ($h^{-1}$) and, $\lambda_B$ and $t$ are the latency and the sampling time, respectively, both expressed in hours (h).

However this equation only will be useful to fit microbial growth in a single phase. Previous works have tried to explain microbial growth in two phases [75]. Nevertheless, in the equation that we propose in this work the maximum microbial growth in the second phase is calculated as $\lim_{t\to\infty} OD_t$ that is the real value for this parameter. So the bilogistic equation is defined as follows:

$$OD_t = \frac{A}{1 + e^{-\frac{4\cdot\mu_A\cdot t}{A}} \cdot \left(-1 + \frac{A}{A_0}\right)} + \frac{B - A}{1 + e^{\frac{2\cdot(B+A+2\cdot\lambda_B\cdot\mu_B)}{B-A} - \frac{4\cdot\mu_B\cdot t}{B-A}}} \tag{35}$$

The first part of the model would be a logistic model, commonly used in the literature to fit microorganism growth or inactivation [199, 49, 51], which would allow us to predict the antifungal effect on the first growth phase. $A_0$ and $A$ is the initial and maximum growth (expressed as OD units), respectively, of the indicator in the presence of antifungal. $\mu_A$ is the maximum specific growth rate ($h^{-1}$) in presence of inhibitor and $t$ (h) is the sampling time.

The second part of the model corresponds with a logistic model reparametrized to shown latency explicitly [195]. In this case latency would refer to cell regeneration time required for the yeast to repair membrane damage caused by pimaricin. Thus, $B$, $\mu_B$ and $\lambda_B$ are the growth parameters described above after the effect of the inhibitor.

**5.1.7. Statistical analysis.** Antimicrobial effectiveness amongst treatments was evaluated by analysis of variance (ANOVA) followed by Bonferroni post-tests for multiple comparisons by using GraphPad Prism™ 5 (GraphPad Software Inc., San Diego, CA, USA).

The fitting data and the significance of the model parameters were assessed using SigmaPlot version 11.0, from Systat Software, Inc. (San Jose California USA).

## 5.2. Results and Discussion

**5.2.1. Pimaricin stability in different matrices.** Degradation kinetics were performed to calculate the pimaricin half-life in the different matrices assayed. Values of the remaining fraction of pimaricin at each time ($F_t$), standarised according to Equation 33 on page 116, are fitted with the following equation:

$$F_t = (F_0 - F_{min}) \cdot e^{-k \cdot t} + F_{min} \tag{36}$$

where $F_t$ and $F_0$ are the fraction of pimaricin at time $t$ and initial time, respectively. $F_{min}$ is the minimum fraction of pimaricin achieved in the different matrices. $k$ is the pimaricin degradation rate ($h^{-1}$) and $t$ is the sampling time (h). The half-life (h) is defined as $\frac{\ln 2}{k}$.

The results of monitoring the pimaricin degradation are depicted in Figure 27 on the facing page and and fitting parameters of the Equation 36 are summarized in Table 13 on page 122. The rate of pimaricin degradation ($k$) in grape juice is 2-fold higher ($p = 0.0091$) than that observed in YPD broth. There are not significant ($p = 0.2393$) differences between the $F_{min}$ achieved in culture broth and grape juice. It seems that, regardless of temperature, the conditions provided by the grape juice (pH 3.5) more importantly affect the degradation of pimaricin. Because, at low pH values, pimaricin is rapidly degraded, producing mycosamine by hydrolysis of the glycosidic bond [99].

When we subject the pimaricin-treated juice to pasteurization temperatures (80 ºC) the pimaricin degradation is significantly increased (Figure 27 on the next page), as the $k$ value is nearly 50 times higher ($p = 0.0021$) at 80 ºC than at 25 ºC in grape juice. Consequently the half-life is also reduced (Table 13 on page 122). There are not significant ($p = 0.1110$) differences between the $F_{min}$ achieved in grape juice at 25 ºC and 80 ºC.

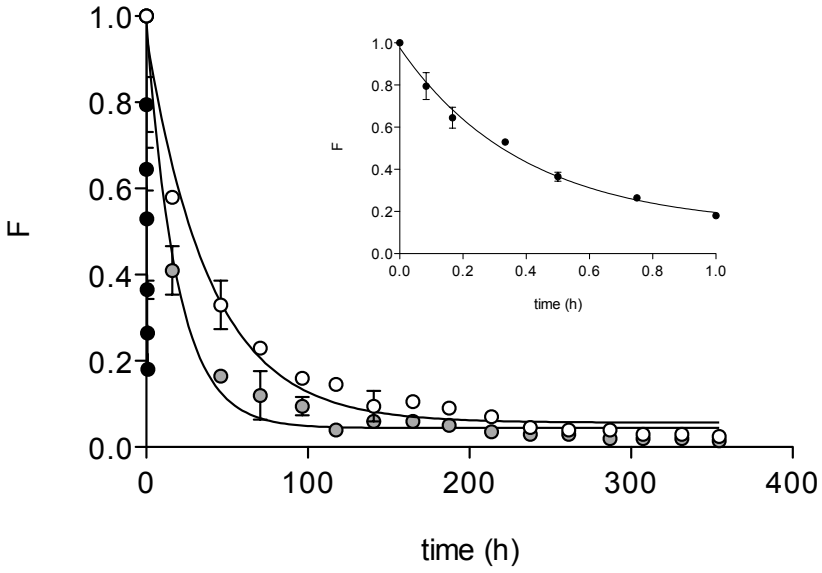


FIGURE 27. Variation of remaining fraction of pimaricin (*F*), standarised according to Equation 33 on page 116, in YPD broth at 37 ºC (○) and grape juice at 25 ºC (●) and 80 ºC (●), the graph inset is an enlarged representation of these data). The lines are the fitting curves generated from Equation 36 on the facing page ($r^2_{\text{YPD broth-37 ºC}}$ = 0.9813; $r^2_{\text{grape juice-25 ºC}}$ = 0.9839; $r^2_{\text{grape juice-80 ºC}}$ = 0.9850).

Pedersen [144] showed losses of 34% at 50 ºC during the preparation of YPD plates, and then the half-life in these plates was 31 d at 6 ºC under dark conditions. In our case the half-life is lowered to 27 h (Table 13 on the next page) in YPD broth, as the assay was performed under light and the storage temperature was 37 ºC. In grape juice half-life of pimaricin is further reduced to 13 h (Table 13 on the following page). These results show that pimaricin have a low stability in usual conditions and treatments (heating, acidification, lighting) for production of fresh (non sterilized) juices reducing potentially their antimicrobial activity. This suggests that a procedure to protect pimaricin degradation could be used to improve their antimicrobial activity.

TABLE 13. Pimaricin degradation parameters in different matrices and temperatures calculated with Equation 36 on page 120

| Matrices | T (ºC) | $F_{min}$ | $k$ ($h^{-1}$) | Half-life (h) |
|---|---|---|---|---|
| YPD broth | 37 | 0.057±0.009*** | 0.025±0.002*** | 27.290±1.697*** |
| Grape juice | 25 | 0.044±0.006*** | 0.053±0.003*** | 13.050±0.807*** |
| | 80 | 0.129±0.043n.s. | 2.551±0.339** | 0.272±0.036** |

Values reported are the means±standard deviation ($n$ = 2).

n.s. ($p > 0.05$): not significant.

* ($p < 0.05$): significant.

** ($p < 0.01$): very significant.

*** ($p < 0.001$): extremely significant.

**5.2.2. Assessment of efficacy of free pimaricin to control microbial growth spoilage.** The response of an indicator microorganism of food spoilage (Sc 1.02) to increasing concentrations of pimaricin was evaluated by dose-response analysis, taking as response the time of latency obtained from the growth curves of Sc 1.02 in the presence of different concentrations of pimaricin after fitting with Equation 34 on page 118.

The half maximal inhibitory concentration ($IC_{50}$, µg $mL^{-1}$) of pimaricin in both matrices, YPD broth and grape juice, is calculated by fitting the dose-response data to the Weibull's equation, reparametrized to make explicit the $IC_{50}$ as proposed Murado et al. [126]:

$$\lambda_D = K \cdot \left(1 - e^{-\ln 2 \cdot \left(\frac{D}{IC_{50}}\right)^{\alpha}}\right) \tag{37}$$

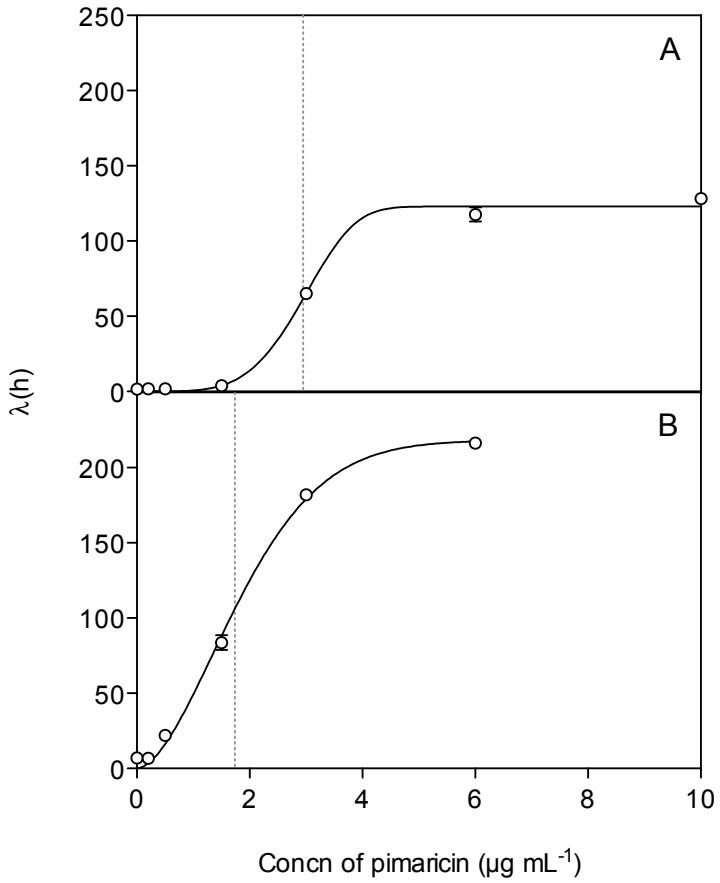


FIGURE 28. Dose-response curves: latency obtained in response to the exposure of a *Saccharomyces cerevisiae* (Sc 1.02) culture in YPD broth at 37 ºC (A) and in grape juice at 25 ºC (B), to increasing concentrations of pimaricin. The lines are the fitting curves generated from Equation 37 on the facing page ($r^2_{\text{YPD broth-37 ºC}} = 0.9984$; $r^2_{\text{grape juice-25 ºC}} = 0.9986$). Dashed lines represent the $IC_{50}$ calculated with Equation 37 on the preceding page.

where $\lambda_D$ is the latency (h) of the indicator microorganism obtained as response to the exposition of different doses of pimaricin ($D$, µg mL$^{-1}$). $K$ is the real maximum response (maximum latency, h) and $\alpha$ is a shape parameter related to the maximum slope of the response.

In Figure 28 on the preceding page is represented the $IC_{50}$ obtained for each matrix. The $IC_{50}$ for pimaricin in culture broth is 2.95±0.06 μg $mL^{-1}$ whilst is 1.74±0.09 μg $mL^{-1}$ in grape juice. This means that the indicator microorganism is more sensitive to pimaricin in grape juice than in culture broth. It must be taking into account that in absence of pimaricin, the latency of Sc 1.02 in grape juice is 4.5 times higher than in culture broth as it provides a poorer media in nitrogen and proteins. Pimaricin acts binding with to ergosterol in membrane cells inhibiting important processes involved in cell regeneration [204], so the absence of an essential nutrient can determine the growth capacity of the microorganism.

**5.2.3. Efficacy of nanohydrogel-pimaricin system to control microbial growth spoilage in a food model system.** To test the antifungal effectiveness of the nanohydrogel-pimaricin system in a liquid food model system, a dialysis against a Sc 1.02 culture at 37 ºC of pimaricin released from the nanohydrogel was performed, measuring the indicator microorganism growth. Thus, experimental growth data (OD) are fitted with the reparametrized logistic model (Equation 34 on page 118) for series without antifungal treatment and reparametrized bilogistic model (Equation 35 on page 119) for series with antifungal treatment.

The results of monitoring the Sc 1.02 growth, depicted in Figure 29 on page 126 and summarized in Table 14 on the facing page, show that the pimaricin-loaded nanohydrogel system was highly effective inhibiting the growth of the indicator strain. Treatments with pimaricin (P, $NP_{PNIPA(5)}$ and $NP_{PNIPA\text{-}20AA(5)}$) lead to a 2-fold reduction ($p < 0.05$) in the yeast growth with regard to samples without pimaricin. Pimaricin-free nanohydrogels ($N_{PNIPA(5)}$ and $N_{PNIPA\text{-}20AA(5)}$) seem to have no negative effect on yeast growth as they do not present significant ($p > 0.05$) differences in growth parameters respect to control cultures without nanohydrogel.

Additionally, the combined effect of antifungal and nanohydrogel is able to extent the latency of Sc 1.02 growth further than the pimaricin alone (Table 14 on the next page). The $\lambda_B$ is increased significantly ($p < 0.05$) from 12.39±0.54 to 81.19±0.17 h with P and

TABLE 14. Growth parameters of *Saccharomyces cerevisiae* (Sc 1.02) in culture broth under different antimicrobial treatments, calculated with Equation 34 on page 118 and Equation 35 on page 119

| Treatment | $A$ | $\mu_A$ ($h^{-1}$) | $A_0$ | B | $\mu_B$ ($h^{-1}$) | $\lambda_B$ (h) | $r^2$ |
|---|---|---|---|---|---|---|---|
| C | - | - | - | $0.433\pm0.009^{***}$ | $0.069\pm0.008^{***}$ | $1.554\pm0.475^{**}$ | 0.9731 |
| $N_{PNIPA(5)}$ | - | - | - | $0.458\pm0.015^{***}$ | $0.105\pm0.025^{**}$ | $1.231\pm0.607^{n.s.}$ | 0.9631 |
| $N_{PNIPA\text{-}20AA(5)}$ | - | - | - | $0.393\pm0.008^{***}$ | $0.059\pm0.007^{***}$ | $1.313\pm0.288^{*}$ | 0.9865 |
| P | $0.049\pm0.004^{***}$ | $0.015\pm0.009^{n.s.}$ | $0.019\pm0.007^{*}$ | $0.219\pm0.004^{***}$ | $0.033\pm0.004^{***}$ | $12.390\pm0.541^{***}$ | 0.9946 |
| $NP_{PNIPA(5)}$ | $0.088\pm0.008^{***}$ | $0.014\pm0.005^{*}$ | $0.023\pm0.009^{*}$ | $0.292\pm0.009^{***}$ | $0.011\pm0.002^{***}$ | $14.500\pm2.230^{***}$ | 0.9856 |
| $NP_{PNIPA\text{-}20AA(5)}$ | $0.052\pm0.002^{***}$ | $0.035\pm0.022^{n.s.}$ | $0.020\pm0.008^{*}$ | $0.243\pm0.008^{***}$ | $0.117\pm0.272^{n.s.}$ | $81.191\pm0.167^{***}$ | 0.9860 |

Values reported are the means±standard deviation ($n = 2$).

$^{n.s.}$($p > 0.05$): not significant.

$^{*}$($p < 0.05$): significant.

$^{**}$($p < 0.01$): very significant.

$^{***}$($p < 0.001$): extremely significant.

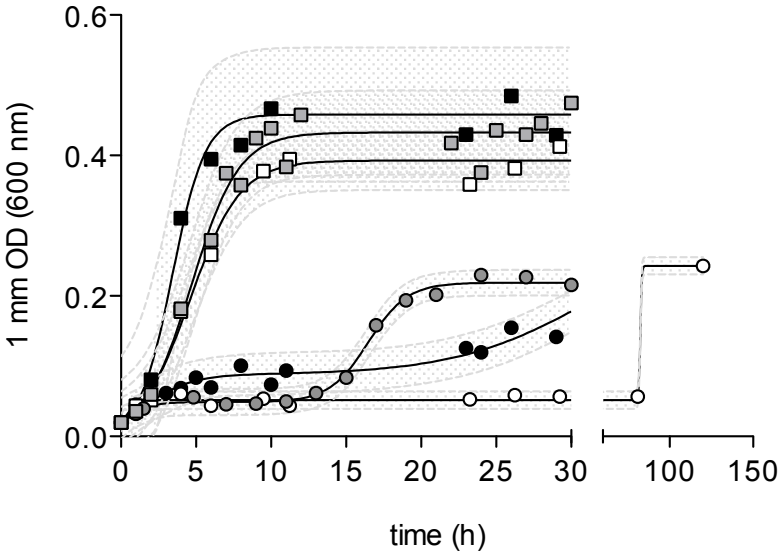


FIGURE 29. Effect of different antimicrobial devices in *Saccharomyces cerevisiae* (Sc 1.02) growth. Control samples without pimaricin: $N_{PNIPA(5)}$ (■), $N_{PNIPA\text{-}20AA(5)}$ (□) and C (■). Samples with pimaricin: $NP_{PNIPA(5)}$ (●), $NP_{PNIPA\text{-}20AA(5)}$ (○) and P (●). The line is the fitting curve generated from Equation 34 on page 118 and 35 on page 119. Dotted area corresponds to the 95% prediction band.

$NP_{PNIPA\text{-}20AA(5)}$ treatments, respectively. Also, the advantage of the use of nanohydrogels with acrylic acid is demonstrated when we compare both inhibition curves. $NP_{PNIPA\text{-}20AA(5)}$ is able to stop completely Sc 1.02 growth during 81.19±0.17 h while $NP_{PNIPA(5)}$ only maintain the inhibition during 14.50±2.32 hours, after which an exponential growth is observed. In addition there is no significant ($p > 0.05$) differences between $\lambda_B$ of samples treated with P and $NP_{PNIPA(5)}$.

These results are consistent with those observed during the release studies in water (Chapter 3 on page 65), and allow to confirm that nanohydrogels can be used to release pimaricin in a slow and continuous way maintaining levels of pimaricin enough to control yeast growth. Additionally the nanohydrogel avoid the pimaricin degradation in the YPD broth and open the possibility to use these release systems in real foods.

**5.2.4. Control of grape juice spoilage employing pimaricin-loaded nanohydrogels.** Pasteurized refrigerated (fresh) juices are the most accepted among commercial juice because its flavour is clearly fresher than juices marketed at room temperature. However the stability of these products depends greatly of limiting the recontamination by preserving the cold chain and limiting the duration of refrigerated storage after opening the package. The use of sulphites, which are usually added to juices can reduce this recontamination. However, allergic disorders associated with this compound suggest the use of alternatives such as pimaricin. Pimaricin could be added after pasteurization treatments but, in Section 5.2.1 on page 120 it was demonstrated that degradation of pimaricin under heat treatments or storage at room temperature in grape juices reduce significantly the pimaricin initially added compromising their efficacy. Also, addition of pimaricin after pasteurization is not possible if the aseptic packaging juice is used.

To address this problem, two alternatives are possible. The first one is increase the initial pimaricin concentration to ensure its stability during prolonged storage times. This mainly occurs in products that are not continuously stored under cooling and may suffer a recontamination, such as juices once purchased by consumers. In view of the good results obtained in the liquid food model system (Section 5.2.3 on page 124) with $NP_{PNIPA\text{-}20AA(5)}$ treatment, the second alternative presented in this work is the use of this system, which can act as protector against pimaricin degradation, while allowing its controlled release. Then, this system enables to adjust the pimaricin dosage over time, reducing the amount of pimaricin present in the juice.

In this sense Figure 30 on the next page shows a comparison of the effect on yeast growth of pimaricin treatments directly added to a grape juice or included into the nanohydrogel. Control treatments with and without nanohydrogels (C and $N_{PNIPA\text{-}20AA(5)}$) seem to have no effect on Sc 1.02 growth in contrast with pimaricin treatments (P and $NP_{PNIPA\text{-}20AA(5)}$). Table 15 on page 129 shows the growth parameters of Sc 1.02 in the presence of different treatments, after fitting the experimental data of growth to Equation 34 on page 118. There are not significant ($p > 0.05$) differences between Sc 1.02 growths

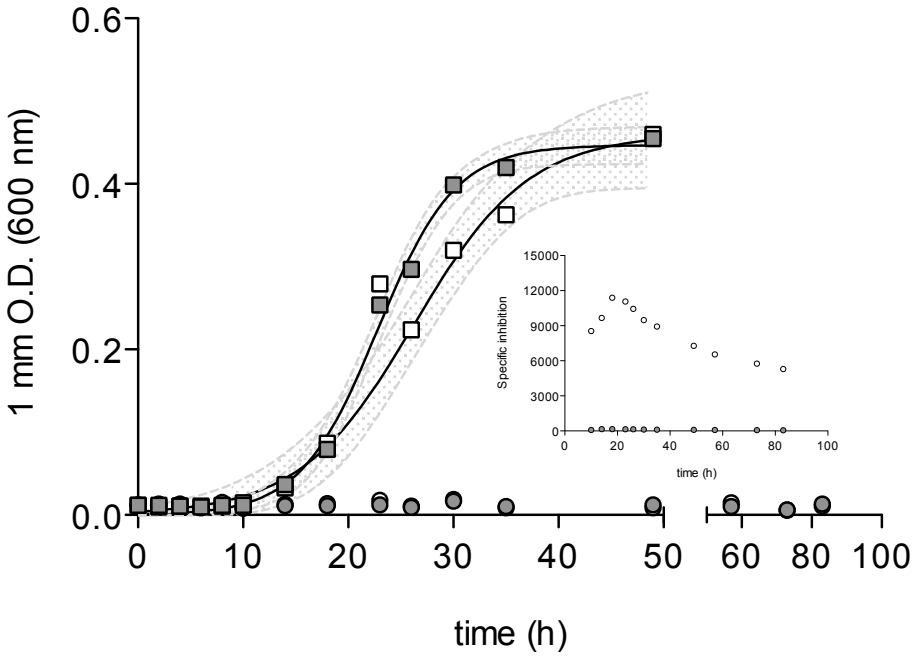


FIGURE 30. Effect of different antimicrobial devices in *Saccharomyces cerevisiae* (Sc 1.02) growth. Control samples without pimaricin: $N_{PNIPA\text{-}20AA(5)}$ (□) and C (■). Samples with pimaricin: $NP_{PNIPA\text{-}20AA(5)}$ (○) and P (●). The line is the fitting curve generated from Equation 34 on page 118. Dotted area correspond to the 95% prediction band. The figure inset represents the specific inhibition at different times.

in control treatments (C and $N_{PNIPA\text{-}20AA(5)}$). So, these results confirm the above obtained in liquid food model system (Section 5.2.3 on page 124) because the nanohydrogel does not interfere with Sc 1.02 growth and, completely inhibiting the pimaricin treatments (P and $NP_{PNIPA\text{-}20AA(5)}$) the growth of Sc 1.02 through the end of the bioassay (Figure 30).

The Equation proposed in Section (Chapter 3) allow us calculate the pimaricin released under the conditions (pH and temperature) assayed during the grape juice storage. So the maximum concentration of pimaricin released during all the experiment would be equal to 0.35±0.02 μg $mL^{-1}$. This concentration is significantly lower ($p < 0.05$) than the $IC_{50}$ calculated in Section 5.2.2 on page 122 for free pimaricin in grape juice (1.74±0.09 μg $mL^{-1}$). Consequently, it seems that the nanohydrogel acts protecting the

TABLE 15. Growth parameters of *Saccharomyces cerevisiae* (Sc 1.02) in grape juice under different antimicrobial treatments, calculated with Equation 34 on page 118

| Treatment | B | $\mu_B$ ($h^{-1}$) | $\lambda_B$ (h) | $r^2$ |
|---|---|---|---|---|
| C | 0.447±0.011*** | 0.030±0.002*** | 15.440±0.628*** | 0.9886 |
| $N_{PNIPA\text{-}20AA(5)}$ | 0.460±0.032*** | 0.021±0.003*** | 15.381±1.770*** | 0.9415 |
| P | - | - | - | - |
| $NP_{PNIPA\text{-}20AA(5)}$ | - | - | - | - |

Values reported are the means±standard deviation ($n$ = 2).

***($p < 0.001$): extremely significant.

pimaricin from the degradation providing a more effective inhibition. In this way we calculated the specific inhibition as follows:

$$\%Inhibition = \frac{OD_0 - OD}{OD_0};\ Specific\,inhibition = \frac{\%Inhibition}{C_t} \tag{38}$$

where, $OD_0$ is the optical density of the samples in control treatments (C and $N_{PNIPA\text{-}20AA(5)}$) and $OD$ is the optical density of samples with pimaricin (P and $NP_{PNIPA\text{-}20AA(5)}$). $C_t$ is de concentration of pimaricin (µg $mL^{-1}$) at each sampling time.

The inset in Figure 30 on the preceding page represents the specific inhibition of Sc 1.02 with P and NP treatment, showing a clearly higher specific inhibition with the $NP_{PNIPA\text{-}20AA(5)}$ treatment compared to P treatment.

CHAPTER 6

# Sumario y conclusiones finales

El trabajo presentado en esta tesis describe la caracterización físico-química y funcional de los nanohidrogeles de poli (*N*-isopropilacrilamida) con (PNIPA) sintetizados con diferente grado de hidrofilia mediante la incorporación de ácido acrílico (AA), para su utilización en el envasado activo de alimentos. Para llevar a cabo estos estudios se han utilizado diversas técnicas de análisis físico-químico, tanto de las nanopartículas sintetizadas como de los alimentos usados como modelo. Asimismo se han puesto a punto diversas técnicas espectrofotométricas y cromatográficas con el fin de cuantificar el agente antimicrobiano usado como modelo (pimaricina), así como diversas técnicas de microbiología clásica y de biología molecular. El conjunto integrado de todos los estudios realizados nos ha permitido conocer mejor el funcionamiento de los nanohidrogeles de PNIPA/AA en función de las condiciones ambientales así como su efectividad en la liberación controlada de antimicrobianos y su aplicación en la conservación de alimentos.

En el **Capítulo 1** de esta tesis se da una visión general del estado del arte del envasado activo de alimentos y como la aplicación de la nanotecnología puede aportar nuevas y prometedoras soluciones dentro de este campo. Asimismo, se han descrito las principales características de la pimaricina, tanto sus ventajas como antimicrobiano de origen natural como sus desventajas asociadas con su baja estabilidad en condiciones que frecuentemente encontramos en los alimentos (pH ácido, exposición a la luz, tratamientos térmicos, ...). Hasta el momento en los estudios realizados usando pimaricina como agente antimicrobiano en alimentos, ésta se ha añadido directamente al alimento o aplicado mediante su inclusión en films que permite su liberación únicamente por difusión por diferencia de concentraciones. Sin embargo, en este trabajo nosotros proponemos el

uso de nanohidrogeles para el transporte y liberación de pimaricina, capaces de liberarla como respuesta a la variación de las condiciones ambientales presentes en el alimento (pH y temperatura).

El **Capítulo 2** describe la síntesis de nanohidrogeles de PNIPA/AA mediante sistemas agua-aceite. Se estudiaron como variables principales la concentración de AA y porcentaje de entrecruzante. Una vez sintetizados se llevó a cabo el estudio de las propiedades físico-químicas de dichos nanohidrogeles (tamaños de partícula, potencial Z, temperatura crítica de colapso) en función de su composición. Asimismo, se ha modelado el comportamiento de los nanohidrogeles de PNIPA que permite establecer una relación empírica entre su composición y sus propiedades termodinámicas asociadas con el grado de colapso en función de pH, la temperatura y el solvente.

Los resultados obtenidos nos muestran como la introducción de más entrecruzante en el polímero aumenta la rigidez de éste limitando su capacidad para hincharse y colapsar de manera que los cambios estructurales asociados con el incremento de la temperatura van a ser más suaves. La introducción de AA en la matriz polimérica también da lugar a cambios importantes en el comportamiento de los nanohidrogeles de PNIPA. El aumento en la carga negativa de las nanopartículas produce una aumento de la repulsión entre cargas del mismo signo que, junto con el aumento de la presión osmótica debido a la presencia de contraiones, va a contribuir a expandir la matriz polimérica dando lugar a un gel más hinchado. El efecto conjunto del aumento en el contenido AA y en el entrecruzante da lugar a interacciones que producen un gel más rígido.

En lo referente al comportamiento de los nanohidrogeles de PNIPA/AA frente a la temperatura y al pH, vimos como la introducción de un grupo hidrófilo va a suavizar los cambios debidos a la temperatura, siempre y cuando el pH del solvente en el que se encuentre el gel esté por encima del $pK_a$ del AA, de manera que su punto crítico de colapso se sitúa en temperaturas más elevadas. A pH < $pK_a$ los grupos carboxilo aportados por el AA no están ionizados dando lugar la dimerización de estos grupos mediante puentes

de hidrógeno dan lugar al colapso del hidrogel. El pH no tuvo influencia alguna en los homopolímeros de PNIPA debido a la ausencia de grupos ionizables.

La influencia de los solventes alcohólicos, como el metanol, en el colapso de los nanohidrogeles de PNIPA/AA va depender en gran medida del fracción alcohólica presente en la mezcla. Así los nanohidrogeles de PNIPA van a colapsar a medida que aumentamos la fracción de metanol en el solvente hasta alcanzar una fracción crítica —en torno a 0,4— a partir de la cual el comportamiento cambia drásticamente de manera que el nanohidrogel se hincha a medida que aumentamos la proporción de metanol. En los nanohidrogeles más hidrófilos (con AA), al igual que en los casos anteriores, el colapso por efecto del metanol es menos intenso. El grado de hinchamiento de los nanohidrogeles en metanol y en agua puros no ofrece diferencias importantes tanto en los geles con AA como en los homopolímeros.

Una vez analizadas las características físico-químicas de los nanohidrogeles de PNIPA-/AA y su comportamiento frente a diferentes condiciones ambientales, en el **Capítulo 3** evaluamos la capacidad de estos nanohidrogeles para transportar y liberar pimaricina en función su composición y de las condiciones ambientales en las que se encuentra con el fin de evaluar su aplicación en el envasado activo de alimentos.

En primer lugar estudiamos la capacidad de los nanohidrogeles de PNIPA/AA para encapsular pimaricina. Los resultados mostraron ésta capacidad aumenta a medida que disminuimos el contenido en entrecruzante en el gel y aumentamos el tiempo de incorporación, siendo más intenso el efecto del incremento en el tiempo de incorporación cuanto mayor es el contenido en entrecruzante. El incremento en el tiempo de incorporación proporciona más tiempo para que la pimaricina difunda al interior de la matriz polimérica.

El contenido en AA prácticamente no afectó a la eficiencia de carga sugiriendo que las interacciones que se puedan producir entre la pimaricina y el nanohidrogel son de carácter débil. No hubo diferencias significativas entre la eficiencia de carga obtenida en

metanol y en agua destilada, en concordancia con lo descrito en el Capítulo 2 en el que vimos que el grado de hinchamiento no varía entre ambos solventes puros.

Para el estudio de la liberación pimaricina desde los nanohidrogeles de PNIPA/AA en primer lugar evaluamos la efectividad del sistema diseñado para tal fin, en el que la pimaricina tiene que difundir a través de dos barreras: la matriz del nanohidrogel y la membrana de diálisis. Se ha visto como la membrana de diálisis no limita la difusión de la pimaricina hacia el medio de liberación, por lo que a la hora de estudiar la difusión desde los nanohidrogeles serán éstos los únicos que influyan en la cinética de liberación.

Se ha estudiado la influencia de la composición y del tiempo de incorporación en la liberación de la pimaricina desde los nanohidrogeles de PNIPA/AA. El aumento en el tiempo de incorporación supuso, para todos los nanohidrogeles estudiados, una disminución de la fracción máxima de pimaricina liberada ($\gamma F_{max}$) debido a que la pimaricina tiene más tiempo para difundir al interior de la matriz polimérica, como vimos cuando estudiamos la eficiencia de carga, de manera que la pimaricina permanece más atrapada impidiendo su posterior liberación. La influencia del contenido en AA y del entrecruzante en la liberación de pimaricina desde los nanohidrogeles de PNIPA/AA está directamente relacionada con la influencia de estos factores sobre las características físico-químicas del gel. Así una disminución en el contenido en entrecruzante da lugar a un gel más flexible que colapsa de forma más intensa en el que la pimaricina va a quedar más atrapada.

Durante el estudio de las cinéticas de liberación en geles con diferente grado de hidrofilia vemos como la introducción de AA en los nanohidrogeles de PNIPA con un 5% de entrecruzante permite a una liberación de pimaricina más lenta y continuada frente al homopolímero de con el mismo contenido en entrecruzante con el cual la liberación se detiene muy pronto obteniendo valores finales de $\gamma F_{max}$ más bajos. Los resultados sugieren que la pimaricina puede quedar en una zona más expuesta en los homopolímeros de PNIPA. Al colapsar éstos con una mayor intensidad debido al aumento de la temperatura expulsan rápidamente esta pimaricina y la liberación se paraliza pronto. En los

homopolímeros con menos entrecruzante el colapso es aún mas intenso aumentando este efecto *burst*.

El ajuste de las cinéticas de liberación al modelo de Korsmeyer-Peppas, que fue el que proporcionó mejores coeficientes de correlación ($r^2 > 0{,}98$), nos permitió clasificar el tipo de difusión desde los nanohidrogeles de PNIPA/AA. Así el mecanismo de liberación desde el homopolímero con un 5% de entrecruzante se clasifica como difusión fickiana en el que la liberación de la biomolécula está únicamente gobernado por la difusión de ésta hacia el medio de liberación. Mientras que la liberación desde el nanohidrogel con AA se clasifica como no-fickiana o transporte anómalo en el cual la liberación de la biomolécula está controlada tanto por la difusión de ésta hacia el medio de liberación como por el propio comportamiento del nanohidrogel (hinchamiento/colapso). Estos resultados concuerdan con los descritos anteriormente, en los que asumimos que la pimaricina liberada desde el nanohidrogel más hidrófobo probablemente sólo se corresponda con aquella que permanece más en la superficie del nanohidrogel y que una vez que el gel colapsa ésta es liberada debido a las fuerzas convectivas generadas hacia el medio de liberación. En el caso del nanohidrogel más hidrófilo, la pimaricina tiene que difundir desde el interior de la matriz polimérica, aparentemente con mayor dificultad que cuando se encuentra en la superficie del nanohidrogel, dando lugar a un incremento en el coeficiente de difusión que clasifica la liberación como no-fickiana.

Además hemos modelado la liberación de la pimaricina desde los nanohidrogeles de PNIPA/AA en función de la temperatura y del pH que nos permite calcular la concentración de pimaricina liberada a un tiempo determinado y para unas condiciones ambientales específicas. Los resultados obtenidos cuando estudiamos el efecto de la temperatura por separado corroboran de nuevo lo explicado anteriormente. El colapso más intenso en los nanohidrogeles sin AA va a generar un mayor atrapamiento de las moléculas de pimaricina paralizando su liberación. Mientras que la introducción de AA reduce el grado de colapso que se produce al aumentar la temperatura de manera que

la pimaricina puede difundir mejor a través de la matriz polimérica prolongando la cantidad liberada y el tiempo de liberación. La temperatura óptima de liberación con el nanohidrogel con AA sería 40,04 ºC mientras que con el nanohidrogel sin AA la temperatura óptima calculada mediante el modelo propuesto sería -1,25 ºC que, aunque obviamente se encuentra fuera del intervalo experimental, indica claramente que la liberación desde este nanohidrogel aumenta a medida que disminuimos la temperatura y el gel se hincha. El comportamiento de los nanohidrogeles con AA frete al pH es similar la observado con la temperatura, esto es, que al disminuir el pH el gel colapsa aumentando la liberación de pimaricina desde el nanohidrogel, pero una vez que el pH disminuye hasta valores inferiores al $pK_a$ del AA el colapso del nanohidrogel es tan intenso que el atrapamiento físico impide la liberación de la pimaricina de la misma forma que lo hacía el homopolímero de PNIPA al aumentar la temperatura.

Por último, estudiamos la capacidad de los nanohidrogeles de PNIPA/AA para liberar la pimaricina cuando alternamos ciclos de temperatura por encima y por debajo del punto crítico de colapso de los nanohidrogeles de PNIPA. Los resultados obtenidos con el homopolímero de PNIPA son consistentes con el mecanismo de liberación positiva, esto es, al aumentar la temperatura la liberación de pimaricina aumenta rápidamente seguida de un proceso de liberación mucho más lento. Al introducir AA en el polímero los cambios de temperatura no afectan tanto a la velocidad de liberación y la liberación continua durante más ciclos que en el caso del homopolímero. En cualquier caso se obtuvieron liberaciones más elevadas alternando varios ciclos de hinchamiento/colapso que un único ciclo y con el gel más hidrófilo se obtuvieron liberaciones más sostenidas en el tiempo. Esto último puede ser de gran utilidad en la industria alimentaria ya que así el efecto antifúngico puede mantenerse durante tiempos más largos. Si el antifúngico se libera en un solo ciclo este podría degradarse más fácilmente y por lo tanto no estar activo para posteriores recontaminaciones.

Teniendo en cuenta entonces el potencial de los nanohidrogeles de PNIPA/AA cargados con pimaricina para el envasado activo de alimentos, en el **Capítulo 4** evaluamos

la efectividad antimicrobiana de estos nanosistemas en el control del crecimiento de hongos empleando en primer lugar un sistema modelo basado en placas de agar para levaduras (PDA) para luego aplicarlo directamente sobre un alimento real, en nuestro caso quesos de la DOP Arzúa-Ulloa.

Con el estudio de la efectividad antimicrobiana de los sistemas nanohidrogel-pimaricina empleando sistemas modelo inoculados con un microorganismo indicador (*Saccharomyces cerevisiae*) comprobamos el efecto protector que ejerce el nanosistema propuesto. Así los mejores resultados se obtuvieron cuando las placas de PDA se incubaron bajo condiciones que comprometían la estabilidad de la pimaricina (pH ácido y almacenamiento con iluminación fluorescente). La reducción en el crecimiento de microorganismo indicador con respecto a un control sin tratamiento antifúngico fue de 80,94±33,02% para el nanohidrogel cargado con pimaricina, que fue significativamente mayor que la observada en las placas tratadas con pimaricina libre, 19,91±6,68%. Mientras en que las placas sin acidificar almacenadas a oscuridad, aunque la reducción fue mayor con el nanohiddrogel cargado con pimaricina (27,07±4,15%), la diferencia con respecto a la reducción con pimaricina libre no fue significativa (17,26±1,34%).

Por lo tanto, el efecto antifúngico de la pimaricina fue potenciado cuando ésta se aplica incluida en el nanohidrogel, probablemente debido a que solamente es liberada cuando las condiciones ambientales lo requieren ralentizando su degradación. Por lo tanto el sistema nanohidrogel-pimaricina puede ser útil en alimentos que se contaminan fácilmente por el crecimiento de hongos (esto es, con pHs ácidos y alto contenido en agua) y que normalmente están expuestos a cambios en la temperatura de almacenamiento durante su transporte y exposición a la venta.

La pimaricina se usa de forma habitual para la prevención de la contaminación superficial de quesos. Es por esto que elegimos este alimento para evaluar la efectividad antimicrobiana del sistema nanohidrogel-pimaricina en un alimento real. La liberación

controlada de pimaricina desde estos nanosistemas puede reducir la cantidad de pimaricina que migra desde la superficie del queso hacia su interior y por tanto reducir la ingestión de conservantes por el consumidor.

Además de la efectividad antimicrobiana también estudiamos el efecto que los nanohidrogeles de PNIPA/AA tienen sobre las características físico-químicas del queso. Los resultados obtenidos sugirieren que el recubrimiento con nanohidrogeles de PNPA/AA no tuvo un efecto negativo sobre la maduración natural del queso. En los quesos en los no se forzó la contaminación no se encontraron diferencias significativas ($p > 0.05$) entre los tratamientos ya que es difícil encontrar diferencias cuando realizamos recuentos microbianos con la muestra entera de queso y no solo en superficie. Es por esto que en el siguiente experimento forzamos la contaminación de los quesos usando como microorganismo indicador *Saccharomyces cerevisiae*. Los recuentos en los quesos tratados con nanohidrogel cargado con pimaricina fueron inferiores a los obtenidos con pimaricina libre aunque estás diferencias sólo fueron significativas ($p < 0.05$) hasta los 22 días. Por lo tanto, a pesar de que el efecto antimicrobiano conseguido no se mantuvo durante mucho tiempo, quizás por partir de una contaminación inicial muy elevada, las diferencias encontradas con respecto a tratamiento con pimaricina libre evidencian el efecto protector del nanohidrogel cargado con pimaricina que ya observamos con los sistemas modelo en placas de PDA y que van a permitir mantener el efecto antimicrobiano durante más tiempo reduciendo la cantidad de pimaricina presente en el alimento.

Además en este Capítulo llevamos a cabo la puesta a punto de un método para cuantificar hongos totales mediante PCR cuantitativa o en tiempo real (qPCR) como alternativa a los métodos tradicionales de recuento en placa más tediosos y que además, en el caso del recuento de hongos, pueden dar lugar a confusión debido a que su recuento depende en gran medida de su estado fisiológico y capacidad para crecer en el medio de cultivo. El ensayo fue lineal a lo largo de 7 órdenes de magnitud siendo el límite de detección de 1 unidad logarítmica para el ADN extraído de cultivos puros. La eficiencia de la reacción fue 0,91±0,08, lo que significa que tasa de amplificación fue

muy eficiente, y el ensayo de qPCR fue muy lineal (r2 = 0,9987). El límite de detección para la cuantificación de hongos totales en queso es de cerca de 2 unidades logarítmicas más alto que el obtenido con los cultivos puros. A pesar de ello el ensayo es lineal a lo largo de 4 órdenes de magnitud. Aunque la amplificación en queso es altamente lineal ($r^2$ = 0,9995), la eficiencia es demasiado alta (1,47±0,17), probablemente debido a la presencia de inhibidores procedentes del queso que no se eliminaron durante la extracción del ADN. También podría ser debido a la presencia de gran cantidad de ADN no-objetivo proveniente otros microorganismos presentes en el queso ya que los valores de $C_T$ de las muestras de control negativo (quesos sin contaminación artificial) son demasiado bajos (23,08 ± 0,59).

Los recuentos de los quesos contaminados con el microorganismo indicador (*Saccharomyces cerevisiae*) realizados mediante recuento en placa fueron comparados con los resultados obtenidos en el análisis mediante qPCR. La correlación entre los recuentos mediante qPCR y recuento en placa fue bueno, alrededor de 100% de precisión. Sin embargo los recuentos obtenidos mediante qPCR fueron más altos que los obtenidos mediante recuento en placa como resultado de la presencia de hongos viables pero no cultivables o más probablemente debido a presencia de células muertas en las muestras de queso.

Por último en el **Capítulo 5** evaluamos la capacidad de los sistemas nanohidrogel-pimaricina para alargar el tiempo de vida útil de zumos de fruta refrigerados (pasteurizados) mediante la liberación controlada del antifúngico. Para ello en primer lugar probamos el nanosistema en un sistema modelo para luego usarlo en zumo de uva.

En primer lugar se ha evaluado un método para cuantificar pimaricina en medio de cultivo para levaduras (YPD) y en zumo de uva mediante cromatografía líquida en fase reversa (RP-HPLC). El ensayo fue altamente lineal ($r^2$ = 0,9996) en el intervalo de concentraciones evaluado (0,05 a 10 μg $mL^{-1}$). Las recuperaciones obtenidas empleando patrones de pimaricina pura fueron bastante altos: 98,11% y 97,32% en el medio de

cultivo y en zumo de uva, respectivamente. Por lo que podemos prescindir de un paso previo de extracción para la detección de pimaricina en las matrices empleadas.

A continuación evaluamos la estabilidad de la pimaricina en medio de cultivo YPD y en zumo de uva. La velocidad de degradación de la pimaricina en zumo fue 2 veces más alta que en medio de cultivo probablemente debido al bajo pH del zumo de uva. El tratamiento de pasteurización también ejerció un efecto importante sobre la degradación de la pimaricina aumentando cerca de 50 veces la velocidad de degradación en zumo de uva. Los resultados mostraron la baja estabilidad de la pimaricina en condiciones que habitualmente podemos encontrar en los alimentos. Por lo tanto, el desarrollo de sistemas que actúen protegiendo a la pimaricina de la degradación podría contribuir a mejorar su actividad antimicrobiana.

Por otro lado evaluamos la capacidad inhibitoria de la pimaricina en las matrices empleadas en este capítulo, medio de cultivo YPD y zumo de uva, mediante la construcción de dosis-respuesta usando *Saccharomyces cerevisiae* como microorganismo indicador. Así la dosis inhibitoria 50 ($IC_{50}$) en medio de cultivo YPD fue 2,95±0,06 μg $mL^{-1}$ mientras que en zumo de uva fue 1,74±0,09 μg $mL^{-1}$. Las condiciones proporcionadas por el zumo con pHs más bajos y la falta de algún nutriente que se encuentra en mayor proporción en el medio de cultivo (fuente de N) hacen que concentraciones más bajas de pimaricina sean más efectivas en esta matriz.

A continuación evaluamos la eficacia del nanohidrogel cargado pimaricina para impedir el deterioro mediante crecimiento microbiano empleando sistemas modelo, que en este caso se basaron en un medio de cultivo YPD inoculado con un microorganismo indicador (*Saccharomyces cerevisiae*). Para el modelado de las curvas de crecimiento en las muestras tratadas con pimaricina, se desarrolló una ecuación bilogística en la que el crecimiento máximo del microorganismo en la segunda fase se calculó como el $\lim_{t \longrightarrow \infty}$, que es el valor real para este parámetro. La primera parte de la ecuación se corresponde con un modelo logístico que nos permite predecir el efecto del antifúngico en la primera

fase del crecimiento del microorganismo indicador. La segunda parte del modelo se corresponde con un modelo logístico reparametrizado para mostrar la latencia de forma explícita y que nos permite modelar el crecimiento del microorganismo indicador tras el efecto del antifúngico, así la latencia se corresponderá con el tiempo necesario para que la levadura se recupere de los daños que pueda causarle la pimaricina y pueda crecer.

Los resultados mostraron que el sistema nanohidrogel-pimaricina propuesto fue muy eficaz inhibiendo el crecimiento del microorganismo indicador, especialmente cuando empleamos el nanohidrogel más hidrófilo. Este nanohidrogel, que como vimos anteriormente proporciona una liberación más lenta y sostenida, incrementó el tiempo de latencia del microorganismo indicador de 12,39±0,54, que proporcionó la pimaricina libre, a 81,19±0,17 h. Además el nanohidrogel por si solo no afectó al crecimiento del microorganismo indicador.

Los zumos refrigerados (pasteurizados) presentan una alta aceptación por los consumidores debido a que tiene un sabor y aroma más natural. Sin embargo la estabilidad de estos productos depende en gran medida de evitar la recontaminación manteniendo la cadena de frío especialmente una vez abiertos. Además el uso de sulfitos, que se añaden de forma habitual para evitar este tipo de recontaminaciones, cada vez está menos aceptado debido a su asociación con problemas de alergia. Una alternativa sería la substitución de estos conservantes químicos por conservantes de origen natural como la pimaricina. Sin embargo, como vimos anteriormente, la pimaricina se ve afectada por el tratamiento térmico de pasteurización por lo que para obtener buenos resultados habría que aumentar la concentración inicial para asegurar que, aunque se degrade parte la cantidad activa, ésta sea suficiente para mantener la estabilidad del alimento durante tiempos prolongados de almacenamiento. Otra posibilidad sería añadirla después del tratamiento de pasteurización pero esto comprometería el envasado aséptico de la bebida.

A la vista de los buenos resultados obtenidos en el sistema modelo con el nanohidrogel cargado con pimaricina en comparación con los obtenidos con la pimaricina libre directamente añadida a las muestras, evaluamos este sistema en zumos. El nanohidrogel puede actuar protegiendo a la pimaricina de la degradación durante el almacenamiento, manteniendo una liberación controlada del antifúngico que permite reducir la cantidad de pimaricina presente en la bebida.

Los resultados mostraron que, nuevamente, el nanohidrogel por si solo no afecta al crecimiento del microorganismo indicador. El sistema nanohidrogel-pimaricina actúa inhibiendo totalmente el crecimiento del microorganismo indicador durante el tiempo ensayado de la misma manera que la pimaricina libre. Sin embargo cuando calculamos la inhibición específica respecto a la cantidad de pimaricina presente en el zumo, ésta resulta claramente más alta para el sistema nanohidrogel-pimaricina que para la pimaricina libre. Cuando calculamos la concentración de pimaricina liberada desde el nanohidrogel en las condiciones presentes en zumo, a partir de los modelo de liberación desarrollado en el Capítulo 3, obtenemos que ésta es de 0,35 ± 0,02 μg $mL^{-1}$. Esta concentración es significativamente inferior a la $IC_{50}$ calculada para esta matriz (1,74 ± 0,09 μg $mL^{-1}$). Por lo que el nanohidrogel parece actuar protegiendo a la pimaricina de la degradación proporcionando una inhibición más efectiva.

Por todo ello, en este trabajo de tesis se ha conseguido demostrar la utilidad de los nanohidrogeles para transportar y liberar pimaricina como respuesta a estímulos externos y su efectividad para controlar el deterioro de los alimentos por el crecimiento de microorganismos, mediante la combinación de dos mecanismos: liberación lenta y controlada y protección frente a la degradación ambiental del antifúngico. Este sistema de liberación permite además reducir la cantidad de pimaricina presente en el alimento para alcanzar un efecto inhibitorio.

Estos resultados resaltan la aptitud de los sistemas nanohidrogel-pimaricina en el envasado activo de alimentos pasteurizados refrigerados mediante su incorporación a

los materiales en contacto con alimentos con el fin de extender su vida útil una vez que abierto el envase.

CHAPTER 7

# Perspectivas

Nunca hasta la realización de este trabajo se había abordado el estudio de la utilización de nanopartículas de PNIPA como sistemas de liberación controlada de conservantes alimentarios. Es, por lo tanto, esta tesis una exploración pionera en este ámbito cuyos resultados permiten vislumbrar con claridad nuevas y diversas líneas de trabajo que han de ser llevadas a cabo en los próximos años.

La variedad en las vías de investigación que ahora se abren son consecuencia directa de las también numerosas derivaciones que resultan de los diferentes capítulos de esta memoria y que previsiblemente generarán conocimientos (algunos de ellos básicos) tan abundantes como lo son las aplicaciones que, con ánimo enumerativo y no exhaustivo, se apuntan en los párrafos siguientes.

Así, en primer lugar, será necesario profundizar en los mecanismos moleculares que subyacen a los procesos de hinchamiento y colapso de las nanopartículas de PNIPA, particularmente en el caso de los heteropolímeros. Este conocimiento permitirá diseñar y formular nanohidrogeles con propiedades más ajustadas a la funcionalidad perseguida. Adicionalmente este conocimiento permitirá construir modelos con los que predecir con mayor precisión cuál será su comportamiento ante una aplicación determinada.

En este mismo sentido resulta de especial interés estudiar la síntesis de nanohidrogeles de PNIPA que respondan a otros estímulos ambientales diferentes a la temperatura. Diseñar materiales que actúen liberando alguna sustancia, por ejemplo, frente a cambios en el pH del medio, abre innumerables aplicaciones alimentarias para mantener la calidad o alargar la vida útil de alimentos cuya acidez bien evoluciona durante el almacenamiento o es indicadora de alteración.

También en el ámbito de la síntesis, el estudio de polímeros de PNIPA que incorporen moléculas direccionadoras es una posibilidad que merece ser explorada. Algunos avances en esta línea ya se han realizado precisamente en el marco del proyecto de investigación coordinado que financió esta tesis. Así, nuestros compañeros de la Universidad del País Vasco y de la Universidad Complutense de Madrid han sintetizado y aplicado con éxito nanohidrogeles que incorporan ácido fólico con el fin de vectorizar la liberación de antineoplásicos en el entorno de las células cancerosas. Del mismo modo podría pensarse en unir a las nanopartículas anticuerpos que reconozcan selectivamente patógenos alimentarios con el fin de que la liberación del antimicrobiano sólo se realice cuando existe en el alimento una población tal que pueda suponer un riesgo para el consumidor. Este ejemplo u otros en la misma línea deberán ser explorados en los próximos años para explotar todas las potencialidades de estos materiales Pero sin duda es la aplicación de estos dispositivos de liberación controlada al desarrollo de sistemas y materiales de envasado activo de alimentos el campo que presenta un mayor recorrido en términos de I+D. Esta tesis puso de manifiesto que era posible controlar el crecimiento microbiano durante el almacenamiento de dos alimentos procesados (queso y zumo), utilizando las nanopartículas de PNIPA cargadas con primaricina. Estos experimentos, realizados poniendo directamente en contacto el conjunto del alimento con las nanopartículas, demostraron la factibilidad de la idea y abrieron el camino para, por una parte, evaluar el comportamiento de los dispositivos frente a otros alimentos tanto frescos como procesados; y por otra, incorporar estas nanopartículas a los materiales de envasado y contacto alimentario para desarrollar envases activos antimicrobianos e inteligentes.

Aunque no se incorporaron a esta tesis ya existen resultados y se han dado algunos avances en esta última dirección en colaboración con el grupo del Dr. Vicente de la Universidade do Minho en Braga (Portugal) para desarrollar films comestibles a escala nano o micro que incorporen las nanopartículas de PNIPA como sistemas de liberación. Los resultados preliminares obtenidos por el momento indican la conveniencia de continuar

las investigaciones mejorando las propiedades tecnológicas (resistencia, integridad, permeabilidad, color) de los sistemas conjuntos (film+nanopartícula) para ser utilizados en alimentos y evaluando su eficacia en alguno de ellos.

Estas investigaciones deberán en un futuro próximo extenderse a otros materiales de contacto alimentario, particularmente los plásticos, tanto en su forma convencional como en presentaciones a escala nanométrica (como las nanofibras) o en plásticos biodegradables, que multiplican las potencialidades de aplicación de los nanodispositivos de PNIPA. En este ámbito resultará crucial intensificar la colaboración con el grupo del Dr. Lagarón del IATA de Valencia (CSIC) con el que ya se mantienen contactos y que deberían enfocarse a conseguir la compatibilidad de los procesos de fabricación de los plásticos con las nanopartículas de PNIPA evitando que éstas se degraden y pierdan sus propiedades durante procesos como la polimerización o la extrusión.

En un apartado de perspectivas no puede dejar de apuntarse el desarrollo de otras aplicaciones alimentarias de los dispositivos de liberación controlada e inteligente de nanopartículas de PNIPA. Las posibilidades en este sentido son muy variadas y tan sólo merece apuntar algunas de ellas para ilustrar la amplitud del campo. Así podrían utilizarse como indicadores de proceso (por ejemplo, liberando una sustancia determinada que provoca un cambio de color cuando se alcanza determinado valor de temperatura o pH), para proteger moléculas lábiles (aromas, antioxidantes) y liberarlos bajo demanda o para diseñar sistemas autoesterilizables (por liberación de un agente como el óxido de titanio) que actúen en una determinada condición ambiental.

Finalmente, todas las posibilidades apuntadas anteriormente implican el desarrollo y puesta a punto de técnicas para el manejo de los sistemas nanométricos que se vayan a emplear y de las técnicas de análisis para la evaluación de su eficacia y, junto con ello, los aspectos toxicológicos y de seguridad. No por ser los últimos citados la importancia de estas cuestiones es menor, todo lo contrario. En los últimos años se han realizado significativos esfuerzos en la evaluación de la seguridad de las aplicaciones de la nanotecnología. Lejos de estar resueltos, el estudio de estos aspectos, cobra más fuerza,

puesto que cada vez es también mayor las exigencias de cara a los consumidores y muy especialmente al medio ambiente.

Así pues, los estudios iniciados con el grupo del Profesor Teijón de la Universidad Complutense de Madrid en el que se evaluó la posible toxicidad de las nanopartículas de PNIPA usadas en esta memoria ha de ampliarse con nuevos ensayos tanto in vitro con líneas celulares como in vivo con animales de experimentación, con el fin de garantizar la viabilidad final de todos los estudios señalados en los párrafos precedentes.

# Bibliography


[1] N. Ahuja, O. P. Katare, and B. Singh. Studies on dissolution enhancement and mathematical modeling of drug release of a poorly water-soluble drug using water-soluble carriers. *European Journal of Pharmaceutics and Biopharmaceutics*, 65(1): 26–38, 2007.

[2] H. R. Allcock and A. M. A. Ambrosio. Synthesis and characterization of ph-sensitive poly(organophosphazene) hydrogels. *Biomaterials*, 17(23):2295–2302, 1996. Cited By (since 1996): 63.

[3] M. Andersson, A. Axelsson, and G. Zacchi. Diffusion of glucose and insulin in a swelling n-isopropylacrylamide gel. *International journal of pharmaceutics*, 157(2): 199–208, 1997.

[4] I. Andorrà, B. Esteve-Zarzoso, J. M. Guillamón, and A. Mas. Determination of viable wine yeast using dna binding dyes and quantitative pcr. *International journal of food microbiology*, 144(2):257–262, 2010.

[5] P. Appendini and J. H. Hotchkiss. Surface modification of poly(styrene) by the attachment of an antimicrobial peptide. *Journal of Applied Polymer Science*, 81(3): 609–616, 2001. Cited By (since 1996): 22.

[6] S. Argentiere, L. Blasi, G. Ciccarella, G. Barbarella, R. Cingolani, and G. Gigli. Nanogels of poly(acrylic acid): Uptake and release behavior with fluorescent oligothiophene-labeled bovine serum albumin. *Journal of Applied Polymer Science*, 116(5):2808–2815, 2010. Cited By (since 1996): 4.

[7] K. Arshak, C. Adley, E. Moore, C. Cunniffe, M. Campion, and J. Harris. Characterisation of polymer nanocomposite sensors for quantification of bacterial cultures.

*Sensors and Actuators, B: Chemical*, 126(1):226–231, 2007. Cited By (since 1996): 15.

[8] H. Auweter, H. Bohn, H. Haberkorn, D. Horn, E. Luddecke, and V. Rauschenberger. Production of carotenoid preparations in the form of coldwater-dispersible powders, and the use of the novel carotenoid preparations, 1999.

[9] G. Bärwald. Über die kaltenkeimung von apfelsaft mit dem fungicid pimaricin. *Die industrielle Obst- und Gemüseverwertung*, 61:453–458, 1976.

[10] L. Bastarrachea, S. Dhawan, and S. S. Sablani. Engineering properties of polymeric-based antimicrobial films for food packaging. *Food Engineering Reviews*, 3(2):79–93, 2011. Cited By (since 1996): 2.

[11] F. Berti, S. Todros, D. Lakshmi, M. J. Whitcombe, I. Chianella, M. Ferroni, S. A. Piletsky, A. P. F. Turner, and G. Marrazza. Quasi-monodimensional polyaniline nanostructures for enhanced molecularly imprinted polymer-based sensing. *Biosensors and Bioelectronics*, 26(2):497–503, 2010. Cited By (since 1996): 10.

[12] A. Bilia, V. Carelli, G. Di Colo, and E. Nannipieri. In vitro evaluation of a ph-sensitive hydrogel for control of gi drug delivery from silicone-based matrices. *International journal of pharmaceutics*, 130(1):83–92, 1996. Cited By (since 1996): 25.

[13] M. D. Blanco, S. Guerrero, C. Teijón, R. Olmo, L. Pastrana, I. Katime, and J. M. Teijón. Preparation and characterization of nanoparticulate poly (n-isopropylacrylamide) hydrogel for the controlled release of anti-tumour drugs. *Polymer International*, 57(11):1215–1225, 2008.

[14] M. D. Blanco, M. Benito, R. Olmo, C. Teijón, E. Pérez, I. Katime, and J. M. Teijón. Synthesis and in vitro biological evaluation as antitumour drug carriers of folate-targeted n-isopropylacrylamide-based nanohydrogels. *Polymer International*, 61(7): 1202–1212, 2012.

[15] C. Blasco and Y. Picó. Determining nanomaterials in food. *TrAC - Trends in Analytical Chemistry*, 30(1):84–99, 2011.

[16] P. Bordes, E. Pollet, and L. AvÃ©rous. Nano-biocomposites: Biodegradable polyester/nanoclay systems. *Progress in Polymer Science (Oxford)*, 34(2):125–155, 2009. Cited By (since 1996): 120.

[17] H. Vanden Bossche, M. Engelen, and F. Rochette. Antifungal agents of use in animal health - chemical, biochemical and pharmacological aspects. *Journal of veterinary pharmacology and therapeutics*, 26(1):5–29, 2003.

[18] H. Bozkurt and O. Erkmen. Predictive modeling of yersinia enterocolitica inactivation in turkish feta cheese during storage. *Journal of Food Engineering*, 47(2): 81–87, 2001.

[19] F. Brandl, F. Kastner, R. M. Gschwind, T. Blunk, J. Teßmar, and A. Göpferich. Hydrogel-based drug delivery systems: Comparison of drug diffusivity and release kinetics. *Journal of Controlled Release*, 142(2):221–228, 2010.

[20] L. Brannon-Peppas and N. A. Peppas. Equilibrium swelling behavior of ph-sensitive hydrogels. *Chemical Engineering Science*, 46(3):715–722, 1991. Cited By (since 1996): 198.

[21] A. L. Brody. "nano, nano" food packaging technology. *Food Technology*, 57(12): 52–54, 2003. Cited By (since 1996): 18.

[22] A. L. Brody, B. Bugusu, J. H. Han, C. K. Sand, and T. H. McHugh. Innovative food packaging solutions. *Journal of Food Science*, 73(8), 2008.

[23] L. E. Bromberg and E. S. Ron. Temperature-responsive gels and thermogelling polymer matrices for protein and peptide delivery. *Advanced Drug Delivery Reviews*, 31(3):197–221, 1998.

[24] M. N. Buffa, A. J. Trujillo, M. Pavia, and B. Guamis. Changes in textural, microstructural, and colour characteristics during ripening of cheeses made from raw, pasteurized or high-pressure-treated goats' milk. *International Dairy Journal*, 11 (11-12):927–934, 2001.

[25] G. G. Buonocore, A. Conte, M. R. Corbo, M. Sinigaglia, and M. A. Del Nobile. Mono- and multilayer active films containing lysozyme as antimicrobial agent. *Innovative Food Science and Emerging Technologies*, 6(4):459–464, 2005. Cited By (since 1996): 20.

[26] M. A. Busolo, P. Fernandez, M. J. Ocio, and J. M. Lagaron. Novel silver-based nanoclay as an antimicrobial in polylactic acid food packaging coatings. *Food Additives and Contaminants - Part A Chemistry, Analysis, Control, Exposure and Risk Assessment*, 27(11):1617–1626, 2010. Cited By (since 1996): 5.

[27] CAGPA. Consellería de agricultura, gandería e política agroalimentaria. orden de 26 de diciembre de 1997 por la que se aprueba el reglamento de la denominación de 641 origen arzúa-ulloa y de su consejo regulador. Diario Oficial de Galicia, 5, 190 - 204, 1998.

[28] A. Cagri, Z. Ustunol, and E. T. Ryser. Antimicrobial, mechanical, and moisture barrier properties of low ph whey protein-based edible films containing p-aminobenzoic or sorbic acids. *Journal of Food Science*, 66(6):865–870, 2001. Cited By (since 1996): 76.

[29] A. Cagri, Z. Ustunol, and E. T. Ryser. Inhibition of three pathogens on bologna and summer sausage using antimicrobial edible films. *Journal of Food Science*, 67 (6):2317–2324, 2002. Cited By (since 1996): 24.

[30] T. Çaykara, S. Kiper, and G. Demirel. Network parameters and volume phase transition behavior of poly(n-isopropylacrylamide) hydrogels. *Journal of Applied Polymer Science*, 101(3):1756–1762, 2006.

[31] R. Censi, T. Vermonden, M. J. van Steenbergen, H. Deschout, K. Braeckmans, S. C. De Smedt, C. F. van Nostrum, P. di Martino, and W. E. Hennink. Photopolymerized thermosensitive hydrogels for tailorable diffusion-controlled protein delivery. *Journal of Controlled Release*, 140(3):230–236, 2009.

[32] J. A. Centeno, J. L. Rodriguez-Otero, and A. Cepeda. Microbiological study of arzua cheese (nw spain) throughout cheesemaking and ripening. *Journal of Food Safety*,

14(3):229–241, 1994.

[33] M. A. Cerqueira, B. W. S. Souza, J. T. Martins, J. A. Teixeira, and A. A. Vicente. Seed extracts of gleditsia triacanthos: Functional properties evaluation and incorporation into galactomannan films. *Food Research International*, 43(8):2031–2038, 2010. Cited By (since 1996): 4.

[34] M. A. Cerqueira, A. I. Bourbon, A. C. Pinheiro, J. T. Martins, B. W. S. Souza, J. A. Teixeira, and A. A. Vicente. Galactomannans use in the development of edible films/coatings for food applications. *Trends in Food Science and Technology*, 22 (12):662–671, 2011. Cited By (since 1996): 2.

[35] Q. Chaudhry, M. Scotter, J. Blackburn, B. Ross, A. Boxall, L. Castle, R. Aitken, and R. Watkins. Applications and implications of nanotechnologies for the food sector. *Food Additives and Contaminants - Part A Chemistry, Analysis, Control, Exposure and Risk Assessment*, 25(3):241–258, 2008. Cited By (since 1996): 109.

[36] F. N. Chearúil and O. I. Corrigan. Thermosensitivity and release from poly n-isopropylacrylamide-polylactide copolymers. *International journal of pharmaceutics*, 366(1-2):21–30, 2009.

[37] G. Chen and A. S. Hoffman. Graft copolymers that exhibit temperature-induced phase transitions over a wide range of ph. *Nature*, 373(6509):49–52, 1995.

[38] H. Chen, J. Weiss, and F. Shahidi. Nanotechnology in nutraceuticals and functional foods. *Food Technology*, 60(3):30–36, 2006. Cited By (since 1996): 57.

[39] H. Chen, Y. Gu, and Y. Hu. Comparison of two polymeric carrier formulations for controlled release of hydrophilic and hydrophobic drugs. *Journal of Materials Science: Materials in Medicine*, 19(2):651–658, 2008.

[40] H. Chen, L. H Liu, L. S Wang, C. B Ching, H. W Yu, and Y. Y Yang. Thermally responsive reversed micelles for immobilization of enzymes. *Advanced Functional Materials*, 18(1):95–102, 2008.

[41] Y. Cheng, Y. Liu, J. Huang, K. Li, W. Zhang, Y. Xian, and L. Jin. Combining biofunctional magnetic nanoparticles and atp bioluminescence for rapid detection

of escherichia coli. *Talanta*, 77(4):1332–1336, 2009. Cited By (since 1996): 18.

[42] J. H. Choi, W. Y. Choi, D. S. Cha, M. J. Chinnan, H. J. Park, D. S. Lee, and J. M. Park. Diffusivity of potassium sorbate in îÂº-carrageenan based antimicrobial film. *LWT - Food Science and Technology*, 38(4):417–423, 2005. Cited By (since 1996): 23.

[43] E. Chollet, Y. Swesi, P. Degraeve, and I. Sebti. Monitoring nisin desorption from a multi-layer polyethylene-based film coated with nisin loaded hpmc film and diffusion in agarose gel by an immunoassay (elisa) method and a numerical modeling. *Innovative Food Science and Emerging Technologies*, 10(2):208–214, 2009. Cited By (since 1996): 12.

[44] L. Cocolin, L. F. Bisson, and D. A. Mills. Direct profiling of the yeast dynamics in wine fermentations. *FEMS microbiology letters*, 189(1):81–87, 2000.

[45] A. L. Cordeiro, R. Zimmermann, S. Gramm, M. Nitschke, A. Janke, N. Schäfer, K. Grundke, and C. Werner. Temperature dependent physicochemical properties of poly(n- isopropylacrylamide-co-n-(1-phenylethyl) acrylamide) thin films. *Soft Matter*, 5(7):1367–1377, 2009.

[46] R. Coronado, S. Pekerar, A. T. Lorenzo, and M. A. Sabino. Characterization of thermo-sensitive hydrogels based on poly(n-isopropylacrylamide)/hyaluronic acid. *Polymer Bulletin*, 67(1):101–124, 2011.

[47] D. C. Coughlan and O. I. Corrigan. Release kinetics of benzoic acid and its sodium salt from a series of poly(n-isopropylacrylamide) matrices with various percentage crosslinking. *Journal of pharmaceutical sciences*, 97(1):318–330, 2008. Cited By (since 1996): 6.

[48] H. M. Crowther and B. Vincent. Swelling behavior of poly-n-isopropylacrylamide microgel particles in alcoholic solutions. *Colloid and Polymer Science*, 276(1):46–51, 1998. Cited By (since 1996): 96.

[49] Y. Dai, L. A. McLandsborough, J. Weiss, and M. Peleg. Concentration and application order effects of sodium benzoate and eugenol mixtures on the growth

inhibition of saccharomyces cerevisiae and zygosaccharomyces bailii. *Journal of Food Science*, 75(7), 2010.

[50] D. Dainelli, N. Gontard, D. Spyropoulos, E. Zondervan van den Beuken, and P. Tobback. Active and intelligent food packaging: legal aspects and safety concerns. *Trends in Food Science and Technology*, 19(SUPPL. 1):S99–S108, 2008. Cited By (since 1996): 14.

[51] P. Dalgaard and K. Koutsoumanis. Comparison of maximum specific growth rates and lag times estimated from absorbance and viable count data by different mathematical models. *Journal of microbiological methods*, 43(3):183–196, 2001.

[52] B. P. F. Day. *Active packaging*, pages 282–302. Food packaging technology. CRC Press, Boca Raton, FL, 2003.

[53] F. Devlieghere, L. Vermeiren, M. Jacobs, and J. Debevere. Effectiveness of hexamethylenetetramine-incorporated plastic for the active packaging of foods. *Packaging Technology and Science*, 13(3):117–121, 2000. Cited By (since 1996): 15.

[54] E. Díez-Peña. *Desarrollo y caracterización de hidrogeles poliméricos con aplicación en la liberación controlada de fármacos*. Phd thesis, Universidad Complutense de Madrid, Madrid, 2002.

[55] R. Dinarvand and A. D'Emanuele. The use of thermoresponsive hydrogels for on-off release of molecules. *Journal of Controlled Release*, 36(3):221–227, 1995. Cited By (since 1996): 68.

[56] G. Le Dréan, J. Mounier, V. Vasseur, D. Arzur, O. Habrylo, and G. Barbier. Quantification of *Penicillium camemberti* and *P. roqueforti* mycelium by real-time pcr to assess their growth dynamics during ripening cheese. *International Journal of Food Microbiology*, 138:100–107, 2010.

[57] F. Eeckman, A. J. Moës, and K. Amighi. Poly (n-isopropylacrylamide) copolymers for constant temperature controlled drug delivery. *International journal of pharmaceutics*, 273(1-2):109–119, 2004.

[58] S. M. Elsaeed, R. K. Farag, and N. S. Maysour. Synthesis and characterization of ph-sensitive crosslinked (nipa-co-aac) nanohydrogels copolymer. *Journal of Applied Polymer Science*, 124(3):1947–1955, 2012.

[59] P. Fajardo, J. T. Martins, C. Fuciños, L. Pastrana, J. A. Teixeira, and A. A. Vicente. Evaluation of a chitosan-based edible film as carrier of natamycin to improve the storability of saloio cheese. *Journal of Food Engineering*, 101(4):349–356, 2010.

[60] C. Fänger, H. Wack, and M. Ulbricht. Macroporous poly(n-isopropylacrylamide) hydrogels with adjustable size "cut-off" for the efficient and reversible immobilization of biomacromolecules. *Macromolecular Bioscience*, 6(6):393–402, 2006.

[61] M. A. Farid, H. A. El-Enshasy, A. I. El-Diwany, and E. S A. El-Sayed. Optimization of the cultivation medium for natamycin production by streptomyces natalensis. *Journal of Basic Microbiology*, 40(3):157–166, 2000.

[62] A. Fernandez, S. Torres-Giner, and J. M. Lagaron. Novel route to stabilization of bioactive antioxidants by encapsulation in electrospun fibers of zein prolamine. *Food Hydrocolloids*, 23(5):1427–1432, 2009. Cited By (since 1996): 17.

[63] Bruce A. Firestone and Ronald A. Siegel. Dynamic ph-dependent swelling properties of a hydrophobic polyelectrolyte gel. *Polymer communications Guildford*, 29(7): 204–208, 1988. Cited By (since 1996): 24.

[64] J. Fu, B. Park, G. Siragusa, L. Jones, R. Tripp, Y. Zhao, and Y. J Cho. An au/si hetero-nanorod-based biosensor for salmonella detection. *Nanotechnology*, 19(15), 2008. Cited By (since 1996): 25.

[65] C. Fuciñosos, N. P. Guerra, J. M. Teijón, L. M. Pastrana, M. L. Rúa, and I. Katime. Use of poly(n-isopropylacrylamide) nanohydrogels for the controlled release of pimaricin in active packaging. *Journal of Food Science*, 77(7):N21–N28, 2012.

[66] V. P. Gadang, N. S. Hettiarachchy, M. G. Johnson, and C. Owens. Evaluation of antibacterial activity of whey protein isolate coating incorporated with nisin, grape seed extract, malic acid, and edta on a turkey frankfurter system. *Journal of Food Science*, 73(8):M389–M394, 2008. Cited By (since 1996): 17.

[67] A. Galdikas, A. Mironas, D. Senuliene, V. Strazdiene, A. Å etkus, and D. Zelenin. Response time based output of metal oxide gas sensors applied to evaluation of meat freshness with neural signal analysis. *Sensors and Actuators, B: Chemical*, 69(3):258–265, 2000. Cited By (since 1996): 19.

[68] N. Garti and A. Benichou. *Recent developments in double emulsions for food applications*, pages 353–412. Food emulsions. Marcel Dekker, New York, USA, 2004.

[69] C. M. GÃÂŒÃ§bilmez, A. YemenicioÇ§lu, and A. ArslanoÇ§lu. Antimicrobial and antioxidant activity of edible zein films incorporated with lysozyme, albumin proteins and disodium edta. *Food Research International*, 40(1):80–91, 2007. Cited By (since 1996): 38.

[70] S. Gemili, A. YemenicioÇ§lu, and S. A. Altinkaya. Development of cellulose acetate based antimicrobial food packaging materials for controlled release of lysozyme. *Journal of Food Engineering*, 90(4):453–462, 2009. Cited By (since 1996): 19.

[71] R. M. Goldsmith. Detection of contaminants in food, 1994.

[72] J. F. Graveland-Bikker and C. G. de Kruif. Unique milk protein based nanotubes: Food and nanotechnology meet. *Trends in Food Science and Technology*, 17(5): 196–203, 2006. Cited By (since 1996): 65.

[73] S. Green, M. Roldo, D. Douroumis, N. Bouropoulos, D. Lamprou, and D. G. Fatouros. Chitosan derivatives alter release profiles of model compounds from calcium phosphate implants. *Carbohydrate research*, 344(7):901–907, 2009.

[74] N. P. Guerra, C. L. Macías, A. T. Agrasar, and L. P. Castro. Development of a bioactive packaging cellophane using nisaplin® as biopreservative agent. *Letters in applied microbiology*, 40(2):106–110, 2005. Cited By (since 1996): 11.

[75] N. P. Guerra, P. Fajardo, C. Fuciños, I. R. Amado, E. Alonso, A. Torrado, and L. Pastrana. Modelling the biphasic growth and product formation by enterococcus faecium cect 410 in realkalized fed-batch fermentations in whey. *Journal of Biomedicine and Biotechnology*, 2010, 2010.

[76] L. G. Guerrero-RamÃ-rez, S. M. NuÃ±o-Donlucas, L. C. Cesteros, and I. Katime. Smart copolymeric nanohydrogels: Synthesis, characterization and properties. *Materials Chemistry and Physics*, 112(3):1088–1092, 2008. Cited By (since 1996): 8.

[77] A. Gutowska, You Han Bae, H. Jacobs, F. Mohammad, D. Mix, J. Feijen, and Sung Wan Kim. Heparin release from thermosensitive polymer coatings: In vivo studies. *Journal of Biomedical Materials Research*, 29(7):811–821, 1995.

[78] M. Hamidi, A. Azadi, and P. Rafiei. Hydrogel nanoparticles in drug delivery. *Advanced Drug Delivery Reviews*, 60(15):1638–1649, 2008. Cited By (since 1996): 121.

[79] J. Han, M. E. Castell-Perez, and R. G. Moreira. Effect of food characteristics, storage conditions, and electron beam irradiation on active agent release from polyamide-coated ldpe films. *Journal of Food Science*, 73(2):E37–E43, 2008. Cited By (since 1996): 5.

[80] J. H. Han and J. D. Floros. Simulating diffusion model and determining diffusivity of potassium sorbate through plastics to develop antimicrobial packaging films. *Journal of Food Processing and Preservation*, 22(2):107–122, 1998. Cited By (since 1996): 28.

[81] K. Hanušová, M. Šťastná, L. Votavová, K. Klaudisová, J. Dobiáš, M. Voldřich, and M. Marek. Polymer films releasing nisin and/or natamycin from polyvinyldichloride lacquer coating: Nisin and natamycin migration, efficiency in cheese packaging. *Journal of Food Engineering*, 99(4):491–496, 2010.

[82] N. Hierro, B. Esteve-Zarzoso, A. González, A. Mas, and J. M. Guillamón. Real-time quantitative pcr (qpcr) and reverse transcription-qpcr for detection and enumeration of total yeasts in wine. *Applied and Environmental Microbiology*, 72(11): 7148–7155, 2006.

[83] A. S. Hoffman. Applications of thermally reversible polymers and hydrogels in therapeutics and diagnostics. *Journal of Controlled Release*, 6(SPEC.NO.):297–305, 1987. Cited By (since 1996): 412.

[84] S. I Hong and W. S Park. Development of color indicators for kimchi packaging. *Journal of Food Science*, 64(2):255–257, 1999. Cited By (since 1996): 9.

[85] S. R. Horner, C. R. Mace, L. J. Rothberg, and B. L. Miller. A proteomic biosensor for enteropathogenic e. coli. *Biosensors and Bioelectronics*, 21(8):1659–1663, 2006. Cited By (since 1996): 18.

[86] K. A. Howard, M. Dong, D. Oupicky, H. S. Bisht, C. Buss, F. Besenbacher, and J. Kjems. Nanocarrier stimuli-activated gene delivery. *Small*, 3(1):54–57, 2007.

[87] X. Huang and T. L. Lowe. Biodegradable thermoresponsive hydrogels for aqueous encapsulation and controlled release of hydrophilic model drugs. *Biomacromolecules*, 6(4):2131–2139, 2005.

[88] M. M. Husein and N. N. Nassar. Nanoparticle preparation using the single microemulsions scheme. *Current Nanoscience*, 4(4):370–380, 2008. Cited By (since 1996): 19.

[89] F. Ilmain, T. Tanaka, and E. Kokufuta. Volume transition in a gel driven by hydrogen bonding. *Nature*, 349(6308):400–401, 1991.

[90] H. Inomata, K. Nagahama, and S. Saito. Measurement and correlation of the swelling pressure of n-isopropylacrylamide gel. *MacromoleculesÂ®*, 27(22):6459–6464, 1994.

[91] Plexus Institute. New nanotechnology food research-if it glows don't eat it, 2006.

[92] R. Jedermann, C. Behrens, D. Westphal, and W. Lang. Applying autonomous sensor systems in logistics-combining sensor networks, rfids and software agents. *Sensors and Actuators, A: Physical*, 132(1 SPEC. ISS.):370–375, 2006. Cited By (since 1996): 56.

[93] R. D. Joerger. Antimicrobial films for food applications: A quantitative analysis of their effectiveness. *Packaging Technology and Science*, 20(4):231–273, 2007. Cited

By (since 1996): 53.

[94] N. Jones, B. Ray, K. T. Ranjit, and A. C. Manna. Antibacterial activity of zno nanoparticle suspensions on a broad spectrum of microorganisms. *FEMS microbiology letters*, 279(1):71–76, 2008. Cited By (since 1996): 116.

[95] K. Kailasapathy and S. Rybka. L. acidophilus and bifidobacterium spp. - their therapeutic potential and survival in yogurt. *Australian Journal of Dairy Technology*, 52(1):28–35, 1997. Cited By (since 1996): 126.

[96] I. Katime, R. Novoa, E. D. De Apodaca, and E. Rodríguez. Release of theophylline and aminophylline from acrylic acid/n-alkyl methacrylate hydrogels. *Journal of Polymer Science, Part A: Polymer Chemistry*, 42(11):2756–2765, 2004.

[97] I.A. Katime, O. Katime, and D. Katime. Materiales inteligentes: Hidrogeles macromoleculares. algunas aplicaciones biomédicas. *Anales de la Real Sociedad Española de Química*, (4):35–50, 2005.

[98] S. Y. Kim, S. Lim, and S. Gunasekaran. Protein interactions in reduced-fat and full-fat cheddar cheeses during melting. *LWT - Food Science and Technology*, 44 (2):582–587, 2011.

[99] J. L. Koontz, J. E. Marcy, W. E. Barbeau, and S. E. Duncan. Stability of natamycin and its cyclodextrin inclusion complexes in aqueous solution. *Journal of Agricultural and Food Chemistry*, 51(24):7111–7114, 2003.

[100] C. Kriegel, K. M. Kit, D. J. McClements, and J. Weiss. Influence of surfactant type and concentration on electrospinning of chitosan-poly(ethylene oxide) blend nanofibers. *Food Biophysics*, 4(3):213–228, 2009. Cited By (since 1996): 15.

[101] M. Kurisawa, M. Yokoyama, and T. Okano. Gene expression control by temperature with thermo-responsive polymeric gene carriers. *Journal of Controlled Release*, 69(1):127–137, 2000.

[102] B. Kuswandi, Y. Wicaksono, Jayus, A. Abdullah, L. Y. Heng, and M. Ahmad. Smart packaging: Sensors for monitoring of food quality and safety. *Sensing and Instrumentation for Food Quality and Safety*, 5(3-4):137–146, 2011.

[103] B. D. Lawrence, M. Cronin-Golomb, I. Georgakoudi, D. L. Kaplan, and F. G. Omenetto. Bioactive silk protein biomaterial systems for optical devices. *Biomacromolecules*, 9(4):1214–1220, 2008. Cited By (since 1996): 49.

[104] C. H. Lee, D. S. An, S. C. Lee, H. J. Park, and D. S. Lee. A coating for use as an antimicrobial and antioxidative packaging material incorporating nisin and î±-tocopherol. *Journal of Food Engineering*, 62(4):323–329, 2004. Cited By (since 1996): 37.

[105] F. V. Leimann, O. H. GonÃ§alves, R. A. F. Machado, and A. Bolzan. Antimicrobial activity of microencapsulated lemongrass essential oil and the effect of experimental parameters on microcapsules size and morphology. *Materials Science and Engineering C*, 29(2):430–436, 2009. Cited By (since 1996): 10.

[106] Y. Li and T. Tanaka. Phase transitions of gels. *Annual Review of Materials Science*, 22(1):243–277, 1992.

[107] Y. Li, Y. T. H. Cu, and D. Luo. Multiplexed detection of pathogen dna with dna-based fluorescence nanobarcodes. *Nature biotechnology*, 23(7):885–889, 2005. Cited By (since 1996): 99.

[108] L. T Lim, I. J. Britt, and M. A. Tung. Sorption and permeation of allyl isothiocyanate vapor in nylon 6,6 film as affected by relative humidity. *Journal of Plastic Film and Sheeting*, 14(3):207–225, 1998. Cited By (since 1996): 5.

[109] C. L Lin, W. Y Chiu, and C. F Lee. Preparation, morphology, and thermoresponsive properties of poly(n-isopropylacrylamide)-based copolymer microgels. *Journal of Polymer Science, Part A: Polymer Chemistry*, 44(1):356–370, 2006.

[110] C. L Lin, W. Y Chiu, and C. F Lee. Preparation, morphology, and thermoresponsive properties of poly(n-isopropylacrylamide)-based copolymer microgels. *Journal of Polymer Science, Part A: Polymer Chemistry*, 44(1):356–370, 2006. Cited By (since 1996): 15.

[111] C. López, A. Torrado, P. Fuciños, N. P. Guerra, and L. Pastrana. Enzymatic hydrolysis of chestnut purée: Process optimization using mixtures of $\alpha - amylase$

and glucoamylase. *Journal of Agricultural and Food Chemistry*, 52(10):2907–2914, 2004.

[112] Douglas B. MacDougall. *Colour measurement of food*, pages 33–63. Colour in food. Woodhead Publishing Limited and CRC Press LLC, Boca Raton, FL, USA and Cambridge, England, 2002.

[113] V. B. V. MacIel, C. M. P. Yoshida, and T. T. Franco. Development of a prototype of a colourimetric temperature indicator for monitoring food quality. *Journal of Food Engineering*, 111(1):21–27, 2012.

[114] H. MacKová and D. Horák. Effects of the reaction parameters on the properties of thermosensitive poly(n-isopropylacrylamide) microspheres prepared by precipitation and dispersion polymerization. *Journal of Polymer Science, Part A: Polymer Chemistry*, 44(2):968–982, 2006.

[115] N. M. Manalili, M. A. Dorado, and R. van Otterdijk. Appropiate food packaging solutions for developing countries. In *Save Food! Interpack2011*, pages 1–28. FAO, 2011.

[116] B. Marcos, T. Aymerich, J. M. Monfort, and M. Garriga. High-pressure processing and antimicrobial biodegradable packaging to control listeria monocytogenes during storage of cooked ham. *Food Microbiology*, 25(1):177–182, 2008. Cited By (since 1996): 20.

[117] J. T. Martins, M. A. Cerqueira, B. W. S. Souza, M. D. O. Carmo Avides, and A. A. Vicente. Shelf life extension of ricotta cheese using coatings of galactomannans from nonconventional sources incorporating nisin against listeria monocytogenes. *Journal of Agricultural and Food Chemistry*, 58(3):1884–1891, 2010. Cited By (since 1996): 10.

[118] M. Blanco Massani, M. R. Fernandez, A. Ariosti, P. Eisenberg, and G. Vignolo. Development and characterization of an active polyethylene film containing lactobacillus curvatus crl705 bacteriocins. *Food Additives and Contaminants - Part A Chemistry, Analysis, Control, Exposure and Risk Assessment*, 25(11):1424–1430,

2008. Cited By (since 1996): 4.

[119] T. Mattila, J. Tawast, and R. Ahvenainen. New possibilities for quality control of aseptic packages: Microbiological spoilage and seal defect detection using headspace indicators. *Lebensmittel Wissenschaft und Technologie*, 23(3):246–251, 1990.

[120] G. Mauriello, D. Ercolini, A. La Storia, A. Casaburi, and F. Villani. Development of polythene films for food packaging activated with an antilisterial bacteriocin from lactobacillus curvatus 32y. *Journal of applied microbiology*, 97(2):314–322, 2004. Cited By (since 1996): 43.

[121] G. Mauriello, E. De Luca, A. La Storia, F. Villani, and D. Ercolini. Antimicrobial activity of a nisin-activated plastic film for food packaging. *Letters in applied microbiology*, 41(6):464–469, 2005. Cited By (since 1996): 38.

[122] Á. Medina, M. Jiménez, R. Mateo, and N. Magan. Efficacy of natamycin for control of growth and ochratoxin a production by aspergillus carbonarius strains under different environmental conditions. *Journal of applied microbiology*, 103(6):2234–2239, 2007.

[123] N. Milainović, N. Milosavljević, J. Filipović, Z. Kneević-Jugović, and M. K. Kruić. Synthesis, characterization and application of poly(n-isopropylacrylamide- co-itaconic acid) hydrogels as supports for lipase immobilization. *Reactive and Functional Polymers*, 70(10):807–814, 2010.

[124] N. Milašinović, M. Kalagasidis Krušić, Z. Knežević-Jugović, and J. Filipović. Hydrogels of n-isopropylacrylamide copolymers with controlled release of a model protein. *International journal of pharmaceutics*, 383(1-2):53–61, 2010.

[125] S. Min, T. R. Rumsey, and J. M. Krochta. Diffusion of the antimicrobial lysozyme from a whey protein coating on smoked salmon. *Journal of Food Engineering*, 84 (1):39–47, 2008. Cited By (since 1996): 7.

[126] M. A. Murado, Ma P. GonzÃ!'lez, and J. A. VÃ!'zquez. Dose-response relationships: An overview, a generative model and its application to the verification of descriptive

models. *Enzyme and microbial technology*, 31(4):439–455, 2002.

[127] A. A. Naddaf, I. Tsibranska, and H. J Bart. Kinetics of bsa release from poly(n-isopropylacrylamide) hydrogels. *Chemical Engineering and Processing: Process Intensification*, 49(6):581–588, 2010. Cited By (since 1996): 5.

[128] N. Nakamura and Y. Amao. An optical sensor for co2 using thymol blue and europium(iii) complex composite film. *Sensors and Actuators, B: Chemical*, 92(1-2):98–101, 2003. Cited By (since 1996): 16.

[129] J. M Nam, C. S. Thaxton, and C. A. Mirkin. Nanoparticle-based bio-bar codes for the ultrasensitive detection of proteins. *Science*, 301(5641):1884–1886, 2003. Cited By (since 1996): 1131.

[130] CTC Nanotechnology. Weitec bio cleaner, 2009.

[131] S. Neethirajan and D. S. Jayas. Nanotechnology for the food and bioprocessing industries. *Food and Bioprocess Technology*, 4(1):39–47, 2011.

[132] A. MartÃ nez Abad, J. M. Lagaron, and M. J. Ocio. Development and characterization of silver-based antimicrobial ethylene-vinyl alcohol copolymer (evoh) films for food-packaging applications. *Journal of Agricultural and Food Chemistry*, 60(21): 5350–5359, 2012.

[133] M. A. Del Nobile, A. Conte, A. L. Incoronato, and O. Panza. Antimicrobial efficacy and release kinetics of thymol from zein films. *Journal of Food Engineering*, 89(1): 57–63, 2008. Cited By (since 1996): 19.

[134] M. Alessandro Del Nobile, D. Gammariello, S. Di Giulio, and A. Conte. Active coating to prolong the shelf life of fior di latte cheese. *Journal of Dairy Research*, 77(1):50–55, 2010.

[135] A. Nopwinyuwong, S. Trevanich, and P. Suppakul. Development of a novel colorimetric indicator label for monitoring freshness of intermediate-moisture dessert spoilage. *Talanta*, 81(3):1126–1132, 2010. Cited By (since 1996): 6.

[136] T. M. De Oliveira, N. De Fátima Ferreira Soares, R. M. Pereira, and K. De Freitas Fraga. Development and evaluation of antimicrobial natamycin-incorporated film

in gorgonzola cheese conservation. *Packaging Technology and Science*, 20(2):147–153, 2007.

[137] K. O'Riordan, D. Andrews, K. Buckle, and P. Conway. Evaluation of microencapsulation of a bifidobacterium strain with starch as an approach to prolonging viability during storage. *Journal of applied microbiology*, 91(6):1059–1066, 2001. Cited By (since 1996): 62.

[138] K. Otake, H. Inomata, M. Konno, and S. Saito. Thermal analysis of the volume phase transition with n-isopropylacrylamide gels. *Macromolecules*, 23(1):283–289, 1990.

[139] B. Ouattara, R. E. Simard, G. Piette, A. BÃ©gin, and R. A. Holley. Diffusion of acetic and propionic acids from chitosan-based antimicrobial packaging films. *Journal of Food Science*, 65(5):768–773, 2000. Cited By (since 1996): 78.

[140] M. Oussalah, S. Caillet, S. SalmiÃ©ri, L. Saucier, and M. Lacroix. Antimicrobial and antioxidant effects of milk protein-based film containing essential oils for the preservation of whole beef muscle. *Journal of Agricultural and Food Chemistry*, 52 (18):5598–5605, 2004. Cited By (since 1996): 72.

[141] A. Pacquit, K. T. Lau, H. McLaughlin, J. Frisby, B. Quilty, and D. Diamond. Development of a volatile amine sensor for the monitoring of fish spoilage. *Talanta*, 69(2 SPEC. ISS.):515–520, 2006. Cited By (since 1996): 40.

[142] A. Pacquit, J. Frisby, D. Diamond, K. T. Lau, A. Farrell, B. Quilty, and D. Diamond. Development of a smart packaging for the monitoring of fish spoilage. *Food Chemistry*, 102(2):466–470, 2007. Cited By (since 1996): 30.

[143] V. Parry. Food fight on the tiny scale, October/21 2006.

[144] J. C. Pedersen. Natamycin as a fungicide in agar media. *Applied and Environmental Microbiology*, 58(3):1064–1066, 1992.

[145] N. A. Peppas. Physiologically responsive hydrogels. *Journal of Bioactive and Compatible Polymers*, 6(3):241–246, 1991. Cited By (since 1996): 80.

[146] N.A. Peppas. *Hydrogels in Medicine and Pharmacy*, volume 1-3. CRC Press Inc., Boca Raton, FL, 1986/1987.

[147] R. Pérez-Masiá, A. López-Rubio, and J. M. Lagarónn. Development of zein-based heat-management structures for smart food packaging. *Food Hydrocolloids*, 30(1): 182–191, 2012. Article in Press.

[148] C. M. B. S. Pintado, M. A. S. S. Ferreira, and I. Sousa. Properties of whey protein-based films containing organic acids and nisin to control listeria monocytogenes. *Journal of food protection*, 72(9):1891–1896, 2009.

[149] A. C. Dos Santos Pires, N. De Fátima Ferreira Soares, N. J. De Andrade, L. H. M. Da Silva, G. P. Camilloto, and P. C. Bernardes. Development and evaluation of active packaging for sliced mozzarella preservation. *Packaging Technology and Science*, 21(7):375–383, 2008. Cited By (since 1996): 10.

[150] Y. Pranoto, S. K. Rakshit, and V. M. Salokhe. Enhancing antimicrobial activity of chitosan films by incorporating garlic oil, potassium sorbate and nisin. *LWT - Food Science and Technology*, 38(8):859–865, 2005. Cited By (since 1996): 90.

[151] P. Puligundla, J. Jung, and S. Ko. Carbon dioxide sensors for intelligent food packaging applications. *Food Control*, 25(1):328–333, 2012.

[152] P. L. Ritger and N. A. Peppas. A simple equation for description of solute release ii. fickian and anomalous release from swellable devices. *Journal of Controlled Release*, 5(1):37–42, 1987.

[153] D. P. T. Roberts, M. J. Scotter, M. Godula, M. Dickinson, and A. J. Charlton. Development and validation of a rapid method for the determination of natamycin in wine by high-performance liquid chromatography coupled to high resolution mass spectrometry. *Analytical Methods*, 3(4):937–943, 2011.

[154] A. RodrÃ-guez, C. NerÃ-n, and R. Batlle. New cinnamon-based active paper packaging against rhizopusstolonifer food spoilage. *Journal of Agricultural and Food Chemistry*, 56(15):6364–6369, 2008. Cited By (since 1996): 22.

[155] P. Rodriguez-Alonso, J. A. Centeno, and J. I. Garabal. Biochemical study of industrially produced arzãÂºa-ulloa semi-soft cows' milk cheese: Effects of storage under vacuum and modified atmospheres with high-nitrogen contents. *International Dairy Journal*, 21(4):261–271, 2011.

[156] M. A. Rojas-GraÃÂŒ, R. J. Avena-Bustillos, M. Friedman, P. R. Henika, O. MartÃ n Belloso, and T. H. Mchugh. Mechanical, barrier, and antimicrobial properties of apple puree edible films containing plant essential oils. *Journal of Agricultural and Food Chemistry*, 54(24):9262–9267, 2006. Cited By (since 1996): 45.

[157] S. Romani, G. Sacchetti, P. Pittia, G. G. Pinnavaia, and M. Dalla Rosa. Physical, chemical, textural and sensorial changes of portioned parmigiano reggiano cheese packed under different conditions. *Food Science and Technology International*, 8 (4):203–211, 2002.

[158] C. Ruengruglikit, H. Kim, R. D. Miller, and Q. Huang. Fabrication of nanoporous oligonucleotide microarrays for pathogen detection and identification. *Polymer Preprints*, 45:526, 2004.

[159] S. Sankaran and S. Panigrahi. Nanoparticulate zinc oxide chemoresistive sensor for volatile acetic acid detection. *Nanoscience and Nanotechnology Letters*, 3(6): 755–762, 2011.

[160] P. Santiago-Silva, N. F. F. Soares, J. E. Nóbrega, M. A. W. Júnior, K. B. F. Barbosa, A. C. P. Volp, E. R. M. A. Zerdas, and N. J. Würlitzer. Antimicrobial efficiency of film incorporated with pediocin (alta â® 2351) on preservation of sliced ham. *Food Control*, 20(1):85–89, 2009. Cited By (since 1996): 16.

[161] B. R. Saunders, H. M. Crowther, and B. Vincent. Poly[(methyl methacrylate)-co-(methacrylic acid)] microgel particles: Swelling control using ph, cononsolvency, and osmotic deswelling. *Macromolecules*, 30(3):482–487, 1997.

[162] R. Saurel, A. Pajonk, and J. Andrieu. Modelling of french emmental cheese water activity during salting and ripening periods. *Journal of Food Engineering*, 63(2): 163–170, 2004.

[163] A. G. M. Scannell, C. Hill, R. P. Ross, S. Marx, W. Hartmeier, and E. K. Arendt. Development of bioactive food packaging materials using immobilised bacteriocins lacticin 3147 and nisaplin(â®). *International journal of food microbiology*, 60(2-3): 241–249, 2000. Cited By (since 1996): 74.

[164] H. G. Schild. Poly (n-isopropylacrylamide): Experiment, theory and application. *Progress in Polymer Science (Oxford)*, 17(2):163–249, 1992.

[165] B. S. Sekhon. Food nanotechnology - an overview. *Nanotechnology, Science and Applications*, 3:1–15, 2010.

[166] J. D. Seldman. *Time-temperature indicators*, pages 74–107. Active food packaging. Chapman and Hall, New York, 1995.

[167] E. Semo, E. Kesselman, D. Danino, and Y. D. Livney. Casein micelle as a natural nano-capsular vehicle for nutraceuticals. *Food Hydrocolloids*, 21(5-6):936–942, 2007. Cited By (since 1996): 51.

[168] K. H Seol, D. G Lim, A. Jang, C. Jo, and M. Lee. Antimicrobial effect of îÂº-carrageenan-based edible film containing ovotransferrin in fresh chicken breast stored at 5 â°c. *Meat Science*, 83(3):479–483, 2009. Cited By (since 1996): 8.

[169] A. Serres, M. BaudyÅ!', and S. W. Kim. Temperature and ph-sensitive polymers for human calcitonin delivery. *Pharmaceutical research*, 13(2):196–201, 1996. Cited By (since 1996): 89.

[170] A. C. Seydim and G. Sarikus. Antimicrobial activity of whey protein based edible films incorporated with oregano, rosemary and garlic essential oils. *Food Research International*, 39(5):639–644, 2006. Cited By (since 1996): 101.

[171] A. Shefer. The application of nanotechnology in the food industry.

[172] Y. Shin, J. H. Chang, J. Liu, R. Williford, Y. K Shin, and G. J. Exarhos. Hybrid nanogels for sustainable positive thermosensitive drug release. *Journal of Controlled Release*, 73(1):1–6, 2001.

[173] R.L. Shirk and W. L. Clark. The effect of pimaricin in retarding the spoilage of fresh orange juice. *Food Technol.*, 17:108–112, 1963.

[174] R. A. Siegel and B. A. Firestone. ph-dependent equilibrium swelling properties of hydrophobic polyelectrolyte copolymer gels. *Macromolecules*, 21(11):3254–3259, 1988. Cited By (since 1996): 371.

[175] R. A. Siegel, M. Falamarzian, B. A. Firestone, and B. C. Moxley. ph-controlled release from hydrophobic/polyelectrolyte copolymer hydrogels. *Journal of Controlled Release*, 8(2):179–182, 1988. Cited By (since 1996): 133.

[176] T. Sivarooban, N. S. Hettiarachchy, and M. G. Johnson. Physical and antimicrobial properties of grape seed extract, nisin, and edta incorporated soy protein edible films. *Food Research International*, 41(8):781–785, 2008. Cited By (since 1996): 43.

[177] M. Smolander, E. Hurme, and R. Ahvenainen. Leak indicators for modified-atmosphere packages. *Trends in Food Science and Technology*, 8(4):101–106, 1997. Cited By (since 1996): 34.

[178] M. Smolander, E. Hurme, R. Ahvenainen, and M. Siika-aho. Indicators for modified atmosphere packages. In *24th IAPRI Symposium 22-24 June*, Rochester, New York, USA, 1998.

[179] M. Smolander, E. Hurme, K. Latva-Kala, T. Luoma, H. L Alakomi, and R. Ahvenainen. Myoglobin-based indicators for the evaluation of freshness of unmarinated broiler cuts. *Innovative Food Science and Emerging Technologies*, 3(3): 279–288, 2002. Cited By (since 1996): 9.

[180] solutions.3m.com. (avalilable 7/8/2012).

[181] I. Sondi and B. Salopek-Sondi. Silver nanoparticles as antimicrobial agent: a case study on e. coli as a model for gram-negative bacteria. *Journal of Colloid and Interface Science*, 275:177–182, 2004.

[182] C. F. Volken De Souza, T. Dalla Rosa, and M. A. Zachia Ayub. Changes in the microbiological and physicochemical characteristics of serrano cheese during manufacture and ripening. *Brazilian Journal of Microbiology*, 34(3):260–266, 2003.

[183] J. Stark and H. S. Tan. *Natamycin*, chapter 9. Food preservatives. Kluwer Academic/Plenum Publishers, USA, 2 edition, 2003.

[184] M. D. Steven and J. H. Hotchkiss. Covalent immobilization of an antimicrobial peptide on poly(ethylene) film. *Journal of Applied Polymer Science*, 110(5):2665–2670, 2008. Cited By (since 1996): 5.

[185] R. A. Stile, W. R. Burghardt, and K. E. Healy. Synthesis and characterization of injectable poly(n-isopropylacrylamide)-based hydrogels that support tissue formation in vitro. *Macromolecules*, 32(22):7370–7379, 1999.

[186] F. J. Stutzenberger, R. A. Latour, Y. Sun, and T. Tzeng. Adhesin-specific nanoparticles and process for using same, 2007.

[187] C. Teijón, S. Guerrero, R. Olmo, J. M. Teijón, and M. D. Blanco. Swelling properties of copolymeric hydrogels of poly(ethylene glycol) monomethacrylate and monoesters of itaconic acid for use in drug delivery. *Journal of Biomedical Materials Research - Part B Applied Biomaterials*, 91(2):716–726, 2009.

[188] S. Theivendran, N. S. Hettiarachchy, and M. G. Johnson. Inhibition of listeria monocytogens by nisin combined with grape seed extract or green tea extract in soy protein film coated on turkey frankfurters. *Journal of Food Science*, 71(2): M39–M44, 2006. Cited By (since 1996): 26.

[189] H. Tokuyama and Y. Kato. Preparation of poly(n-isopropylacrylamide) emulsion gels and their drug release behaviors. *Colloids and Surfaces B: Biointerfaces*, 67 (1):92–98, 2008.

[190] H. Türe, E. Eroglu, F. Soyer, and B. Özen. Antifungal activity of biopolymers containing natamycin and rosemary extract against aspergillus niger and penicillium roquefortii. *International Journal of Food Science and Technology*, 43(11):2026–2032, 2008.

[191] H. Türe, E. Eroğlu, B. Özen, and F. Soyer. Physical properties of biopolymers containing natamycin and rosemary extract. *International Journal of Food Science and Technology*, 44(2):402–408, 2009.

[192] H. Ture, E. Eroglu, B. Ozen, and F. Soyer. Effect of biopolymers containing natamycin against aspergillus niger and penicillium roquefortii on fresh kashar cheese. *International Journal of Food Science and Technology*, 46(1):154–160, 2011.

[193] S. K. Vakkalanka, C. S. Brazel, and N. A. Peppas. Temperature- and ph-sensitive terpolymers for modulated delivery of streptokinase. *Journal of Biomaterials Science, Polymer Edition*, 8(2):119–129, 1996. Cited By (since 1996): 75.

[194] J. Vartiainen, E. Skytta, J. Enqvist, and R. Ahvenainen. Properties of antimicrobial plastics containing traditional food preservatives. *Packaging Technology and Science*, 16(6):223–229, 2003. Cited By (since 1996): 16.

[195] J. A. Vázquez and M. A. Murado. Mathematical tools for objective comparison of microbial cultures. application to evaluation of 15 peptones for lactic acid bacteria productions. *Biochemical engineering journal*, 39(2):276–287, 2008.

[196] J. A. Vázquez, S. F. Docasal, M. A. Prieto, Ma P. González, and M. A. Murado. Growth and metabolic features of lactic acid bacteria in media with hydrolysed fish viscera. an approach to bio-silage of fishing by-products. *Bioresource technology*, 99(14):6246–6257, 2008.

[197] L. Vermeiren, F. Devlieghere, M. Van Beest, N. De Kruijf, and J. Debevere. Developments in the active packaging of foods. *Trends in Food Science and Technology*, 10(3):77–86, 1999. Cited By (since 1996): 126.

[198] L. Vermeiren, F. Devlieghere, and J. Debevere. Effectiveness of some recent antimicrobial packaging concepts. *Food additives and contaminants*, 19(SUPPL.):163–171, 2002. Cited By (since 1996): 57.

[199] D. E. Wachenheim, J. A. Patterson, and M. R. Ladisch. Analysis of the logistic function model: Derivation and applications specific to batch cultured microorganisms. *Bioresource technology*, 86(2):157–164, 2003.

[200] D. F. H. Wallach and A. Novikov. Methods and devices for detecting spoilage in food products, 1998.

[201] F. Wang, J. Yao, M. Russel, H. Chen, K. Chen, Y. Zhou, B. Ceccanti, G. Zaray, and M. M. F. Choi. Development and analytical application of a glucose biosensor based on glucose oxidase/o-(2-hydroxyl)propyl-3-trimethylammonium chitosan chloride nanoparticle-immobilized onion inner epidermis. *Biosensors and Bioelectronics*, 25 (10):2238–2243, 2010. Cited By (since 1996): 5.

[202] C. Wanihsuksombat, V. Hongtrakul, and P. Suppakul. Development and characterization of a prototype of a lactic acid-based time-temperature indicator for monitoring food product quality. *Journal of Food Engineering*, 100(3):427–434, 2010. Cited By (since 1996): 4.

[203] J. Weiss, P. Takhistov, and D. J. McClements. Functional materials in food nanotechnology. *Journal of Food Science*, 71(9), 2006.

[204] Y. M. Te Welscher, H. H. Ten Napel, M. M. Balagué, C. M. Souza, H. Riezman, B. De Kruijff, and E. Breukink. Natamycin blocks fungal growth by binding specifically to ergosterol without permeabilizing the membrane. *Journal of Biological Chemistry*, 283(10):6393–6401, 2008.

[205] Y. M. Te Welscher, L. Jones, M. R. Van Leeuwen, J. Dijksterhuis, B. De Kruijff, G. Eitzen, and E. Breukink. Natamycin inhibits vacuole fusion at the priming phase via a specific interaction with ergosterol. *Antimicrobial Agents and Chemotherapy*, 54(6):2618–2625, 2010.

[206] Y. M Weng, M. J Chen, and C. Wenlung. Antimicrobial food packaging materials from poly(ethylene-co-methacrylic acid). *LWT - Food Science and Technology*, 32 (4):191–195, 1999. Cited By (since 1996): 21.

[207] Yih-Ming Weng and Joseph H. Hotchkiss. Anhydrides as antimycotic agents added to polyethylene films for food packaging. *Packaging Technology and Science*, 6(3): 123–128, 1993. Cited By (since 1996): 47.

[208] J. Y Wu, S. Q Liu, P. W. S Heng, and Y. Y Yang. Evaluating proteins release from, and their interactions with, thermosensitive poly (n-isopropylacrylamide) hydrogels. *Journal of Controlled Release*, 102(2):361–372, 2005.

[209] www.azonano.com. Nanotechnology and food packaging.

[210] www.fresh check.com. (available 26/8/2012).

[211] www.meatandpoultryonline.com/doc.mvc/FreshTag 0001. (available 26/8/2012).

[212] www.mgc.co.jp/eng/products/abc/ageless/eye.html. (available 26/8/2012).

[213] www.ripesense.com. (available 26/8/2012).

[214] www.tetrapak.com. (available 7/8/2012).

[215] www.timestrip.com. (available 7/8/2012).

[216] www.vitsab.com. (available 7/8/2012).

[217] W. Xue, S. Champ, and M. B. Huglin. Network and swelling parameters of chemically crosslinked thermoreversible hydrogels. *Polymer*, 42(8):3665–3669, 2001.

[218] S. Yan, C. Huawei, Z. Limin, R. Fazheng, Z. Luda, and Z. Hengtao. Development and characterization of a new amylase type time-temperature indicator. *Food Control*, 19(3):315–319, 2008. Cited By (since 1996): 15.

[219] M. Yildirim, F. Güleç, M. Bayram, and Z. Yildirim. Properties of kashar cheese coated with casein as a carrier of natamycin. *Italian Journal of Food Science*, 18 (2):127–138, 2006.

[220] M. K. Yoo, Y. K. Sung, Y. M. Lee, and C. S. Cho. Effect of polyelectrolyte on the lower critical solution temperature of poly(n-isopropyl acrylamide) in the poly(nipaam-co-acrylic acid) hydrogel. *Polymer*, 41(15):5713–5719, 2000.

[221] H. Zhang, R. Elghanian, L. Demers, N. Amro, S. Disawal, and S. Cruchon-Dupeyrat. Direct-write nanolithography method of transporting ink with an elastomeric polymer coated nanoscopic tip to form a structure having internal hollows on a substrate, 2009.

[222] X. Z Zhang, R. X Zhuo, J. Z Cui, and J. T Zhang. A novel thermo-responsive drug delivery system with positive controlled release. *International journal of pharmaceutics*, 235(1-2):43–50, 2002.

[223] R. Zhao, P. Torley, and P. J. Halley. Emerging biodegradable materials: Starch- and protein-based bio-nanocomposites. *Journal of Materials Science*, 43(9):3058–3071, 2008. Cited By (since 1996): 31.

[224] X. Zhao, L. R. Hilliard, S. J. Mechery, Y. Wang, R. P. Bagwe, S. Jin, and W. Tan. A rapid bioassay for single bacterial cell quantitation using bioconjugated nanoparticles. *Proceedings of the National Academy of Sciences of the United States of America*, 101(42):15027–15032, 2004. Cited By (since 1996): 229.

[225] P. W. Zhu and D. H. Napper. Coil-to-globule type transitions and swelling of poly(n-isopropylacrylamide) and poly(acrylamide) at latex interfaces in alcohol-water mixtures. *Journal of colloid and interface science*, 177(2):343–352, 1996.

[226] R. X Zhuo and W. Li. Preparation and characterization of macroporous poly(n-isopropylacrylamide) hydrogels for the controlled release of proteins. *Journal of Polymer Science, Part A: Polymer Chemistry*, 41(1):152–159, 2002. Cited By (since 1996): 25.

[227] M. H. Zwietering, I. Jongenburger, F. M. Rombouts, and K. Van't Riet. Modeling of the bacterial growth curve. *Applied and Environmental Microbiology*, 56(6):1875–1881, 1990. Cited By (since 1996): 709.

# ANEXO

C. Fuciños, N. P. Guerra, J. M. Teijón, L. M. Pastrana, M. L. Rúa, and I. Katime. Use of poly(*N*-isopropylacrylamide) nanohydrogels for the controlled release of pimaricin in active packaging. *Journal of Food Science*. 77(7):N21-N28, 2012.

# Use of Poly(N-isopropylacrylamide) Nanohydrogels for the Controlled Release of Pimaricin in Active Packaging

C. Fuciños, N.P. Guerra, J.M. Teijón, L.M. Pastrana, M.L. Rúa, and I. Katime

**Abstract:** We propose here a delivery drug-polymer system using poly(N-isopropylacrylamide) (PNIPA) nanohydrogels that enables pimaricin to be protected from hostile environments and allows the controlled release of the antifungal through environmental stimuli. We synthesized 2 nanohydrogels, 1 with 100% N-isopropylacrylamide (PNIPA(5)) and 1 with 80% N-isopropylacrylamide copolymerized and 20% acrylic acid (PNIPA-20AA(5)). Both were then, loaded with a pimaricin aqueous solution. The pimaricin release profiles of these 2 nanohydrogels were considerably different: PNIPA(5) released 10% and PNIPA-20AA(5) released 30% with respect to the free pimaricin release. Moreover, the diffusion experiments showed that pimaricin was released from the PNIPA-20AA(5) nanohydrogel for up to 3 times longer than free pimaricin. Therefore, incorporating acrylic acid as comonomer into the PNIPA nanohydrogel resulted in a slower but more continuous release of pimaricin. The highest pimaricin levels were reached when the most hydrophilic nanohydrogel was used. The bioassay results showed that the pimaricin-nanohydrogel system was highly effective in inhibiting the growth of the indicator strain in conditions of thermal abuse. The spoilage in acidified samples stored under fluorescent lighting was reduced by 80.94% ± 33.02% in samples treated with a pimaricin-loaded nanohydrogel, but only by 19.91% ± 6.68% in samples treated with free pimaricin. Therefore, 2 conclusions emerge from this study. One is that the nanohydrogel delivery system could impede the degradation of pimaricin. The other is that the inhibitory effect of the antifungal on yeast growth is more pronounced when it is added included into the nanohydrogel to the food, especially in an acidic environment.

**Keywords:** active packaging, controlled release, nanohydrogel, pimaricin, poly(N-isopropylacrylamide)

**Practical Application:** This article presents relevant results on the use of nanohydrogels in food packaging. Nanohydrogels could provide protection so that the pimaricin remains active for a longer time. They also allow the controlled release of pimaricin, which thus regulates the unnecessary presence of the antifungal in the food.

## Introduction

In recent years, the interest in antimicrobials for extending the shelf life of food products has focused on using natural substances such as essential oils (allyl isotiocyanate), bacteriocins (nisin), and pimaricin. Pimaricin (natamycin) is a polyene antifungal produced by *Streptomyces natalensis* and related species. As it has low toxicity and prevents the growth of mould and yeast, pimaricin is very useful in the food industry as a preservative on the surface of cheese, fruit, and other nonsterile products, such as meat and sausages (Farid and others 2000; Vanden Bossche and others 2003).

There are 2 technological problems associated with pimaricin as a food preservative. They are its low water solubility and its sensitivity to ultraviolet light (Koontz and others 2003; Stark and Tan 2003). In addition, when there is continuous contact between preservatives and microorganisms, microbial resistance can develop and so the preservative becomes ineffective. This occurs frequently when antimicrobials are added directly to the food product. Active packaging can reduce, but not eliminate, this effect.

Currently, there is enormous interest in applying nanoscience to the food industry, particularly for developing new functional materials to improve food safety and quality (Weiss and others 2006; Neethirajan and Jayas 2011). Nanoparticles can be used to encapsulate functional ingredients and can perform a number of different roles, such as protecting the functional ingredient against degradation during food processing, storage and usage, carrying it to the site of action, and controlling its release as in active packaging. In this last application, nanoscale has several advantages which are, better dispersion of nanoparticles in the food packaging material and the possibility of controlling the release rate as a response to specific environmental conditions (for example, pH, ionic strength, or temperature).

Thermally sensitive and nontoxic poly(N-isopropylacrylamide) (PNIPA) hydrogels are widely used. Some applications include the controlled release of insulin (Andersson and others 1997) and

*MS 20111500 Submitted 12/15/2011, Accepted 03/29/2012.* *Authors Fuciños, Guerra, Pastrana, and Rúa are with Biotechnology Group, Dept. of Analytical Chemistry and Food Science, Univ. of Vigo, 32004, Ourense, Spain. Author Teijón is with Polymeric Materials Group for the Controlled Release of Bioactive Compounds in Biomedicine, Dept. of Biochemistry and Molecular Biology, Complutense Univ. of Madrid, 28040 Madrid, Spain. Author Katime is with Group of New Materials and Supramolecular Spectroscopy, Dept. of Physical Chemistry, Univ. of País Vásco, 48940 Leioa, Spain. Direct inquiries to author Fuciños (E-mail: clarafg@gmail.com).*


doi: 10.1111/j.1750-3841.2012.02781.x


Journal of Food Science A Publication of the Institute of Food Technologists

5-fluorouracil (Blanco and others 2008) in pharmaceutical applications as well as antifungals and macromolecules such as benzoates and bovine serum albumin (Caykara and others 2006). PNIPA has a hydrophilic/hydrophobic balance in the side chains, and thus hydrogen bonds can form between water molecules and hydrophilic groups of the hydrogel. These hydrogen bonds act cooperatively to form a stable shell around the hydrophobic groups, which means that the PNIPA hydrogel has good solubility at low temperatures. As the temperature increases, these interactions become weak and the entrapped water molecules are slowly released. When the hydrogel reaches its lower critical solution temperature (LCST, around 33 °C) or above, these interactions are destroyed and the hydrophobic interactions among the hydrophobic groups are strengthened dramatically and abruptly, which leads to the collapse of the polymer chains and thus the phase transition of the hydrogel network (Zhang and others 2002).

Developing active packages with controlled delivery systems is a promising alternative, particularly if pimaricin is released as a response to particular triggers. Several different approaches that include pimaricin in packaging films to avoid mould spoilage have been reported, for example, chitosan-based edible films (Fajardo and others 2010), wheat gluten and methyl cellulose biopolymers (Türe and others 2008), and polyethylene films coated with commercially available polyvinylchloride (PVC) lacquer (Hanušová and others 2010). However, thermosensitive hydrogels have never been assayed for this purpose.

Therefore, the aim of this work was to synthesize PNIPA nanohydrogels with different grades of hydrophilicity by adding acrylic acid (AA) as comonomer and evaluating their capacity to transport and release pimaricin under different temperature conditions. In addition, the effectiveness of the pimaricin-loaded PNIPA nanodevices in controlling mould spoilage was assayed with a food model system consisting in potato dextrose agar (PDA) plates. In order to assess the protective effect of nanohydrogels, mould spoilage was evaluated under favorable and unfavorable conditions for the chemical stability of pimaricin.

## Materials and Methods

The commercial materials employed in this work are listed in Table 1.

### Synthesis of PNIPA/AA nanohydrogels

The microemulsion polymerization experiments were prepared using water in oil (W/O) systems. The W/O microemulsion composition was 58% aqueous phase (AP), 17% oil phase (OP), and 25% surfactant (ST). The AP consisted of 80% water and 20% monomers. For pure PNIPA nanohydrogels (PNIPA(5)), the relation (w/w) of N-isopropylacrylamide (NIPA) based on the monomers ($m_{NIPA}/m_{monomer}$) was 1. For NIPA copolymerized with AA (PNIPA-20AA(5)) nanohydrogels $m_{NIPA}/m_{monomer}$ was 0.80 and $m_{AA}/m_{monomer}$ was 0.20. To preserve the shape and size of the particles during handling we used the cross-linking agent N,N′-methylenebisacrylamide (NMBA) ($m_{NMBA}/m_{monomer} = 0.05$). The OP consisted entirely of Isopar™ M, which was mixed directly with surfactants (ST) Atlas™ G-1086 ($m_{AtlasG-1086}/m_{ST} = 0.97$) and Span™ 83 ($m_{Span83}/m_{ST} = 0.03$).

The 2 phases were solubilized then mixed in a 100 mL reactor thermostatized at 25 °C, equipped with mechanical stirring and a thermal sensor. To eliminate oxygen, 10 min before the polymerization began (by adding the initiator at a ratio $m_{NaHSO_3}/m_{monomer} = 0.01$) and during the entire reaction, the reaction medium was purged by bubbling nitrogen through it. The polymerization conversion was monitored via the temperature increase inside the glass reactor. The polymer was purified using selective precipitation with chloroform and diethyl ether. The pure polymer was dried overnight in an oven (50 °C) and then ground in a colloid mill (IKA® -Werke GmbH & Co. KG, Staufen, Germany).

The particle size distribution was analysed with a dynamic light scattering (DLS) measurement technique using a Zetasizer Nano ZS (Malvern Instruments, Worcestershire, U.K.) at 25 °C. Nanohydrogel samples were prepared by dispersing PNIPA powder in distilled water (0.5 mg/mL), the samples were agitated for 3 h at ambient temperature to allow the nanoparticles to swell properly. Each analysis was performed in triplicate.

### Preparation of pimaricin-loaded PNIPA/AA nanohydrogels

PNIPA/AA nanohydrogel powder was dispersed in distilled water by agitation for 3 h at ambient temperature to allow the nanoparticles to swell properly. This suspension was then mixed with a pimaricin water solution to obtain final concentrations of 12.5 mg of nanohydrogel per mL and 0.4 mg of commercial pimaricin per mL. The mixture was stirred overnight at 25 °C (below the LCST) to guarantee that the pimaricin was incorporated into the nanohydrogel particles. This mixture was used in further release studies. A nanohydrogel sample without pimaricin was processed in the same conditions and used as a control. The experiments were carried out in duplicate.

### Pimaricin release from PNIPA/AA nanohydrogels

For the release studies, 3 mL of pimaricin-loaded nanohydrogel samples, obtained as explained in the previous section, were placed in a dialysis bag (the SnakeSkin™ pleated dialysis bag with a molar mass cut-off of 3500 g/mol was obtained from Pierce, Rockford, Ill., U.S.A.) and dialyzed against 12 mL of distilled water at a constant temperature while agitating constantly. Samples of 1 mL were taken at intervals from the solution in order to determine the pimaricin concentration. The volume removed from the probe was returned after measurements had been made.

**Table 1–Commercial materials.**

| Material | Company |
|---|---|
| N-isopropylacrylamide, stabilized 99% | Acros Organics (Geel, Belgium) |
| Acrylic acid (stabilised with hydroquinone monomethyl ether) for synthesis | Merck (Darmstadt, Germany) |
| N,N′-methylenebisacrylamide for synthesis | Merck (Darmstadt, Germany) |
| Sodium bisulfite for analysis | Merck (Darmstadt, Germany) |
| Isoparaffinic synthetic hydrocarbon (Isopar™ M), 98% | Esso Chemie (Cologne, Germany) |
| Sorbitan sesquiolate (Span™ 83), 98% | Uniquema (Wilmington, Del., U.S.A.). |
| PEG-40 Sorbitol Hexaoleate (Atlas™ G-1086), 98% | Uniquema (Wilmington, Del., U.S.A.) |
| Chloroform stabilized with ethanol | Panreac (Barcelona, Spain) |
| Diethyl ether stabilized with approximately 6 ppm of BHT | Panreac (Barcelona, Spain) |
| Commercial pimaricin (50% pure pimaricin, 50% lactose) | VGP Pharmachem (Barcelona, Spain) |
| Pure pimaricin from *Streptomyces chattanoogensis*, ≥95% (HPLC) | Sigma-Aldrich (Munich, Germany) |
| Potato dextrose agar (PDA) | Difco™ (Detroit, Mich., U.S.A.) |
| L(+)-tartaric acid *PRS* | Panreac (Barcelona, Spain) |

A nanohydrogel sample without pimaricin was processed under the same conditions and used as a control. All experiments were carried out in duplicate.

In order to determine the time required to reach dialysis equilibrium, a pimaricin solution (3 mL) with the same concentration loaded into the nanohydrogels (0.4 mg powder per mL) was dialyzed against 12 mL of distilled water, as indicated above.

The data were fitted with GraphPad Prism™ 5 (GraphPad Software Inc., San Diego, Calif., U.S.A.). The significance of the model parameters was assessed with Mathematica 7 (Wolfram Research, Inc., Champaign, Ill., U.S.A.).

### Pimaricin detection and quantification

The pimaricin concentration in the dialysis media was determined spectrophotometrically at 319 nm (Beckman Coulter Inc., Brea, Calif., U.S.A.). Pimaricin has maximum absorption at 304 nm; however, the suboptimal peak (90% of the maximum) observed at 319 nm showed the highest value for the pimaricin/dialyzed PNIPA absorbance ratio.

The molar absorption coefficient ($\varepsilon$) for pimaricin was extrapolated from the linear fit of the absorbance measurements of pure aqueous pimaricin solutions with known concentrations from 0.3 to 30 ppm (within the solubility limit). A value of $0.077 \pm 0.006$ L/$\mu$g/cm was obtained.

### Measurement of the gel phase transition temperature

The phase transition was examined by measuring the transmittance of polymer suspensions at 500 nm using a spectrophotometer with a Peltier temperature control module (Beckman Coulter Inc., Brea, Calif., U.S.A.) at temperature intervals from 15 to 50 °C with increments of 2 °C between each measurement.

### Inhibition studies employing a food model system

We designed a food model system consisting of Petri dishes with 5 mL of PDA agar. In order to simulate favorable (A) and unfavorable (B) conditions for the chemical stability of pimaricin, we considered the following conditions:

A) PDA agar without acidification and plate storage under dark conditions.
B) Acidified PDA agar (pH 3) with 10% L(+)-tartaric acid (w/v) and plate storage under fluorescent lighting.

The antimicrobial effectiveness of the nanohydrogel-pimaricin system (NP) was evaluated together with control treatments in which the nanohydrogel-pimaricin system was substituted by distilled water (C), the nanohydrogel (N), and free pimaricin (P). The nanohydrogel and pimaricin concentrations and ratios were the same as those used for the release studies.

An aliquot of 25 $\mu$L of a 12 h-culture of *Saccharomyces cerevisiae* (Sc 1.02) ($30 \times 10^7$ UFC/mL) was inoculated in triplicate into the Petri dishes. After 1 h in the fridge to allow the inoculated culture to be absorbed properly, 100 $\mu$L of each antimicrobial sample (NP, N, C, and P) was spread over the plate surface. All plates were incubated at 4 °C for 7 d and then at 25 °C until the end of the experiment (15 d).

### Statistical treatment

The results of pimaricin diffusion were analysed with Student's *t*-test ($\alpha = 0.05$). The antimicrobial effectiveness of the treatments was evaluated by analysis of variance (2-way ANOVA) followed by Bonferroni posttests for multiple comparisons. All the statistical tests were performed with GraphPad Prism™ 5.

## Results and Discussion

### Synthesis of PNIPA/AA nanohydrogels

The mean particle size (r. nm) and polydispersitivity index (PDI) of the PNIPA(5) and PNIPA-20AA(5) nanohydrogels determined by DLS at the end of the inverse microemulsion polymerization were $79.19 \pm 10.06$ (PDI $= 0.25 \pm 0.10$) and $114.19 \pm 13.80$ (PDI $= 0.29 \pm 0.11$), respectively.

### Pimaricin release from PNIPA/AA nanohydrogels

The 1st objective of this work was to study the release kinetics of pimaricin from nanohydrogels. Due to the experimental difficulties in separating the nanohydrogel from free pimaricin, we placed the loaded nanohydrogel in dialysis bags and determined the free pimaricin concentration over time in the dialysis media (distilled water). Therefore, during the release process, the pimaricin needed to diffuse through 2 release layers: the nanohydrogel matrix and the dialysis bag (Figure 1).

The membrane of the dialysis bag could become a barrier to pimaricin molecules, either because they adhere to the membrane or because they form aggregates (Stark and Tan 2003) that are larger than the pores of the dialysis bag. Therefore, we studied the diffusion of free pimaricin through the dialysis bag. The results obtained (data not shown) indicate that diffusion continued until equilibrium was reached and that the dialysis bag did not influence the release of pimaricin. Hence, the free pimaricin transition to the release media would only be governed by the capacity of the molecule to diffuse at the tested temperature.

However, all of the pimaricin that had been loaded could not be released in the dialysis process because the process stopped when it reached the equilibrium concentration. Thus, the amount of pimaricin released in the dialysis experiments with free pimaricin was considered to be the maximum amount of pimaricin released from the nanohydrogels.

Thus, the relative fraction of pimaricin released ($\gamma F_t$) was defined by the following expression:

$$\gamma F_t = C_{t\ \mathrm{PNIPA-Pim}} / C_{\mathrm{max\,Pim}} \qquad (1)$$

where $C_{t\ \mathrm{PNIPA-Pim}}$ is the amount of pimaricin ($\mu$g) released from the nanohydrogel to the dialysis medium (passing through the dialysis membrane) and $C_{\mathrm{max\,Pim}}$ is the amount of pimaricin ($\mu$g) under the steady-state conditions determined in the dialysis experiments with free pimaricin (without nanohydrogel).

To calculate the maximum relative amount of pimaricin released ($\gamma F_{\max}$), experimental data were fitted according to the following equation, adapted from López and others (2004):

$$\gamma F_t = \gamma F_{\max} + (\gamma F_0 - \gamma F_{\max}) \times \exp(-m \times t) \qquad (2)$$

where $\gamma F_{\max}$ and $\gamma F_0$ are the maximum relative amount of pimaricin and initial relative amount of pimaricin, respectively, released from the nanohydrogels through the dialysis membrane. The parameter $m$ (min$^{-1}$) is the maximum release rate and $t$ (min) is the sampling time.

Equation 2 is valid in the entire experimental domain, that is, it is able to fit the pimaricin released in a time interval from $t_0$ (initial time) to $t_{\mathrm{eq}}$ (equilibrium dialysis time). Considering that $\gamma F_{\max} = \lim \gamma F_t$ when $t$ tends to infinity, the time needed to

reach $\gamma F_{max}$ would be infinity. For the sake of practicality, we decided to calculate $t_{eq}$ as the time to reach 99% of $\gamma F_{max}$.

**Pimaricin release from the PNIPA(5) nanohydrogel.** The most characteristic features of the release of pimaricin from PNIPA(5) were the strong burst effect associated with the pimaricin release curve of the pimaricin-loaded PNIPA(5) nanohydrogel and the plateau observed at around 10% release (Figure 2).

Data derived from Eq. 2 (Table 2) indicate that the maximum relative fraction of pimaricin released ($\gamma F_{max}$) from the PNIPA(5) nanohydrogel at 37 °C was only 9%, and most of the antifungal remained trapped in the collapsed nanogel. The maximum release rate ($m$) was significantly higher ($P = 0.0335$) than that obtained in the dialysis experiments with free pimaricin (data not shown), and the time necessary to reach equilibrium was 0.13 times shorter.

It is well documented that at 37 °C (above the LCST) hydrophobic interactions among PNIPA chains strengthen dramatically, which leads to the collapse of the polymer and the release of significant amounts of water (Zhang and others 2002; Huang and Lowe 2005).

It has been reported that loaded molecules can become entrapped in the external part of PNIPA xerogels. Blanco and others (2008) found that methotrexate was released from PNIPA over 25 h with a burst effect of 71% at 15 min. It has been suggested that the fast release of the externally entrapped methotrexate is the cause of the burst effect. The large size and hydrophobicity of the methotrexate incorporated into the nanohydrogel structure might contribute to slowing down their release at 37 °C. Zhang and others (2002) have described similar effects with 5-fluorouracil entrapped in PNIPA hydrogels. In this case, some of the drug became entrapped in the shrunken matrix due to the collapse of the polymer chains and gel volume shrinkage, which slowed down the drug release.

We suggest that because pimaricin is larger (665.725 g/mol) than methotrexate (454.46 g/mol) and 5-Fluorouracil (130.08 g/mL) and also due to its amphiphilic nature, pimaricin could not be released from the PNIPA nanohydrogel (and/or the pimaricin was entrapped in the shrunken matrix). The burst effect at the beginning could be because the pimaricin was in a very exposed location within the nanohydrogel structure and so it could be released quickly when the water was expelled from the inside, coinciding with the collapse of the nanogel network.

**Pimaricin release from the PNIPA-20AA(5) nanohydrogel.** It has been demonstrated that the physical properties (LCST) of PNIPA nanohydrogels can be modulated by copolymerization with hydrophilic monomers (Schild 1992; Eeckman and others 2004; Milašinović and others 2010). In this work, we used AA as the hydrophilic monomer to synthesize a PNIPA nanohydrogel with 20% AA (PNIPA-20AA(5)). It is expected that adding AA will promote the formation of new hydrogen bonds with water. As explained above, PNIPA-20AA(5) nanoparticles are larger than PNIPA(5) nanoparticles because they are able to capture more water.

The release kinetic from the PNIPA-20AA(5) nanohydrogel showed a very different profile from that of the PNIPA(5) nanohydrogel (Figure 2). There was no burst effect, but rather the pimaricin was released steadily. According to Milašinović and others (2010), the absence of the initial burst suggests that the pimaricin is trapped in the nanogel structure, unlike the previous assayed nanogel in which significant amounts of pimaricin seem to remain exposed on the surface of the nanogel particles.

The maximum amount of pimaricin released from the PNIPA-20AA(5) nanohydrogel was also significantly higher ($P = 0.0309$) than that released from the PNIPA(5) nanohydrogel (Table 2), although it took a very long time to reach the steady state. The $m$ value was significantly lower than that obtained for the PNIPA(5) nanohydrogel ($P = 0.0272$) and the dialysis experiments with free pimaricin ($P = 0.0087$). This continuous efflux of pimaricin to the medium indicates that the PNIPA-20AA(5) nanohydrogel imposed less diffusional restrictions than PNIPA(5).

## The effect of temperature on the release of pimaricin from nanohydrogels

To clarify the processes involved in the release of pimaricin from nanohydrogels with and without AA, we conducted a new experiment in which the nanohydrogels were loaded with pimaricin at

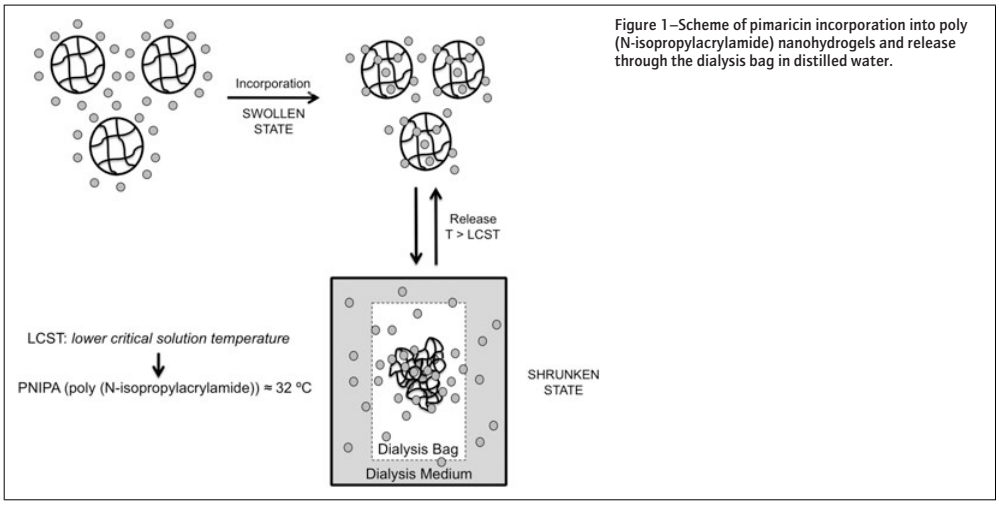


Figure 1–Scheme of pimaricin incorporation into poly (N-isopropylacrylamide) nanohydrogels and release through the dialysis bag in distilled water.

25 °C as in the previous assays and then used to obtain the different kinetic profiles by dialysis at 15, 25, 37, and 47 °C.

As the temperature increased, the $\gamma F_{max}$ value of the PNIPA-20AA(5) nanohydrogel increased up to a maximum and then decreased slightly. However, significantly less pimaricin was released from the PNIPA(5) nanohydrogel as the temperature increased (Figure 3). Therefore, by plotting the maximum relative fractional release ($\gamma F_{max}$) against temperature ($T$), it was possible to observe a well-defined optima, and thus the following second-order polynomial function was fitted to the experimental data:

$$\gamma F_{max} = a_0 + a_1 \times T + a_2 \times T^2 \quad (3)$$

By deriving the functions obtained in relation to the temperature and solving the roots of the resulting functions, the optimal temperature at which the largest amount of pimaricin was released was calculated to be 40.04 °C for the PNIPA-20AA(5) nanohydrogel and −1.25 °C for the PNIPA(5) nanohydrogel. This latter optimum temperature value is obviously located outside the experimental domain. Even so, the trend predicted by the model clearly indicates that for the PNIPA(5) nanohydrogel a decrease in temperature would lead to an increase in the amount of pimaricin released (Figure 3).

The observed behavior could be interpreted as resulting from the temperature causing the nanohydrogel collapse. Hydrophobic interactions are one of the main factors leading to the collapse of a nanohydrogel above the LCST (Eeckman and others 2004). The presence of AA might also affect the deswelling rate, and give rise to a more hydrated collapse state that facilitates the continuous diffusion of pimaricin to the medium. However, the collapse of the less hydrated PNIPA(5) nanohydrogel would be more intense, trapping pimaricin molecules within the shrunken matrix and aborting their release (Figure 3).

In order to verify this hypothesis, we examined the LCST phase transitions of the nanohydrogels according to the transmittance measurements at different temperatures, a methodology widely used in the literature. To facilitate interpretation, the data obtained were transformed to optical density values (Figure 4) with the following equation:

$$OD_{500} = -\mathrm{Log}_{10}(T_{500}) \quad (4)$$

where $OD_{500}$ and $T_{500}$ are the optical density and the transmittance of the nanohydrogel suspension at 500 nm, respectively.

As hypothesized, in Figure 4 we can see a sharp volume phase transition for the PNIPA(5) nanohydrogel and that the introduction of 20% AA almost completely stopped the LCST transition for the PNIPA-20AA(5) nanohydrogel. Milašinović and others (2010) observed similar behavior when they increased the hydrophilicity of the PNIPA homopolymer by increasing the percentage of itaconic acid. The homopolymer showed a sharp phase transition (34.2 °C) that became less pronounced when 5% or 10% itaconic acid was added, and the transition became practically nonexistent with 15% itaconic acid.

## Sustained controlled release

After studying the different capacities of PNIPA nanohydrogels to transport and release pimaricin when the temperature is increased above its LCST, we then alternated temperature cycles to determine whether or not this release is sustained over time. This

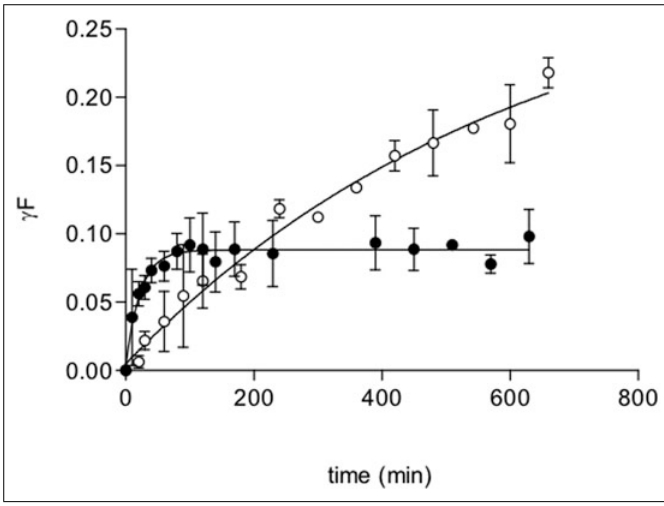


**Figure 2–Relative fraction of pimaricin released ($\gamma F_t$) from the PNIPA(5) (●) and PNIPA-20AA(5) (○) nanohydrogels through the dialysis bag of 3500 g/mol in distilled water at 37 °C. The lines are the fitting curves generated from Eq. 2 ($r^2_{PNIPA(5)} = 0.9693$; $r^2_{PNIPA-20AA(5)} = 0.9833$).**

**Table 2–Maximum relative fraction of pimaricin released ($\gamma F_{max}$) from the nanohydrogels, maximum release rate ($m$), and equilibrium dialysis time ($t_{eq}$) at 37 °C.**

| Nanohydrogel | $\gamma F_{max}$ (37 °C) | $m$ (37 °C) ($min^{-1}$) | $t_{eq}$ (37 °C) (h) |
|---|---|---|---|
| PNIPA(5) | $0.09 \pm 0.002^a$ | $44.27 \times 10^{-3} \pm 5.76 \times 10^{-3a}$ | 1.72 |
| PNIPA-20AA(5) | $0.31 \pm 0.06^b$ | $1.62 \times 10^{-3} \pm 0.48 \times 10^{-3b}$ | 47.31 |

Values reported are the means ± standard deviation ($n = 2$).
[a–b]Different lower case letters in the same column indicate a statistically significant difference ($P < 0.05$).

is important because in the food industry it may be necessary to release the antifungal in various cycles.

Therefore, we analysed pimaricin release from nanohydrogels with stepwise temperature changes between 15 and 37 °C. The cumulative pimaricin release profiles as well as the pimaricin release rate as a function of pulsatile temperature are shown in Figure 5.

The results for the PNIPA(5) nanohydrogel were consistent with the positive squeezing mechanism reported in the literature (Bromberg and Ron 1998; Shin and others 2001; Wu and others 2005). When the temperature was increased, the release rate peaked rapidly followed by a very slow release process. Pimaricin release stopped after 2 temperature pulses and during these cycles 15% was released, which indicates that the deswelling process did not help to squeeze more pimaricin out of the gel matrix.

However, when AA was added to the PNIPA-20AA(5) nanohydrogel, the temperature changes did not affect the release rate as dramatically. Although the biggest release peak occurred in the 1st cycle at 37 °C, after the 3rd cycle at this temperature the release rate still remained apparently constant.

Therefore, higher releases were obtained by alternating on/off cycles, and consequently there were larger amounts of pimaricin in the release medium than in a single cycle at 37 °C, although with the PNIPA-20AA(5) nanohydrogel a more sustained release over time was achieved.

### Inhibition studies employing food model systems

To evaluate the antimicrobial effectiveness of the pimaricin-nanohydrogel system proposed, we conducted experiments using a food model system consisting of PDA plates. In addition, this

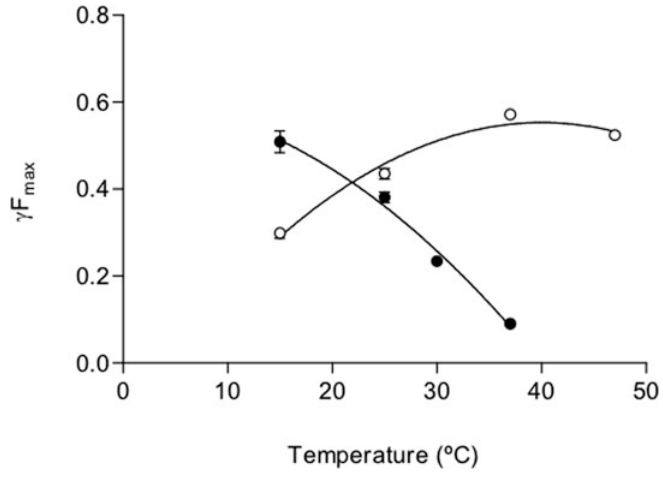


Figure 3–Variation of the maximum relative fraction of pimaricin released ($\gamma F_{max}$) from the PNIPA(5) (●) and PNIPA-20AA(5) (○) nanohydrogels through the dialysis bag of 3500 g/mol in distilled water in relation to temperature. The lines are the fitting curves generated from Eq. 3 ($r^2_{PNIPA(5)} = 0.9896$; $r^2_{PNIPA-20AA(5)} = 0.9725$).

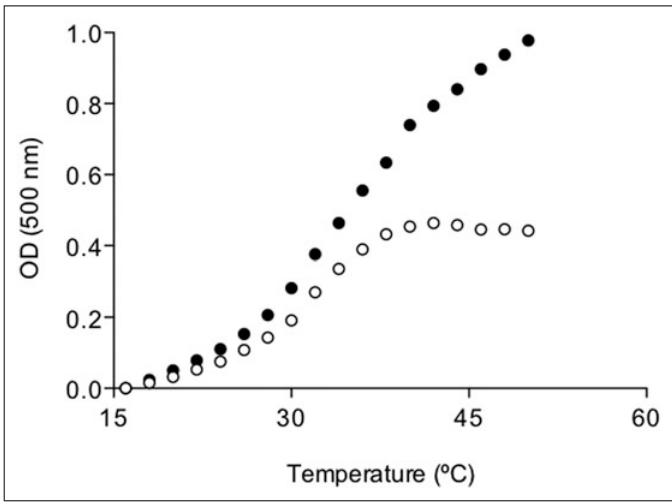


Figure 4–Optical density (OD) at 500 nm of the aqueous solutions (12.5 mg/mL) of the PNIPA(5) (●) and PNIPA-20AA(5) (○) nanohydrogels.

assay was used to assess the capacity of nanohydrogels to protect the pimaricin by keeping it chemically stable under favorable (A) and unfavorable (B) conditions since critical amounts of pimaricin could be degraded under acidic conditions (Stark and Tan 2003) and fluorescent lighting. Koontz and others (2003) addressed this problem and studied how forming inclusion complexes of pimaricin and cyclodextrins increased the stability of pimaricin compared to free pimaricin in cheese products stored under high-intensity fluorescent lighting in supermarket freezer showcases.

No growth was observed at 4 °C (Table 3) in any of the plates or storage conditions (A or B) assayed. When the temperature was increased up to 25 °C and under favorable conditions for pimaricin stability (A), growth peaked rapidly and counts were above the limit (CFU > 75, in 5 mL of medium) for controls without pimaricin (C and N). Nonetheless, when pimaricin was present, there was much less growth, especially in those plates containing pimaricin in the nanohydrogel (Table 3).

In plates under unfavorable conditions (B: acidic medium and storage under fluorescent lighting), counts were low for all treatments because yeast grows more slowly in acidic media; however, the poorest growth was again observed on plates with the pimaricin-loaded nanohydrogel (Table 3).

In order to quantify these effects, we calculated the percentage reduction in microbial growth as follows:

$$\%R = ((N_0 - N)/N_0) \times 100 \quad (5)$$

where $N_0$ is the mean count on control plates (C) and $N$ is the mean count on plates with pimaricin (P) and pimaricin-loaded nanohydrogel (NP), both expressed as Log (CFU/mL).

For plates under (A) conditions, the NP treatment showed a reduction of 27.07 ± 4.15%, which was higher than that observed on plates with the P treatment, which showed a reduction of 17.26% ± 1.34%, although the difference between the 2 treatments was not significant ($P > 0.05$). However, under (B) conditions, there was a larger difference between the NP and P treatments. The reduction on plates with the NP treatment was 80.94% ± 33.02%, which was significantly higher ($P < 0.01$) than that observed on plates with the P treatment, 19.91% ± 6.68%. In any case, the ANOVA analysis at a 95% confidence level of the percentage reduction (%$R$) showed that the effect of the treatment was very significant ($P = 0.0069$) and the effect of growth conditions (pH, light) was significant ($P = 0.0205$). The interaction between these 2 factors was also significant ($P = 0.0311$), that is, the treatment did not have the same effect under the 2 growth conditions assayed.

Therefore, the antifungal effect of pimaricin was potentiated when it was applied loaded into the PNIPA-20AA(5) nanohydrogel probably because pimaricin was released slowly when environmental conditions required it. This seems to indicate that the nanohydrogel had a protective effect against degrading conditions (pH, light), which thus made the antifungal effect of pimaricin more intense.

Therefore, the nanohydrogel-pimaricin system proposed in this work would be useful in packaging for food products that are easily spoiled by fungal growth (that is, which have low pH and a high moisture content) and that are normally exposed to changes in storage temperature due to transport and shelf time. As pimaricin is usually used to prevent moulds and yeasts growing on the surface of cheese we are currently performing experiments with cheese samples to test PNIPA-nanohydrogel systems. The controlled

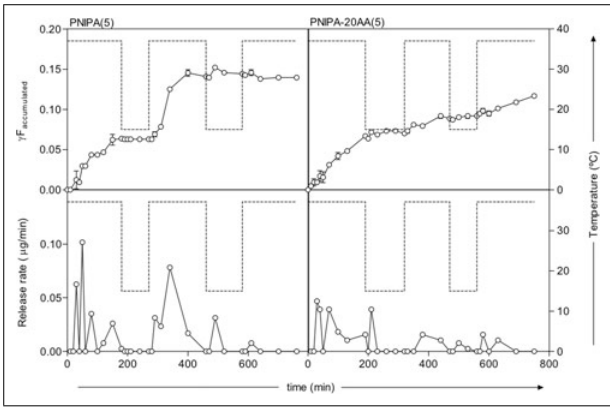


Figure 5–Relative fraction of accumulated pimaricin released and the release rate of pimaricin from the PNIPA(5) and PNIPA-20AA(5) nanohydrogels through the dialysis bag of 3500 g/mol in distilled water. The dashed line shows the temperature cycling of the release medium between 37 and 15 °C.

**Table 3–Counts (CFU) of *Saccharomyces cerevisiae* (Sc 1.02) on PDA agar plates without acidification stored under dark conditions (A), and acidified PDA agar plates stored under fluorescent lighting (B), treated with distilled water (C), nanohydrogel (N), free pimaricin (P), and the nanohydrogel-pimaricin system (NP).**

| | 4 °C | | | | 25 °C | | | |
|---|---|---|---|---|---|---|---|---|
| | Two days | | Seven days | | Nine days | | Fifteen days | |
| | A | B | A | B | A | B | A | B |
| C | – | – | – | – | 347.0 ± 33.1 | 11.7 ± 12.6 | 327.3 ± 23.8 | 19.7 ± 13.5 |
| N | – | – | – | – | 405.7 ± 46.5 | 54.0 ± 26.1 | 346.7 ± 37.3 | 57.0 ± 22.7 |
| P | – | – | – | – | 65.7 ± 3.8 | 0.3 ± 0.6 | 64.0 ± 7.8 | 4.7 ± 2.1 |
| NP | – | – | – | – | 29.3 ± 10.0 | – | 26.3 ± 9.1 | 0.3 ± 0.6 |

Values reported are the means ± standard deviation ($n = 3$).

release of pimaricin from PNIPA nanohydrogels could reduce the amount of pimaricin on the surface of the cheese, and therefore reduce the amount that migrates to the cheese bulk.

## Conclusion

Our results suggest that the degree of hydrophilicity determines how the pimaricin is released from PNIPA nanohydrogels, and can lead to a slower but more continuous release of pimaricin, thus increasing the amount of the antifungal released. Pimaricin-loaded PNIPA-20AA(5) nanohydrogels could be an effective system for controlling the release of pimaricin because they protect the antifungal against environmental degradation and release it slowly. Pimaricin-loaded nanohydrogels could therefore be used in active packaging in the future.

## Acknowledgments

This work was funded by grant (MAT 2006–11662-CO3-CO2-C01/MAT 2010-21509-C03-01/EUI 2008–00115) from the "Ministerio de Educación y Ciencia" (Spain). Clara Fuciños was funded by a predoctoral scholarship from Univ. of Vigo (Spain).

## References

Andersson M, Axelsson A, Zacchi G. 1997. Diffusion of glucose and insulin in a swelling N-isopropylacrylamide gel. Intl J Pharm 157(2):199–208.

Blanco MD, Guerrero S, Teijón C, Olmo R, Pastrana L, Katime I, Teijón JM. 2008. Preparation and characterization of nanoparticulate poly(N-isopropylacryl-amide) hydrogel for the controlled release of anti-tumour drugs. Polym Intl 57(11):1215–25.

Bromberg LE, Ron ES. 1998. Temperature-responsive gels and thermogelling polymer matrices for protein and peptide delivery. Adv Drug Deliv Rev 31(3):197–221.

Caykara T, Bulut M, Dilsiz N, Akyüz Y. 2006. Macroporous poly(acrylamide) hydrogels: swelling and shrinking behaviours. J Macromol Sci Pure Appl Chem 43(6):889–97.

Eeckman F, Moës AJ, Amighi K. 2004. Poly(N-isopropylacrylamide) copolymers for constant temperature controlled drug delivery. Intl J Pharm 273(1–2):109–19.

Fajardo P, Martins JT, Fuciños C, Pastrana L, Teixeira JA, Vicente AA. 2010. Evaluation of a chitosan-based edible film as carrier of natamycin to improve the storability of Saloio cheese. J Food Eng 101(4):349–56.

Farid MA, El-Enshasy HA, El-Diwany AI, El-Sayed E-A. 2000. Optimization of the cultivation medium for natamycin production by *Streptomyces natalensis*. J Basic Microbiol 40(3): 157–66.

Hanušová K, Šťastná M, Votavová L, Klaudisová K, Dobiáš J, Voldřich M, Marek M. 2010. Polymer films releasing nisin and/or natamycin from polyvinyldichloride lacquer coating: nisin and natamycin migration, efficiency in cheese packaging. J Food Eng 99(4): 491–6.

Huang X, Lowe TL. 2005. Biodegradable thermoresponsive hydrogels for aqueous encapsulation and controlled release of hydrophilic model drugs. Biomacromolecules 6(4):2131–9.

Koontz JL, Marcy JE, Barbeau WE, Duncan SE. 2003. Stability of natamycin and its cyclodextrin inclusion complexes in aqueous solution. J Agric Food Chem 51(24):7111–4.

López C, Torrado A, Fuciños P, Guerra NP, Pastrana L. 2004. Enzymatic hydrolysis of chestnut purée: process optimization using mixtures of $\alpha$-amylase and glucoamylase. J Agric Food Chem 52(10):2907–14.

Milašinović N, Kalagasidis Krušić M, Knežević-Jugović Z, Filipović J. 2010. Hydrogels of N-isopropylacrylamide copolymers with controlled release of a model protein. Intl J Pharm 383(1–2):53–61.

Neethirajan S, Jayas DS. 2011. Nanotechnology for the food and bioprocessing industries. Food Bioprocess Technol 4(1):39–47.

Schild HG. 1992. Poly(N-isopropylacrylamide): experiment, theory and application. Prog Polym Sci 17(2):163–249.

Shin Y, Chang JH, Liu J, Williford R, Shin Y-, Exarhos GJ. 2001. Hybrid nanogels for sustainable positive thermosensitive drug release. J Control Release 73(1):1–6.

Stark J, Tan HS. 2003. Natamycin. In: Russell NJ, Gould GW, editors. Food preservatives. 2nd ed. New York, USA: Kluwer Academic/Plenum Publishers. pp. 179–183.

Türe H, Eroglu E, Soyer F, Özen B. 2008. Antifungal activity of biopolymers containing natamycin and rosemary extract against *Aspergillus niger* and *Penicillium roquefortii*. Intl J Food Sci Technol 43(11):2026–32.

Vanden Bossche H, Engelen M, Rochette F. 2003. Antifungal agents of use in animal health – chemical, biochemical and pharmacological aspects. J Vet Pharmacol Ther 26(1):5–29.

Weiss J, Takhistov P, McClements DJ. 2006. Functional materials in food nanotechnology. J Food Sci 71(9): R107–16.

Wu JY, Liu SQ, Heng PW, Yang YY. 2005. Evaluating proteins release from, and their interactions with, thermosensitive poly (N-isopropylacrylamide) hydrogels. J Control Release 102(2):361–72.

Zhang X-Z, Zhuo R-X, Cui J-Z, Zhang J-T. 2002. A novel thermo-responsive drug delivery system with positive controlled release. Intl J Pharm 235(1–2):43–50.